Application of Internal Curing to Improve Concrete Bridge Deck Performance

SPR-P1(19) M083

Arman Abdigaliyev
Graduate Research Assistant
Department of Civil and Environmental Engineering
University of Nebraska-Lincoln

Yong-Rak Kim, PhD
Professor
Department of Civil & Environmental Engineering
Texas A&M University

Jiong Hu, PhD
Associate Professor
Department of Civil and Environmental Engineering
University of Nebraska-Lincoln

A Report on Research Sponsored by

Nebraska Department of Transportation

April 2020

Technical Report Documentation Page

1. Report No SPR-P1(19) M083	2. Government Accession No.	3. Recipient's Catalog No.	
4. Title and Subtitle Application of Internal Curing to Improve Concrete Bridge Deck Performance		5. Report Date April 2020	
		6. Performing Organization Code	
7. Author/s Arman Abdigaliyev, Yong-Rak Kim, and Jiong Hu		8. Performing Organization Report No.	
9. Performing Organization Name and Address University of Nebraska-Lincoln, Department of Civil Engineering Peter Kiewit Institute, Omaha, NE 68182-0178		10. Work Unit No. (TRAIS)	
		11. Contract or Grant No.	
12. Sponsoring Organization Name and Address Nebraska Department of Transportation 1400 Highway 2, PO Box 94759, Lincoln, NE 68509		13. Type of Report and Period Covered	
		14. Sponsoring Agency Code	
15. Supplementary Notes			

16. Abstract

Due to the relatively high cement content and low water-to-cement ratio (w/c) used, bridge deck concrete is prone to premature cracking. Internal curing has been found to greatly reduce the chance of premature cracking as well as concrete deterioration. This research project was intended to develop internally cured bridge deck concrete based on a local mix design in Nebraska. Four different lightweight fine aggregate (LWFA) as internal curing agents were evaluated, and their effects on fresh, mechanical, durability, and shrinkage properties of concrete were studied. To identify the most effective LWFA dosage for shrinkage reduction, different replacement rates of sand and gravel with LWFA were adopted to account for the moisture loss during the construction and drying period. Aggregate blends of internally cured mixes were also optimized to account for the disturbed aggregate gradations due to the introduced LWFA. The research study demonstrated that it is possible to develop a local internally cured concrete mix that is both technical and economically feasible. Even though the replacement of fine aggregates by LWFAs results in decreases of 28-day modulus of elasticity, and modulus of rupture, the overall mechanical properties still meet bridge deck criteria. As the curing age decreases, internally cured mixes were found to be less affected owing to the curing water from within the concrete matrix provided by the saturated LWFAs, which demonstrated that internal curing could potentially decrease the required amount of curing period in the field. The developed internally curing mixes were also found to have comparable chloride penetrability compared to the control mix and were also categorized as either very low or low chloride ion penetrability based on lab study.

17. Key Words lightweight fine aggregate, internal curing, shrinkage, cracking, aggregate	18. Distribution Statement		
19. Security Classification (of this report) Unclassified	20. Security Classification (of this page) Unclassified	21. No. of Pages 89	22. Price

Form DOT F 1700.7 (8-72) Reproduction of form and completed page is authorized

Table of Contents

LIST OF FIGURES

LIST OF TABLES

ACKNOWLEDGMENTS

The authors would like to thank the Nebraska Department of Transportation (NDOT) for funding the research project. In particular, the authors thank NDOT Technical Advisory Committee members for their technical support and valuable inputs and assists throughout the project. The authors would also like to thank Lyman-Richey Corp., Arcosa Lightweight, Buildex Inc., and Ash Grove Cement Company for the kind donation of materials for this research. Finally, the authors would like to thank Brandon Faltin, Flavia Ribeiro Furtado De Mendonca, Hani Alanazi, Joey Malloy, Jose Olvera Cortes, and Miras Mamirov for their valuable assistance throughout the project.

DISCLAIMER

The contents of this report reflect the views of the authors who are responsible for the facts and the accuracy of the data presented herein. The contents do not necessarily reflect the official views or policies of the Nebraska Department of Transportation, nor of the University of Nebraska-Lincoln. This report does not constitute a standard, specification, or regulation. Trade or manufacturers' names, which may appear in this report, are cited only because they are considered essential to the objectives of the report. The United States (U.S.) government and the State of Nebraska do not endorse products or manufacturers.

This material is based upon work supported by the Federal Highway Administration under SPR-P1(19) M083. Any opinions, findings, and conclusions or recommendations expressed in this publication are those of the author(s) and do not necessarily reflect the views of the Federal Highway Administration.

ABSTRACT

Due to the relatively high cement content and low water-to-cement ratio (w/c) used, bridge deck concrete is prone to premature cracking. Internal curing has been found to greatly reduce the chance of premature cracking as well as concrete deterioration. This research project was intended to develop internally cured bridge deck concrete based on a local mix design in Nebraska. Four different lightweight fine aggregate (LWFA) as internal curing agents were evaluated, and their effects on fresh, mechanical, durability, and shrinkage properties of concrete were studied. To identify the most effective LWFA dosage for shrinkage reduction, different replacement rates of sand and gravel with LWFA were adopted to account for the moisture loss during the construction and drying period. Aggregate blends of internally cured mixes were also optimized to account for the disturbed aggregate gradations due to the introduced LWFA. The research study demonstrated that it is possible to develop a local internally cured concrete mix that is both technical and economically feasible. Even though the replacement of fine aggregates by LWFAs results in decreases of 28-day modulus of elasticity, and modulus of rupture, the overall mechanical properties still meet bridge deck criteria. As the curing age decreases, internally cured mixes were found to be less affected owing to the curing water from within the concrete matrix provided by the saturated LWFAs, which demonstrated that internal curing could potentially decrease the required amount of curing period in the field. The developed internally curing mixes were also found to have comparable chloride penetrability compared to the control mix and were categorized as either very low or low chloride ion penetrability based on lab study.

CHAPTER 1. INTRODUCTION

1.1 Background

Due to the relatively high cement content and low water-to-cement ratio (w/c) or water-to-binder ratio (w/b) used, bridge deck concrete is prone to early-age cracking. As shown in Figure 1, bridge deck cracking and deterioration, coupled with the application of deicing chemicals during winter operations, have been a primary concern. Nebraska Department of Transportation (NDOT) has employed mitigating reactionary strategies such as crack sealing and overlay to address this issue of early-age deck cracking. However, these strategies are costly and could have an impact on traffic operations. NDOT will clearly benefit if concrete decks are free from premature cracking associated with initial construction.

Figure 1. Examples of bridge deck cracking
(photos from NDOT Bridge Inspection Database)

In recent years, several states have examined the concept of internal curing of concrete bridge decks to address the early-age cracking. According to American Concrete Institute (ACI) (ACI 308, 2013), "*Internal curing refers to the process by which the hydration of cement occurs because of the availability of additional internal water that is not part of the mixing water.*" Internal curing has been found to greatly reduce the chance of early-age cracking as well as concrete deterioration. Besides, the success of internal curing could reduce the current required extensive wet curing period, which is expensive and difficult to enforce and monitor. Even though internal curing could lead to an increase in materials cost to some extent due to the use of lightweight fine aggregates (LWFA), there is a great potential to save life cycle costs by extending service life and shortening external curing. This research will provide NDOT with a cost-effective practice for internal curing. Successful accomplishment of this research project will allow NDOT to apply the internal curing concept in various concrete projects, particularly for bridge deck construction, which will bring significant benefits to both short-term and long-term performance of concrete structures.

1.2 Research Objectives

The overall goal of this study is to identify a cost-effective practice for internal curing of bridge deck concrete for NDOT. To achieve the goal, three specific objectives of this study are to

(1) summarize the best practice of internal curing concrete for bridge deck application through an extensive literature review and survey; (2) determine the appropriate source and addition rate of LWFA for internal curing of Nebraska concrete bridge decks; and (3) evaluate the technical feasibility and benefits of internal curing for Nebraska bridge deck construction.

1.3 Organization of the Report

This project report is divided into six chapters. Following the introduction, the report provides a detailed background of internal curing in Chapter 2, covering such topics as mechanisms of the method, materials for internal curing, mix designs and proportioning, properties of internally cured concrete, and, finally, DOT experience from both laboratory and field. Chapter 3 presents the overview of materials used in the study, including various types of locally available LWFA, as well as concrete mixing procedures and testing methods. Next, Chapter 4 explains the experimental program and analyzes the results of the project in detail. Based on the project goals and needs, it was divided into three phases, each with its own goals and testing matrix. Chapter 5 of the report includes the analysis of the feasibility and cost-effectiveness of the proposed method, and recommendations for construction practice of internally cured concrete. Finally, Chapter 6 concludes the report by summarizing the findings, and suggesting further work that needs to be done for the successful implementation of the technique in the state of Nebraska.

CHAPTER 2. BACKGROUND

This chapter provides a summary of state-of-the-practice and recent advances in the internal curing of concrete. While internal curing is still a relatively new concept, several states have successfully conducted field projects with internal curing bridge deck concrete. The research team conducted an extensive review of past experience, current practice, and specifications for internal curing concrete, with the focus on mixture design, batching, and placing. Measures and practices to ensure the successful construction of internal curing concrete, particularly the saturation (pre-wetting) and control of moisture content of LWFA in the field were also summarized.

2.1 Concrete Shrinkage and Cracking

By its nature, concrete experiences significant volumetric changes starting from the moment water comes into contact with cement. This process can last for years. When dealing with unrestrained concrete elements or structures, volumetric changes possess no harm to concrete. However, in real case scenarios, concrete is always restrained or fixed in some way. Continuous volumetric expansions and contractions will cause stress build-up in the concrete matrix, which will eventually lead to cracking and durability issues. Before discussing internal curing, it is essential to define the different types of concrete volumetric change, or shrinkage, and cover the governing mechanism behind each of them. This will later help in understanding the concepts behind internal curing. Concrete shrinkage is a broad topic with numerous types and details. This report will cover only the basics of the most relevant types of concrete shrinkage.

2.1.1 Chemical Shrinkage

Chemical shrinkage accounts for the total volume reduction during the chemical reaction between water and cement. In other words, there is a volumetric difference between the combined volume of a predefined amount of cement and water and the total volume of hydrated cement paste. That volume difference is accounted for as a chemical shrinkage (Kosmatka and Wilson, 2011).

It is also important to define the chemical shrinkage before and after the set. Before the initial set, cement paste is in the plastic state, which means that it can deform freely. However, after the initial set has occurred, cement paste hardens and can no longer deform. As a result, the major part of chemical shrinkage is compensated by the generation of stress-induced air voids in the paste matrix (Kosmatka and Wilson, 2011).

2.1.2 Autogenous Shrinkage

Autogenous shrinkage accounts for the visible part of chemical shrinkage, which occurs at the macro-level and can be visually measured. The remaining part of the chemical shrinkage is comprised of capillary voids, which are generated in the paste matrix after setting and due to surface tension of the capillaries. In other words, capillary voids compensate for the major part of the stresses induced by continuous chemical shrinkage of the paste after the development of the self-supporting cement matrix (Kosmatka and Wilson, 2011). Figure 2 and Figure 3 illustrate the difference between chemical and autogenous shrinkage.

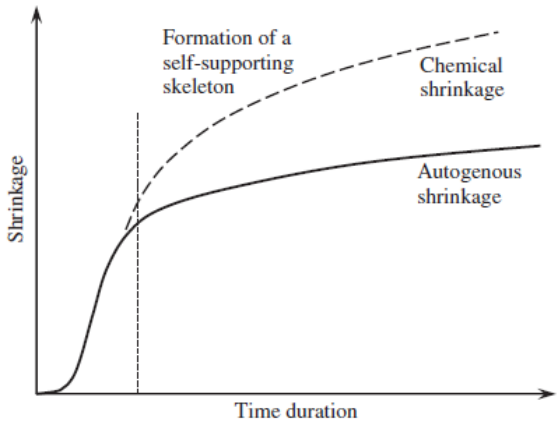

Figure 2. Schematic diagram of the difference between chemical and autogenous shrinkage (adapted from Li, 2011)

In general, autogenous shrinkage and chemical shrinkage are equivalent before the setting of concrete. However, there are some debates on whether autogenous shrinkage includes a pre-set part of the shrinkage. Some researchers and standards prefer to define autogenous shrinkage as the visible volume change occurred only after the set (Neville, 2011; ASTM C1698, 2009) whereas others claim that autogenous shrinkage accounts for visible volume change both before and after the set (Li, 2011; ACI 209 2005; ACI 209 1992). It should be noted that autogenous shrinkage does not occur with the presence of water. Figure 3 provides a graphic illustration of autogenous shrinkage and chemical shrinkage.

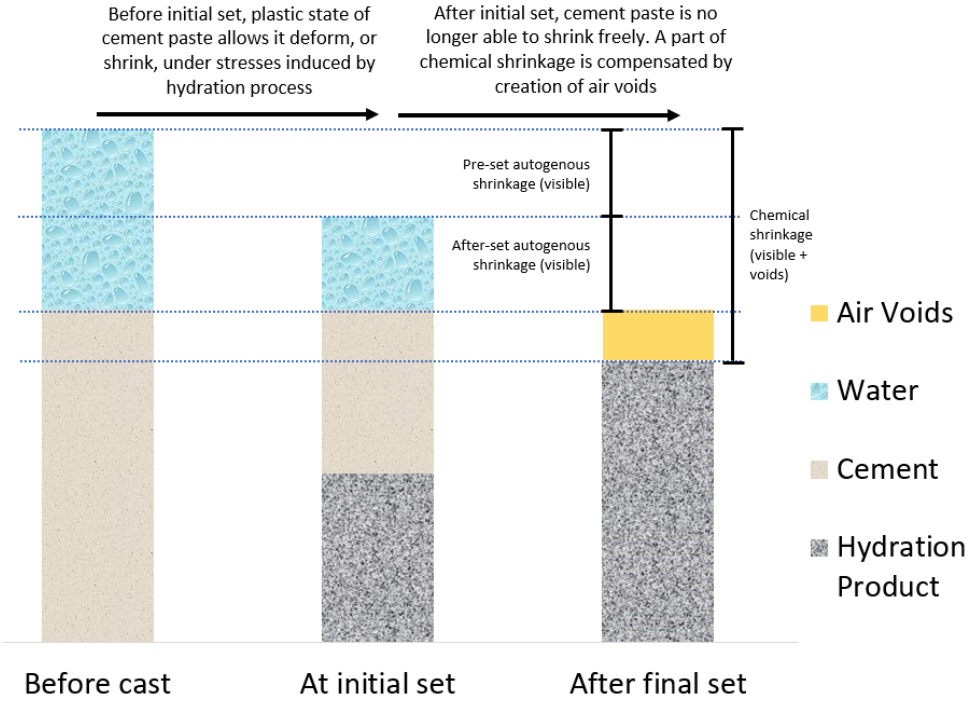

Figure 3. Schematic diagram of chemical shrinkage of cement paste (adapted from Kosmatka and Wilson, 2011)

2.1.3 Drying Shrinkage

As concrete starts losing moisture, drying shrinkage occurs, which can last for years. The amount of drying shrinkage highly depends on various factors, such as concrete curing conditions, cement type, w/c or w/b, concrete ingredients, and others (Kosmatka and Wilson, 2011). Figure 4 illustrates how chemical and drying shrinkage results in a stress build-up inside the concrete matrix.

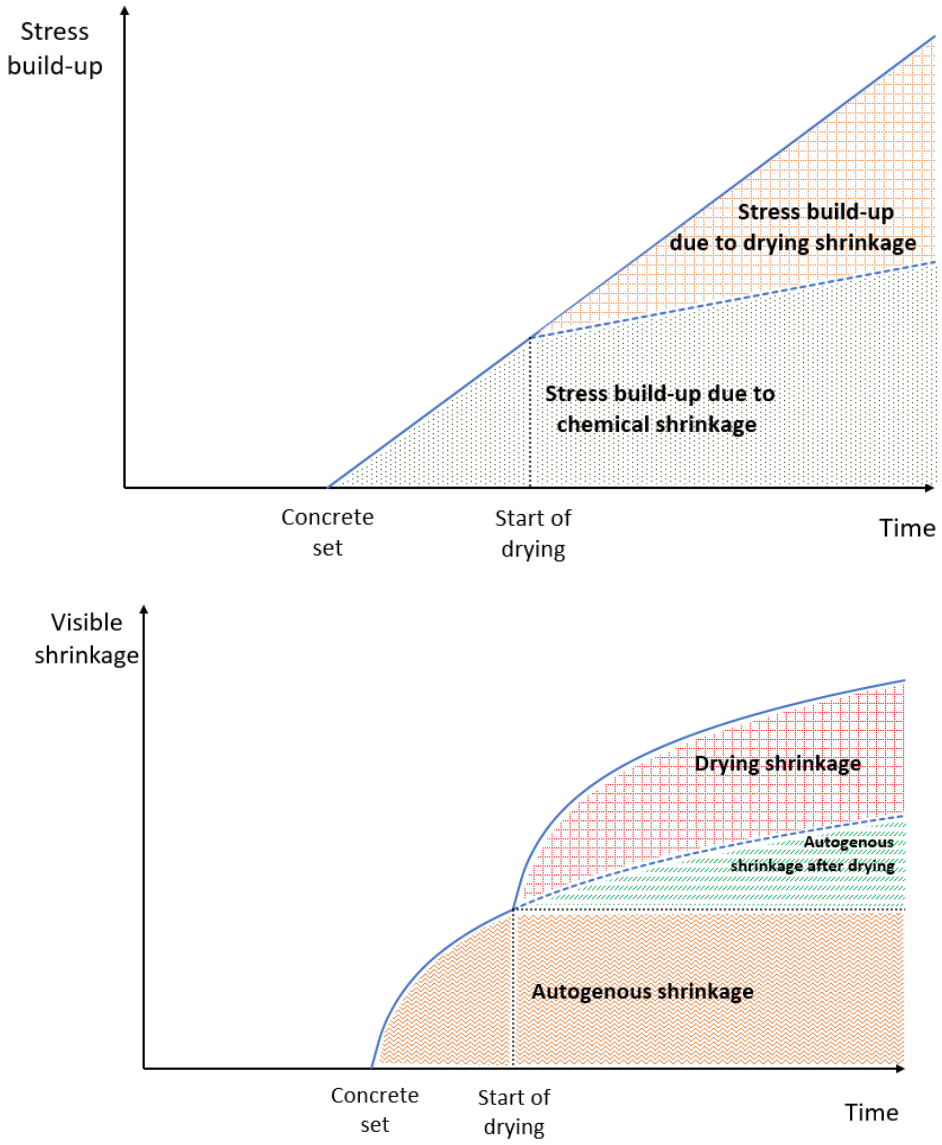

Figure 4. Schematic diagram of the relationship between concrete shrinkage and stress build-up at the early ages

2.1.4 Issues Associated with Concrete Shrinkage and Cracking

Premature cracking of bridge decks has been a major problem in the United States at the nationwide level for decades. It is not uncommon to observe surface cracks as early as two months after the construction. Many reports identify early-age shrinkage of concrete as one of the driving factors of crack development (Rettner et al., 2014; MNDOT, 2011).

The development of cracks in concrete leads to faster deterioration of the structure by means of rapid transport of contaminants, such as chloride from deicing salts, from the surface to the reinforcement. Corroding reinforcement expands, which results in more cracks, and subsequently, accelerated deterioration. According to Lindquist et al. (2006), the corrosion level of the bridge deck reinforcement could start to exceed the acceptable limit in less than a year in case of a local crack, whereas the chloride content at non-cracked regions rarely exceeds even the conservative levels. However, most importantly, the research group, which studied three different types of bridge decks: monolithic bridge decks and decks with two different types of overlays, identified that the presence of overlay does not have a major impact on the chloride content in the concrete (Lindquist, 2006). In other words, the current reactive measure of cracking treatment is not as efficient as it should be. It seems that the bridge deck cracking issue should be treated in a proactive way. One of the measures to address early-age shrinkage of concrete includes the internal curing of concrete.

2.2 Mechanism of Internal Curing

According to American Concrete Institute (ACI): "*Internal curing refers to the process by which the hydration of cement occurs because of the availability of additional internal water that is not part of the mixing water*" (ACI Committee 308-213, 2013). Unlike traditional curing method, in which water is mostly supplied from outside sources, such as burlaps and fogging, internal water is generally supplied via internal reservoirs, such as saturated lightweight fine aggregates (LWFA), superabsorbent polymers (SAP), saturated wood fibers, or saturated crushed (returned) concrete aggregates. By replacing a portion of the conventional fine aggregate in the mixture with LWFA, internal curing can be induced by moisture that is provided from the concrete mix for later-stage cement hydration over time. As shown in Figure 5, high relative humidity can be maintained within the pore structure of concrete, which could reduce shrinkage, extend hydration, and increase strength and durability performance.

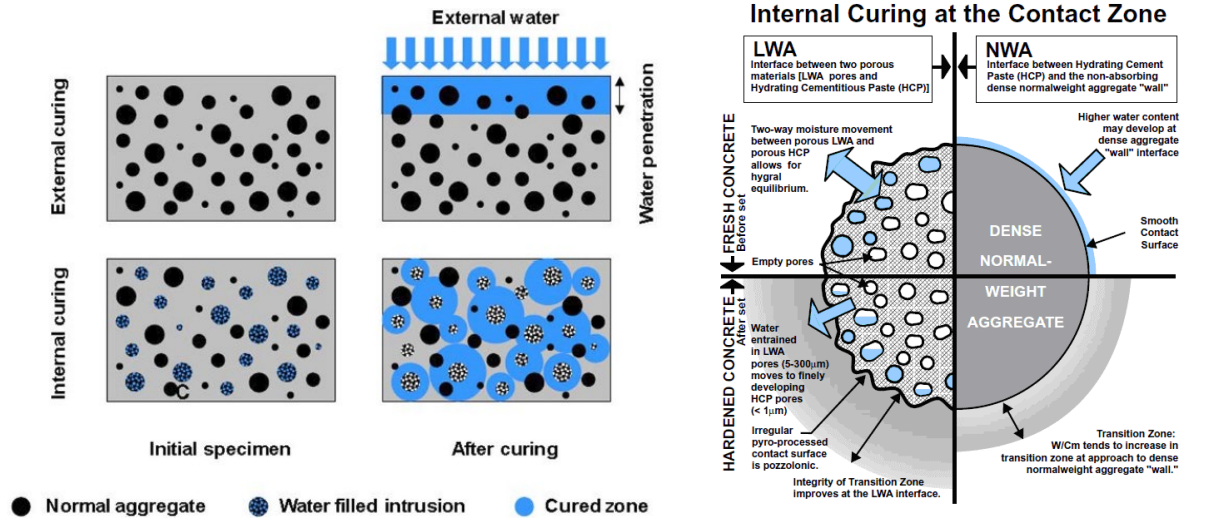

(a) Mechanism (b) Aggregates and interfacial transition zone

Figure 5. Schematic illustration of the mechanism of internal curing
(adapted from Expanded Shale, Clay and Slate Institute; Arcosa Lightweight)

Theoretically, water supplied by internal curing is intended to compensate for the difference between chemical and after-set autogenous shrinkage (Henkensiefken et al., 2009). However, in practice, the ignorance of shrinkage before the concrete set is an insignificant correction, which is challenging to measure. Instead, it is more feasible to assume the volume of total chemical shrinkage as a required volume of internal curing water (Schlitter et al., 2010). Thus, the effect of internal curing minimizes the conventional stress build-up and shrinkage, as shown in Figure 4, to the levels illustrated in Figure 6.

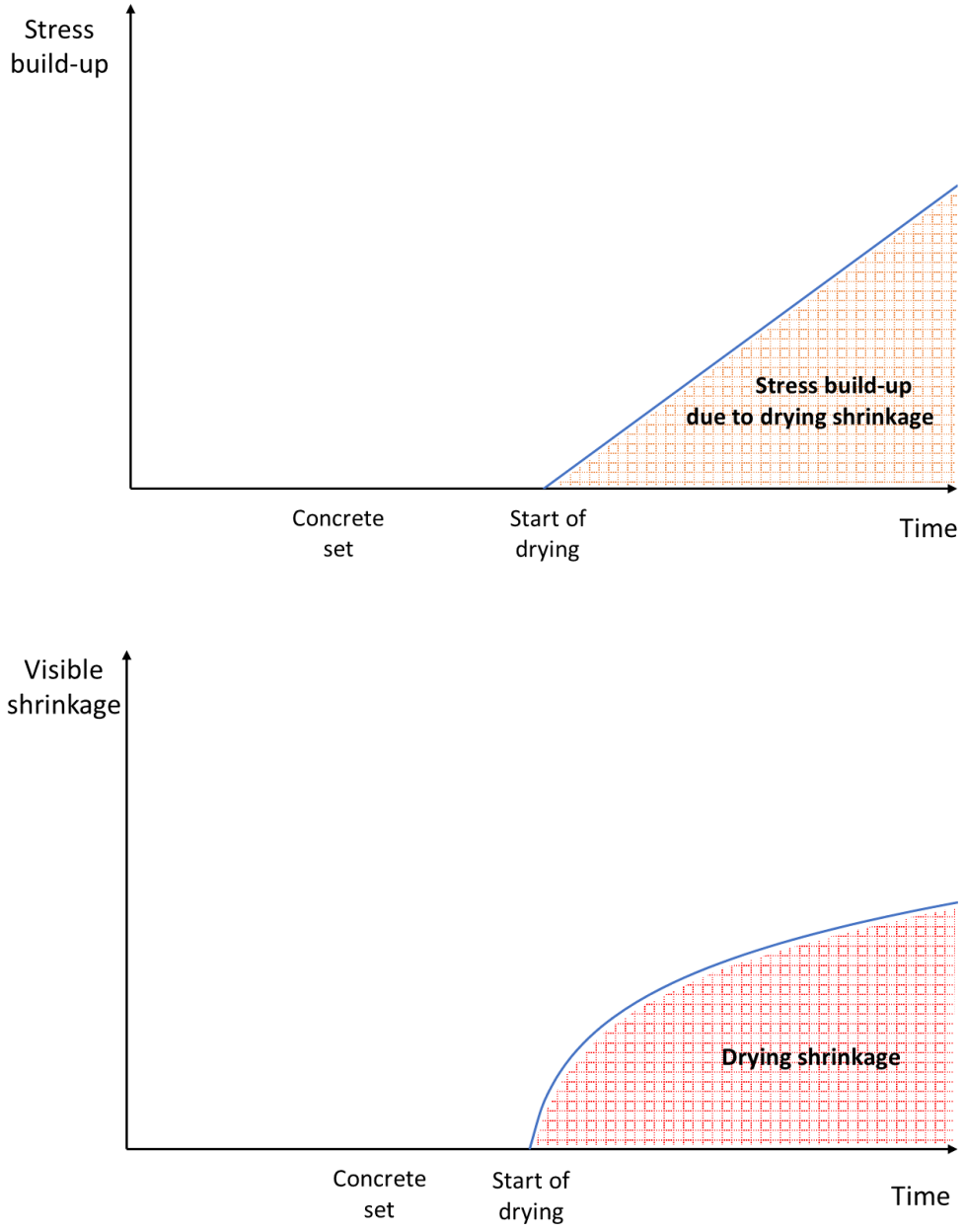

Figure 6. Schematic diagram of the relationship between concrete shrinkage and stress build-up at the early ages with internal curing

As exemplified in Figure 7, several studies have demonstrated that internal curing can provide better concrete performance in various ways. Firstly, mortar with presoaked LWFA at a dosage rate higher than 14.3% by volume experienced little autogenous shrinkage and lesser drying shrinkage compared to the control specimen, which is illustrated in Figure 7a and Figure 7c respectively. Furthermore, delayed cracking age from the restrained shrinkage test with the same mortar mixes may be observed in Figure 7b. Finally, another study revealed higher electrical resistivity of internally cured concrete compared to the plain mix at the later ages, which is illustrated in Figure 7d. All the findings indicate that internal curing contributes to mitigating chemical shrinkage, reducing self-desiccation, and improving cement hydration, which in turn minimizes the harmful effect of previously discussed issues associated with concrete shrinkage. As a result, reduced early-age cracking, higher concrete strength and stiffness, and reduced permeability and rebar corrosion are obtained by introducing internal curing to the concrete.

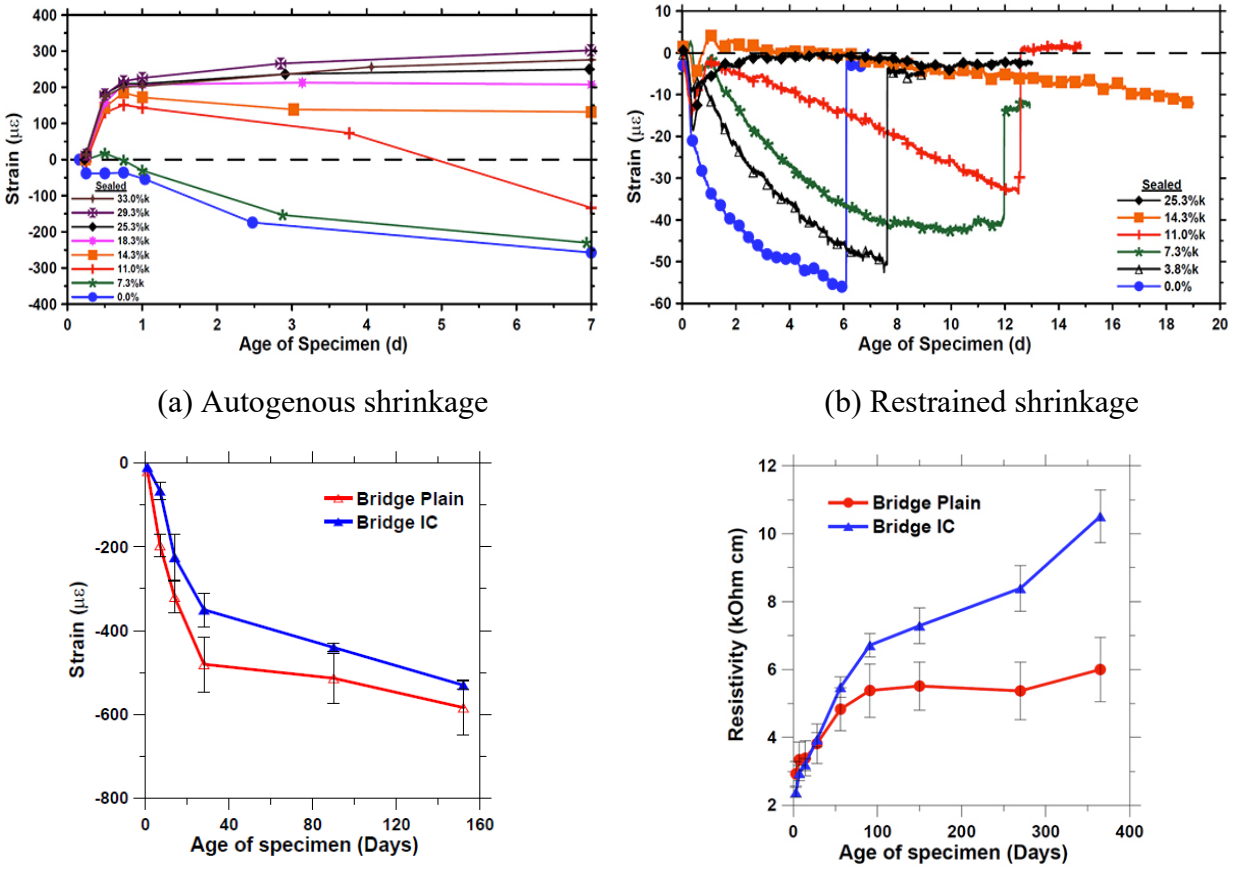

(a) Autogenous shrinkage

(b) Restrained shrinkage

(c) Drying shrinkage

(d) Electrical resistivity

Figure 7. Benefits of internal curing on various concrete properties
(adapted from Schlitter et al., 2010; Di Bella et al., 2012)

2.3 DOT Experience of Internal Curing

Internal curing of concrete is not a new concept. In recent years, several states have examined the internal curing efficiency of concrete bridge decks to address the early-age cracking. In 2009, Kansas DOT led a research project, which evaluated the impact of internal curing on low-cracking high-performance concrete (Reynolds et al., 2009). In 2010, Indiana DOT worked on the

development of internally cured pavement concrete and assessment of its mechanical, shrinkage, and durability properties (Schlitter et al., 2010). Five years later, Indiana DOT documented the construction of four internally cured bridge decks, which applied findings of the previously mentioned study. The report provides a comparison of mechanical, shrinkage, and durability properties of internally cured and reference mixtures (Barrett et al., 2015). In 2012, a research team from Purdue University conducted a full-scale field study to compare the performance of two bridge decks, one of which utilized the concept of internal curing (Di Bella et al., 2012). In 2014, Colorado DOT funded a research project, which enhanced CDOT bridge deck mixtures with internal curing and studied its mechanical, shrinkage, and transport properties with a particular focus on freeze-thaw resistance (Jones et al., 2014). In 2015, New York State DOT summarized its positive experience on internally cured bridge decks, which were constructed several years prior to paper publication (Streeter et al.). In 2016, Louisiana DOTD published a report on laboratory and field evaluation of internally cured bridge deck concrete (Rupnow et al., 2016). In 2017, Iowa DOT investigated both laboratory and field performance of internally cured pavement concrete for the purpose of increasing joint spacing (Vosoughi et al., 2017). The following sections cover some of the essential details of each project, such as the materials used and their physical properties. In order to avoid confusion, each project report or paper was given an identification number (ID), which is comprised of an abbreviation of a governing agency and year published, and hereinafter will be referred by their respective IDs. Table 1 provides a summary of project IDs, their main purposes, and respective report codes.

Table 1. List of projects focused on internal curing of bridge deck concrete

ID	Governing/ Leading Agency	Year published	Project Objectives	Reference
ODOT-2007	Ohio DOT	2007	Evaluate the impact of high absorptive materials on cracking tendencies	Delatte et al., 2007
KDOT-09	Kansas DOT	2009	Evaluate the potential of LWA to be used as an internal curing aggregate in high-performance concrete	Reynolds et al., 2009
INDOT-10	Indiana DOT	2010	Develop an internally cured concrete to be used in bridge decks	Schlitter et al., 2010
PURDUE-12	Purdue University	2012	Evaluate and compare plain and internally cured concrete bridge decks	Di Bella et al., 2012
UDOT-13	Utah DOT	2013	Evaluate deck performance in terms of early-age cracking with distress surveys	Guthrie and Stevens, 2013
ORDOT-13	Oregon DOT	2013	Evaluate long-term drying shrinkage performance with internal curing and shrinkage reducing admixtures	Ideker et al., 2013
AKDOT-14	Arkansas DOT	2014	Evaluate the performance of concrete with two types of coarse LWA	Goad et al., 2014
CDOT-14	Colorado DOT	2014	Evaluate laboratory performance of internally cured bridge deck concrete	Jones et al., 2014
INDOT-15	Indiana DOT	2015	Implement findings of KDOT-09 and evaluate the performance of internally cured full-scale bridge decks	Barrett et al., 2015
FLDOT-2015	Florida DOT	2015	Evaluate performance and usability of internally cured concrete for both bridge decks and concrete pavement slabs	Tia et al., 2015
NYSDOT-15	New York State DOT	2015	Inspect internally cured bridge decks and summarize their performance	Streeter et al. 2015
LADOTD-16	Louisiana DOTD	2016	Evaluate laboratory and field performance of internally cured bridge deck concrete	Rupnow et al., 2016
IADOT-17	Iowa DOT	2017	Evaluate laboratory and field performance of internally cured pavement concrete	Vosoughi et al., 2017
NCDOT-19	North Carolina DOT	2019	Evaluate shrinkage and permeability of internally cured concrete and performance of bridge deck with internally cured concrete	Cavalline et al., 2019

2.4 Materials for Internal Curing

2.4.1 General Material Requirement and Selection

The primary principle behind the internal curing of concrete lies in water reservoirs, which are preserved in the concrete matrix and supply additional water during ongoing hydration of cementitious materials. Jensen and Lura (2006) claimed that successful internal curing requires

water to be readily available both thermodynamically and kinematically after the final set has occurred. Thermodynamic availability refers to the activity of absorbed water, which should be close to 1.0. Kinematic availability refers to both uniform and effective spatial distribution of water reservoirs and the ability of water to transport to the surrounding matrix when its relative humidity starts to decrease (Jensen and Lura, 2006). In 2013, the American Concrete Institute published a report, ACI 308-213 R-13 (ACI 308, 2013), on internally cured concrete. At that time, due to a lack of studies, there were no specific guidelines on the physical properties of lightweight aggregates. Thus, the report has covered a limited part on material selection, stating that lightweight aggregates should:

1. Not reduce the compressive strength of mortar;
2. Not break down during mixing action;
3. Provide water to the surrounding matrix during early plastic state;
4. Provide enough water for continuous cement hydration;
5. Be compatible with replacing aggregate in terms of gradation;

Many materials possess the required properties mentioned previously, such as LWFA, SAP, pumice, zeolite, perlite, and recycled aggregates. Out of them, only the former two were commonly used due to their availability, extensively studied, and evaluated as potential internal curing agents during the last decade (Liu et al., 2017). The main disadvantage found for the SAP is that they tend to significantly decrease in volume during water desorption, which leaves air voids inside the concrete matrix and may negatively affect its mechanical properties (Liu et al., 2017; Jones et al., 2014). As a result, it led to the complete dominance of LWFA for internally cured concrete at the current construction market.

American Society for Testing and Materials (ASTM) has also published a standard (ASTM C1761) entitled "Standard Specification for Lightweight Aggregate for Internal Curing of Concrete" (ASTM 2017), which covers two types of aggregates: expanded and processed. The main physical properties for fine aggregates required by the standard are shown in Table 2. Gradation requirements are illustrated later in Table 4.

Table 2. ASTM C1761 requirements on lightweight aggregates for internal curing

Maximum Dry Loose Bulk Density (pcf)	70
Minimum 72-hr Water Absorption (%)	5
Minimum Desorption at 94% RH (%)	85

Construction practices and research trends show that expanded lightweight aggregates, namely expanded shale, clay, and slate, are currently the most appropriate choice for internal curing and are available nationwide. They can absorb up to 25% of water by mass, and proven to effectively reduce early-age cracking of concrete decks (Henkensiefken et al., 2009). Table 3 summarizes the physical properties of internal curing materials utilized in documented DOT projects. It can be clearly seen that expanded lightweight fine aggregates are the most widely used materials for internal curing.

Table 3. Physical properties of LWFAs utilized in the projects

Project ID	Type of LWFA	Absorption (%)	Fineness Modulus	Specific Gravity	
				App	SSD
KDOT-09	Expanded shale	16.0	N/A	N/A	1.15
	Expanded shale	16.0	N/A	N/A	1.15
	Expanded shale	16.0	N/A	N/A	1.15
INDOT-10	Expanded shale	10.5	3.10	1.56	N/A
	Expanded shale	5.8	3.10	1.56	N/A
	Crushed concrete aggregate	9.8	N/A	N/A	N/A
INDOT-15	Expanded shale	15-20	N/A	N/A	1.75
PURDUE-12	Expanded shale	10.4	N/A	N/A	1.56
CDOT-14	Expanded LWFA	16.5	N/A	N/A	1.85
	Expanded LWFA	16.5	N/A	N/A	1.65
	Expanded LWFA	18.8	N/A	N/A	1.87
NYSDOT-15	Expanded LWFA	19.0	N/A	N/A	N/A
LADOTD-16	Expanded clay	N/A	N/A	N/A	N/A
IDOT-17	Expanded clay	22.2	N/A	N/A	1.23

Table 4 illustrates the gradation of materials used in projects listed in Table 3. As can be seen, preference is given to fine aggregates ranging mostly from No.4 to No.100 in size.

Table 4. Gradation of LWFAs utilized in the projects

Project ID	Gradation (% Passing)							
	3/8”	No.4	No.8	No.16	No.30	No.50	No.100	No.200
ASTM C1761	100	65-100	N/A	15-80	N/A	0-35	0-25	N/A
KDOT-09	100	95.51	69.81	33.3	16.15	7.05	3.37	1.84
	100	76.62	2.89	1.69	1.58	1.38	0.99	0.58
	100	77.9	2.04	0.57	0.49	0.47	0.45	0.41
INDOT-10	100	100	85-90	60-70	35-40	15-25	10-15	0-5
	100	100	80-85	55-65	35-40	15-25	10-15	0-5
	N/A	N/A	N/A	N/A	N/A	N/A	N/A	N/A
INDOT-15	N/A	N/A	N/A	N/A	N/A	N/A	N/A	N/A
PURDUE-12	N/A	N/A	N/A	N/A	N/A	N/A	N/A	N/A
CDOT-14	N/A	N/A	N/A	N/A	N/A	N/A	N/A	N/A
	N/A	N/A	N/A	N/A	N/A	N/A	N/A	N/A
	N/A	N/A	N/A	N/A	N/A	N/A	N/A	N/A
NYSDOT-15	N/A	N/A	N/A	N/A	N/A	N/A	N/A	N/A
LaDOTD-16	N/A	N/A	N/A	N/A	N/A	N/A	N/A	N/A
IDOT-17	100	100	80-85	50-60	20-30	10-15	0-5	0-2

Figure 8 further illustrates the gradation of those materials in a graphic version. Also, it should be noted that little attention was given to control the overall fineness modulus and gradation of aggregates. Since combined aggregate gradation is changed, both fresh and mechanical properties might directly be affected by the replacement of fine aggregates. Combined aggregate gradation will be one of the topics addressed in this study.

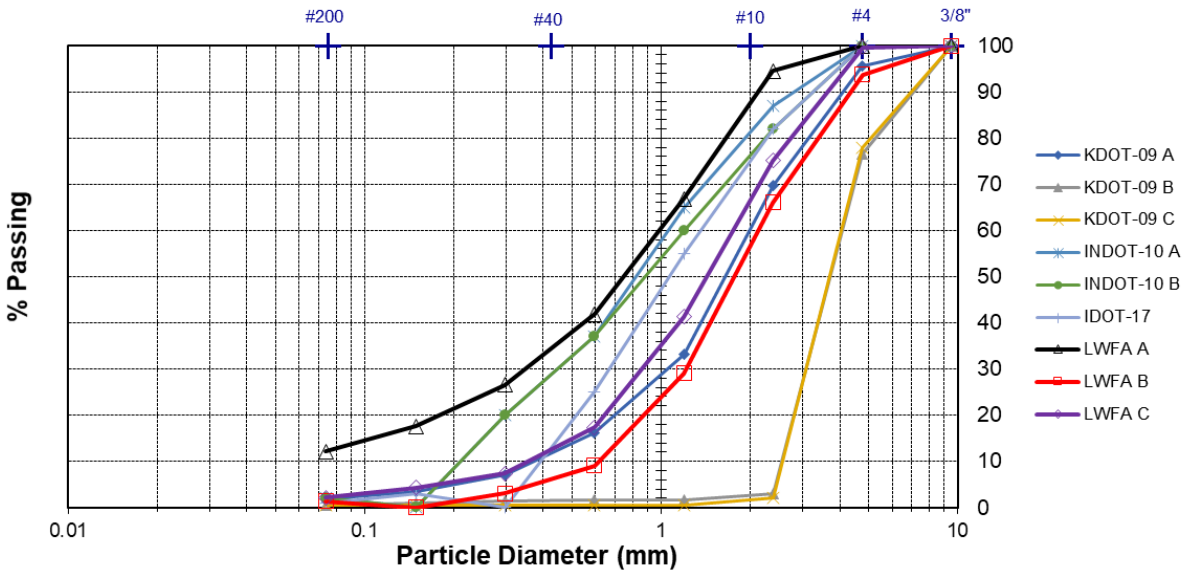

Figure 8. Gradation of materials used in documented DOT internal curing studies compared to materials used in this study

2.4.2 LWFA Test Methods

The majority of the tests on physical properties of LWFAs, such as absorption capacity, desorption value, and specific gravity, require the material to be in a saturated surface-dry (SSD) condition. This state can be achieved relatively easily for the normal fine aggregate or coarse lightweight aggregate using standard test procedures. However, a certain degree of difficulty can be experienced with LWFA. This section covers several methods for bringing LWFA to SSD condition.

2.4.2.1 "Brown Paper Towel" Method

The following test method is implemented and approved by NYSDOT and outlined in ASTM C1761 (NY 703-19 E, 2008; ASTM 2017). As the test title implies, paper towels are used to wipe fine aggregates in order to remove surface water, which is illustrated in Figure 9. After the aggregates were soaked with water, and the top layer of free water was decanted, a sample representative is taken and placed on top of several layers of paper towels. Then, an operator should pat and stir the aggregates with dry paper towels as quickly as possible and ensuring that no aggregates are lost. If the bottom paper towels are wet and cannot absorb more water, they should be carefully replaced. The patting and stirring procedure can be stopped when moisture is no longer observed on the paper towels, meaning that aggregates were finally brought to SSD condition.

Figure 9. The process of bringing LWFA to SSD condition by a brown paper towel method

Even though the "brown paper towel" test method is standardized, the human factor plays a key role in the procedure. In addition, a significant part of the fine aggregates might be lost during patting and stirring. Finally, several studies concluded that the test method might take up to one hour and is not repeatable, and may result in ranging values (Miller, 2014).

2.4.2.2 Centrifuge Method

In 2014, Miller proposed utilizing a centrifuge method for bringing fine aggregates to SSD condition. The example of centrifuge equipment can be seen in Figure 10. In his extensive research, he utilizes a similar concept described in ACI 211.2 (1990) for lightweight coarse aggregates. A sample of wet fine aggregates are placed in a centrifuge, where the surface water is removed by the action of centrifugal force (Miller, 2014)

This method is believed not only to eliminate a human factor present in "brown paper towel" method, but also to significantly reduce procedure duration down to 15 minutes and provide repeatable results. However, the absorption capacity value is highly influenced by both rotation speed and duration, which should be carefully chosen and remain identical throughout the whole research study (Miller, 2014). In order to be able to compare test results from different studies, this test method needs to be standardized.

Figure 10. A typical centrifuge setup
(Miller, 2014)

2.4.2.3 ASTM C128 Method

ASTM C128 (2015) is the standard test method for the relative density and absorption capacity of fine aggregates. After soaking period, it requires a sample of wet fine aggregates to be placed on a non-absorbent surface and to be exposed to a flow of gentle warm air, which can be produced by a commercially available hairdryer as shown in Figure 11a. At the same time, aggregates should be stirred and tumbled to accelerate the drying process. When fine aggregates reach a free-flowing condition, a small cone mold should be filled with fine aggregates and lifted. Slump flow will indicate that the aggregates reached SSD condition (see Figure 11b). Otherwise, if the aggregates retain the shape of a mold, the drying procedure should be further continued.

(a) Bringing aggregates to SSD condition (b) Cone mold for examing moisture condition of LWFA

Figure 11. Water absorption test by ASTM C128 method

There are several problems associated with this test method utilized for LWFA. Firstly, after some period of drying, a portion of fine aggregates may become airborne and can be easily lost due to airflow (Reynolds et al., 2009). Secondly, the test method is time-consuming and may take up to one hour for LWFA. Finally, since the human factor is also present, it is easy to over-dry or under-dry fine aggregates.

2.5 Mix design of IC Concrete

2.5.1 Mix Proportioning Methods of Internal Curing

Since the main principle behind internal curing is to provide water to compensate for the water lost due to chemical shrinkage of cement paste, the amount of additional required curing water is a function of cement content. Bentz et al. (Bentz and Snyder, 1999; Bentz et al., 2005) proposed an equation for calculating the amount of LWFA needed to compensate water loss, which is as follows:

$$\mathbf{M_{LWA}} = \frac{\mathbf{c_f \times cs \times \alpha_{max}}}{\mathbf{s \times \phi_{LWA}}} \qquad \textbf{(Eq. 1)}$$

where:

M_{LWA} is dry mass of LWFA needed in the mix design (lb/yd^3)
c_f is the cement content in the mix design (lb/yd^3)

cs is chemical shrinkage coefficient of cement (lb of water/lb of cement)

α_{max} is the degree of cement hydration (unitless)

s is the degree of LWFA saturation (0-1, where the value of 1 corresponds to complete saturation)

ϕ_{LWA} is LWFA water absorption (lb of water/lb of dry LWFA)

Equation 1, also known as the Bentz equation, was used as a basis for mix design and proportion in all of the covered projects from Table 1, except for LADOTD-16, where standard aggregate replacement values were chosen.

It has been reported that the Bentz equation (Eq. 1) overlooks several details. Firstly, the absorption capacity of LWFA varies with the duration of soaking. For example, a difference between 24hr and 72hr water absorption might be up to several percents. Thus, it is important that soaking time is the same for both water absorption tests and concrete mixtures. Secondly, the desorption of LWFA is overlooked in the equation. At a relative humidity of 94%, it is uncommon that the aggregates release only a part of absorbed water with the other part remaining inside of the aggregate (Castro, 2011).

Castro (2011) modified the Bentz equation to address the time-dependent parameter of water absorption and include the desorption value of LWFA. This equation (Eq. 2) will be utilized as a basis for mix proportioning in the study:

$$\mathbf{M_{LWA}} = \frac{\mathbf{c_f \times cs \times \alpha_{max}}}{\mathbf{t^A \times \phi_{LWA,24hr} \times \psi}} \qquad \textbf{(Eq. 2)}$$

where:

t^A is time-dependent coefficient normalized for 24-hour water absorption

$\phi_{LWA,24\text{hr}}$ is LWFA water absorption at 24 hours (lb of water/lb of dry LWFA)

Ψ is desorption coefficient, or the fraction of total water released at 94% RH (unitless)

There are still some issues, which the modified Bentz ignores. Firstly, the equation assumes that all of the water provided by the internal curing agents will be used towards hydration. In other words, the equation does not account for the water, which might be lost during concrete production and drying.

Secondly, no attention is given to the gradation of the fine aggregates and combined aggregate. In most cases, LWFA is finer compared to natural fine aggregates. In these cases, issues might arise with the replacement of fine aggregates. For example, Iowa DOT reported a slight reduction in workability with the introduction of internal curing aggregates. Furthermore, the state of Nebraska utilizes sand and gravel as fine aggregates, which is much coarser than most of the LWFA. A plain replacement of aggregates by volume without addressing the gradation may disturb the overall aggregate blend gradation, as well as aggregate packing, which may lead to potential workability issues.

2.5.2 Examples of Internal Curing Concrete Mix Design

Table 5 provides an overview of concrete mix designs evaluated by other DOT studies. It should be noted that most studies evaluated the effect of the calculated amount of LWFA based on the Bentz equation (Eq. 1), and some studies replaced fine aggregates by the fixed amount based on their experience. With regard to the limitations mentioned previously, only a few studies tried to study different replacement rates of LWFA. Furthermore, some of the studies determined the

amount of LWFA based on the rule of thumb with no explanation to support the decision. Also, no attention was given to overall aggregate blend gradation.

Table 5. Concrete mix designs published in DOT studies

ID	w/b	Replacement of FA (%)	Cement (pcy)	Fly Ash (pcy)	Silica Fume (pcy)	Slag (pcy)	Water (pcy)	CA (pcy)	FA (pcy)	LWFA (pcy)
IDOT-17	0.45	20	457	114	0	0	257	1698	942	200
LaDOTD-16	0.35	5, 10, 15	600	0	0	0	210	2031	819	291
NYSDOT-15	0.40	30	500	135	40	0	270	N/A	N/A	N/A
INDOT-15	0.40	N/A	435	115	25	0	228	1740	825	340
CDOT-14	N/A	N/A	N/A	N/A	N/A	N/A	N/A	N/A	N/A	N/A
PURDUE-12	0.39	57	657	0	0	0	256	1763	528	455
INDOT-10	0.30	21	1091	0	0	0	327	1168	598	564
KDOT-09	0.44	8.4	384	0	0	149	234	1807	923	195

2.5.3 Mix Design Adjustment and Optimization Methods

Concrete is a complex material, where aggregates of various shapes, sizes, and specific gravities make up the basis of the final product. The proportions of each aggregate, their combined gradation and packing density, as well as fineness modulus have a direct impact on many concrete properties, such as workability. Disturbing the aggregate blend by plain replacement of fine aggregates may cause workability issues. For instance, a slight decrease of workability was reported by Iowa DOT in their field project, when sand was replaced by LWFA (Vosoughi et al., 2017). For the case of Nebraska, the situation might be even more severe since Nebraska utilizes sand and gravel as fine aggregates, which are generally coarser.

Throughout this particular study, the need for aggregate optimization for better workability was identified. The research team decided to overcome this issue by investigating the two following approaches:

1. General adjustment method. The workability of the mixes was improved by the addition of water-reducing admixtures.
2. Aggregate blend optimization. As the replacement of sand and gravel by finer lightweight aggregates disturbs the overall gradation of the blend and leads to lower workability, this approach will modify the blend proportions of the aggregates based on experimental void content tests, which were also compared to theoretical and empirical particle packing models.

This section will describe various aggregate packing theories and models, which will be utilized in the project to obtain the optimum blend proportions.

In the Modified Toufar Model, the packing density, ϕ, and characteristic diameter, d_{char}, of each material are used to calculate the packing densities of particle combinations (Goltermann et al., 1997). For multi-particle calculations, the model is used firstly to calculate the d_{char}, and ϕ of the combination of the two materials. Next, the model is used to integrate this initial combination with the next constituent material, and the process is repeated until all materials have been included and the resulting overall packing density of the mix has been calculated. Combined packing degree of the binary blend is estimated with the following equation:

$$\Phi = \frac{1}{[\frac{V_1}{\varphi_1}+\frac{V_2}{\varphi_2}-V_2(\frac{1}{\varphi_2}-1)k_d k_s} \quad \textbf{(Eq. 3)}$$

where $$k_d = \frac{d_2-d_1}{d_2+d_1} \quad \textbf{(Eq. 4)}$$

$$k_s = (\frac{x}{x_0}) \times k_0 \text{ for } x < x_0 \quad \textbf{(Eq. 5)}$$

$$k_s = 1 - \frac{(1+4x)}{(1+x)^4} \text{ for } x > x_0 \quad \textbf{(Eq. 6)}$$

where V_1, V_2 and ϕ_1, ϕ_2 are the aggregate fractions by volume and packing degrees of each aggregate respectively, k_d is a diameter ratio factor, k_s is a statistical factor, x_0=0.4753, k_0=0.3881, and $x = \frac{(\frac{V_1}{V_2})\times(\frac{\varphi_1}{\varphi_2})}{(1-\varphi_2)}$.

The Modified Toufar Model was utilized in the research project, the main aim of which was to optimize the pavement concrete in the state of Nebraska for better workability and performance. The research team of the project conducted an extensive study on various theoretical particle packing theories and concluded that the Modified Toufar Model is the most suitable for the pavement concrete, which was optimized (Mamirov, 2019).

In Dewar's model, the voids ratio, U, and the log mean size, d_m of each single material are used to calculate the voids ratio of a particular combination of materials (Dewar, 1999). For multi-particle calculations, a similar stepwise process, as described above, is used, except that it is a requirement of the Dewar method that the combination process should start from the finest two materials before the next coarser material can be added. The relationship between ϕ and U is as follows:

$$\varphi = \frac{1}{U+1} \quad \textbf{(Eq. 7)}$$

In 1960s, a standard combined gradation graph was issued by the Federal Highway Administration. It yields the linear line of the highest density of the blend based on the maximum aggregate size. The graph, which is commonly known as the 0.45 power graph, has been used in aggregate gradation control in the hot mix asphalt industry for decades (Roberts et al., 1996). Figure 12 illustrates the examples of the chart for different maximum aggregate sizes.

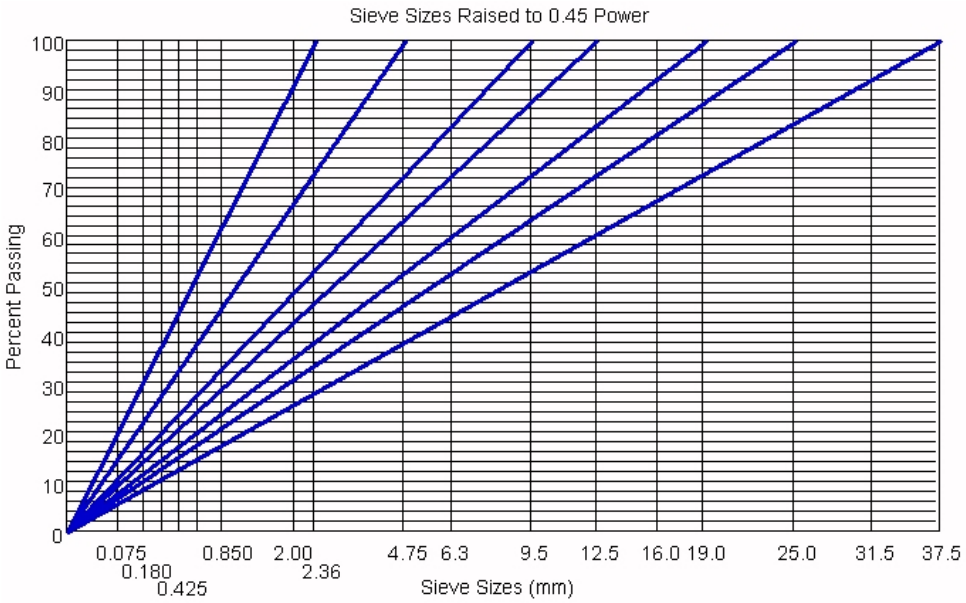

Figure 12. Maximum density curves for 0.45 power gradation graph for a different maximum aggregate size (adapted from Pavement Interactive, 2019)

Tarantula Curve is an empirical method to proportion aggregate content developed by Ley et al. (2012) after comparing the workability of the mixtures with different gradations using the Box test. As illustrated in Figure 13, Tarantula Curve includes boundary limits on an individual percent retained chart, and provides recommendations for the amount of coarse sand to provide appropriate cohesion and the amount of fine sand to provide adequate workability.

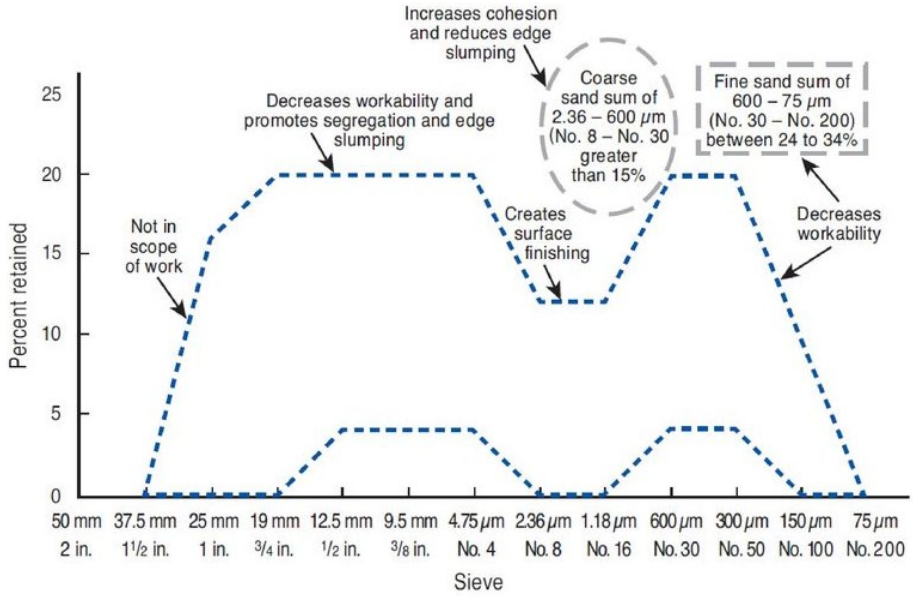

Figure 13. Tarantula curve (adapted from Ley et al, 2012)

2.6 Properties of IC Concrete

The following section covers the effect of internal curing on various concrete properties, which were reported in other DOT studies. Each subsection covers the impact of internal curing on a specific property.

2.6.1 Fresh Concrete Properties

No major issues associated with the workability of concrete mixes were reported in most of the studies. However, as mentioned before, Iowa DOT experienced a slight reduction in workability, which was successfully addressed by a higher dosage of high-range water reducer.

No major issues associated with the air content of the concrete mixes were reported in any of the studies. The air contents of the mixes varied from 2% to 8%, which satisfied the local state requirements.

In all cases, as it is expected, the fresh unit weight of concrete drops with the introduction of lightweight aggregates, which can reach up to 10%. However, most reports claim that the reduction of unit weight is insignificant, and the concrete still remains in the category of "normal-weight" concrete.

2.6.2 Mechanical Properties

Other DOT studies on internal curing report either a slight improvement or no change in compressive strength of concrete with LWFA. Colorado DOT, Indiana DOT, and New York State DOT reported up to 13%, 12%, and 4.6% increase of the compressive strength, respectively, with lightweight aggregates. Furthermore, Louisiana DOT experienced the same or slightly higher compressive strength for the case of internally cured concrete (Rupnow et al., 2016). Finally, some studies, such as Iowa DOT and Kansas DOT, claimed either no change or slight reduction in the compressive strength of the mixes (Vosoughi et al, 2017; Reynolds et al., 2009).

With regards to the modulus of elasticity, Colorado DOT, Iowa DOT, and Louisiana DOT all reported a 10-20% reduction in their studies. The following findings are supported by several studies, which claim that "softer" lightweight aggregates will eventually lead to the lower modulus of elasticity (Schlitter et al., 2010; Raoufi et al., 2011).

2.6.3 Volume stability and Cracking

In general, all studies on internal curing identified lower shrinkage for internally cured specimens in the cases of autogenous shrinkage and restrained shrinkage.

The findings of Kansas DOT (Reynolds et al., 2009)project indicate a reduction of free shrinkage for the majority of internally cured specimens. Among slag-free mixes, the most effective behavior in terms of free shrinkage was shown by a 14-day cured mix with the highest replacement of LWFA, 64% by volume of the pea gravel. 30-day and 90-day free shrinkage values of the mix were estimated as 220 με and 347 με respectively, compared to 313 με and 410 με of the plain mix.

Indiana DOT (Schlitter et al., 2012) reports a significant reduction, and sometimes complete elimination, of autogenous shrinkage of concrete. A reduction in plastic shrinkage cracking was also observed. The internal curing of concrete resulted in lower cracking potential in large scale tests as well.

Colorado DOT (Jones et al., 2014) signifies a reduction in autogenous and drying shrinkage as well as expansion in a sealed environment. The improvement in restrained shrinkage is more noticeable in mixtures with lower w/c.

2.6.4 Durability

Most studies provide promising findings on the durability of internally cured concrete, which at least is comparable compared to the control mix.

Both Indiana DOT (Schlitter et al., 2010) and Iowa DOT (Vosoughi et al., 2017) experienced the same trend with the surface resistivity of the concrete. At the very early ages, the surface resistivity of internally cured concrete was found to be either lower or almost the same compared to control ones. However, after 28 to 56 days, the resistivity of internally cured concrete becomes higher. The reason behind the trend might be explained by the presence of saturated aggregates at an early age, which lowers resistivity (Di Bella et al., 2012). As time passes, water desorbs from the aggregates and hydrates the surrounding cement particles, which improves the resistivity of the concrete.

Furthermore, Colorado DOT (Jones et al., 2014) reported that with properly air entrainment, internally cured concrete should have sufficient resistance to freeze-thaw cycles. However, overdosage of LWFA, i.e., mixtures that have more prewetted LWFA than needed, could potentially have freeze-thaw resistance concerns. In addition, internally cured concrete showed scaling resistance, which was comparable to those of control mixes. Next, the study identified the reduction in chloride diffusion coefficient and permeability due to improved hydration.

Finally, Indiana DOT (Barrett et al., 2015) paid close attention to various chloride transportation tests, such as rapid chloride penetration test, surface resistivity, rapid chloride migration test, migration cell, and chloride ponding and profiling in their study. Their results indicated better performance of internally cured concrete in all of the tests above.

2.7 Construction Practice of Internally Cured Concrete

2.7.1 Field Handling of Lightweight Fine Aggregates

LWFAs require continuous water supply prior to batching, which might be a difficult task in the field due to the physical nature of the material. New York DOT project implemented the same concept of prewetting coarse aggregates for fine aggregates (Streeter et al. 2015). Stockpiles for LWFA were constructed, where a sprinkler system continuously provided water for at least 48 hours, or until the absorbed moisture content of LWFA reached the required value. After the prewetting process is done, stockpiles were drained of excess water for 12 to 15 hours. At the end of the draining, LWFAs were immediately used in batching. The prewetting duration of stockpiles was determined based on the time-dependent absorption capacity of LWFAs. It was determined that most water was absorbed in the first 24 hours with a little further difference. A 48 hours of the prewetting period was established, taking safety factor into account. In addition, stockpiles were turned several times during the prewetting period for uniform soaking of aggregates (Streeter et al. 2015).

The same method and procedures for prewetting LWFAs prior to batching are outlined in the Guide Specification for Internally Curing Concrete (Weiss and Montanari, 2017).

2.7.2 Mixing Procedure

New York State DOT (Streeter et al., 2015) implied that no differences in batching were needed to accommodate internally cured concrete. The LWFA was batched first, followed by the fine aggregate, coarse aggregate, admixtures, cement, pozzolan, microsilica, and remaining mixing water and then mixed completely.

Furthermore, no major adjustments for the mixing procedure were introduced in the study conducted by Purdue University research group (Di Bella et al. 2012). The coarse and fine

aggregate were first placed in the pan mixer. Water was then added to the mixture (along with lightweight aggregate in the case of the internally cured mixture). Cement and admixtures were then added. After all the materials were placed in the mixer, they were mixed in accordance with ASTM C192 (ASTM 2007).

Colorado DOT (Jones et al., 2014) implemented the following mixing procedure. The fine and coarse aggregates were first combined in a "buttered" mixer, adding a portion of the batch water to control dust and ensure proper water absorption for the aggregate. Next, cement and fly ash were added to the mixer and combined with the aggregates until a uniform distribution was achieved. The remaining batch water was slowly added, and the time of water to cement contact was noted. Immediately following the addition of water, the water-reducing and air-entraining admixtures were slowly added directly to the concrete. The concrete was mixed for three minutes, rested for three minutes, and then mixed for an additional two minutes.

2.7.3 Placing, Finishing, and Curing

The following subsection briefly discusses the issues and guidelines associated with placing, finishing, and curing of internally cured concrete.

With regards to placing, New York State DOT (Streeter et al. 2015) placed an internally cured concrete using the same techniques and procedures as the control mix. Typically, the concrete would be pumped onto the deck, where no any difference in pumpability was noticed between internally cured and conventional concrete. Purdue University research group (Di Bella et al. 2012) had concerns on pumping the internally cured concrete. It was thought initially that pumping the concrete could result in water squeezed into the pores of the lightweight aggregate. Thus, the contractors were pouring concrete using the buckets. Later, after the discussion with NYSDOT about their successful experience with pumping internally cured concrete, the research team of Purdue University suggested pumping concrete in any future work.

Finishability of internally cured concrete was improved in most of the studies. Contractors in the Louisiana DOT study (Rupnow et al. 2016) noted that the visual appearance of internally cured concrete is no different than conventional concrete and it finishes "slightly better". In the study conducted by New York State DOT (Streeter et al. 2015), contractors also noted similar finishability and "less sticky" concrete.

Louisiana DOT (Rupnow et al., 2016), as well as some other studies, stress that internal curing by no means should replace conventional curing of the concrete. Rather, it serves as a means for the reduction of cracking in addition to already established practices. The findings of Louisiana DOT project suggested combining the internal curing method with a 7-day wet burlap curing. In the case of Purdue University study (Di Bella et al. 2012) and New York State DOT project (Streeter et al. 2015), the curing durations were also not changed and remained at 7 days and 14 days of curing respectively with soaker hoses and wet burlaps, which were periodically wetted by the construction personnel.

2.8 Field Studies from Other DOTs

Since the final goal of the project is to successfully implement the internal curing technique in the state of Nebraska, it is essential to analyze field-related studies of other DOTs. Table 6 provides a summary of documented internal curing concrete field projects performed at different states with the locations and details of decks being constructed. The following section of the chapter includes five case studies that highlight some details of construction and performance of the field studies with bridge decks using internal curing concrete.

Table 6. List of documented field projects of internal curing of bridge deck concrete

Constructed Year	Location	Deck Details	References
2009	Court Street Overpass I-81, Syracuse, NY	Steel girder 3 Spans: 180', 197', 125' Deck width: 65'	Streeter et al., 2015
2010	Interstate 81 over East Hill Road, Lisle, NY	Steel girder Single span: 74.2' Deck width: 42.4'	Streeter et al., 2015
2010	Mt. Gilead and Gettys Creek road, Bloomington, IN	Composite reinforced concrete deck 2 Spans: 50' and 39.5' Deck width: 27'-8" Deck thickness: 8"	Di Bella et al., 2012
2011	Interstate 190 / Interstate 290 interchange, Tonawanda, NY	Curved steel girder 2 Spans: 376' and 365' Deck width: 42.4'	Streeter et al., 2015
2013	NB I-69 over Little Black Creek, Grant County, IN	Continuous Reinforced Concrete Slab 3 Spans: 21', 28', 219' Deck thickness: 15.50"	Barrett et al., 2015
2013	US 150 over Lost River, Orange County, IN	Continuous Composite Steel Beam 3 Spans: 69'-9", 84'-6", 69'-9" Deck thickness: 8"	Barrett et al., 2015
2013	US 31 over Hutto Creek, Scott County, IN	Composite Steel Beam Single Span: 55' Deck thickness: 8"	Barrett et al., 2015
2013	SR 933 over Baugo Creek St., Joseph County, IN	Continuous Composite Prestressed Concrete Bulb-T Beam 2 Spans: 84'-6", 84'-6" Deck thickness: 8"	Barrett et al., 2015
2014	US Hwy 54 and US Hwy 169, La Harpe, KS	Pavement Length: 500'	ESCSI, 2020
2016	U.S. 80 KCS Railroad Crossing, Ada, LA	Span: 270' Deck width: 50' Deck thickness: 8"	Rupnow et al., 2016
2016	Western Lafayette Parish on West Congress Street, Lafayette, LA	3 Spans: 25', 20', 20'	Rupnow et al., 2016
2017	Interstate 271 in Mayfield Heights, OH	2 Spans: 193 feet (in total)	CPTech, 2020
2017	NC 55 Alston Avenue crossing over NC 147 Durham Expressway, Durham, NC	Span: 124'-6"	Cavalline et al., 2019

2.8.1 Indiana 2010

In 2010, the research team of Purdue University conducted and documented the construction of plain and internally cured bridge decks (Di Bella et al. 2012). Two bridges were constructed 1000 ft away from each other in Bloomington, Indiana. Both of them are similar structurally and utilize a composite reinforced concrete deck 27'-8" wide. The thickness of bridge

decks was 8” at the center and 4.5” at the edges in both cases. The spans of the bridges were 50 ft (plain) and 39.5 ft (internally cured), respectively.

Due to the initial concern that pumping the concrete could result in water preferentially squeezed into the pores of the LWFA, the internally cured concrete deck was placed using a bucket, as shown in Figure 14. However, the researcher pointed out that they discussed with NYSDOT that have reported with experience of no difficulties in pumping internally cured mixtures since the time of this project, and later made the recommendation that pumping would be permitted for future internal curing applications.

Figure 14. Internally cured bridge deck placed by means of a bucket

Visual inspection of bridge decks after one year revealed two cracks on the plain bridge deck, whereas no deficiencies were observed for internally cured concrete deck, as shown in Figure 15.

(a) Crack on a plain bridge deck

(b) Internally cured bridge deck with no cracks

Figure 15. Condition of both bridge decks with plain and internally cured concretes one year after placement

2.8.2 New York 2010

As a part of their internal curing evaluation program, NYSDOT constructed seventeen bridge decks with internally cured concrete in 2010 (Streeter et al. 2015)

From prior experience with prewetting coarse lightweight aggregate for use in structural lightweight concrete, it was determined that the use of a sprinkler on the stockpile was the best method to prewet the LWFA, see **Figure** 16. It was reported that there were no differences in batching that were needed to accommodate internally curing concrete. However, with cases with small concrete batch plants with an insufficient number of bins, two aggregates were pre-blended and placed into one bin, which left a bin space to batch LWFA.

Figure 16. Sprinkler system used for soaking LWFA prior to batching

As for placement, which all concrete were placed with pumps (see Figure 17), no differences were observed in the pumpability of the mix when compared to a similar mix without internal curing. Finishability was similar between conventional and internal curing concrete. At the beginning of the job, the engineer compared the air content measured by the pressure method and the volumetric method and found that the difference was within 0.5%, and the pressure meter was used throughout the pour. The burlap and soaker hoses were left in place for 14 curing days to provide continuous, uniform wetting for the entire curing period.

(a) Interstate 190/ Interstate 290 Interchange (b) Court Street Deck Placement

Figure 17. Internally cured bridge deck placed by means of pump trucks

2.8.3 Indiana 2013

In the summer of 2013, collaborated with a research team from Purdue University, Indiana Department of Transportation (INDOT) constructed four bridge decks utilizing internally cured high-performance concrete. A report from Barrett et al. (2015) provided detailed documentation of INDOT's experience and construction of the four bridge decks.

For each of the mix, a trial batch was held a minimum of 28 days prior to the date of construction to identify and solve potential issues for production prior to the date of construction.

As shown in Figure 18, prior to batching, the lightweight aggregate pile was soaked for a minimum of 48 hours and allowed to drain for a minimum of 12 hours. Variability in moisture states within a stockpile of prewetted lightweight aggregate should be controlled or monitored and accounted for throughout concrete production.

Figure 18. LWA piles being soaked prior to batching of internally cured concrete

The research team recommended that additional training and education for batch plant operators to fully understand how to make moisture adjustments and change scale jog rates when producing mixtures containing LWFA may serve to avoid potential issues during batching. Similar to experiences from NYDOT projects, due to the lack of additional aggregate bins for LWFA, the producer was required to refill the LWFA hoppers throughout production. A few issues were also encountered during the construction, including lower air content than desired. However, it was later determined that the excess free fall to the point of placement because of the pump geometry may have contributed to this issue. The research team also commented that pumping issues were observed, which would be present regardless of the concrete mixture proportions are avoidable with additional training and education. All four bridge decks were successfully constructed and are now in service.

2.8.4 Louisiana 2016

In 2016, Louisiana DOT conducted a field investigation on the performance of internally cured bridge deck concrete. Two concrete placements were evaluated:

1. U.S. 80 near Ada, North Louisiana. As illustrated in Figure 19, the placement was 8"-thick section, which is 50 ft wide and 270 ft long. The total volume of the concrete placed is 350 cu yd. The experience from the ready-mix plant operator and contractor showed that LWFA had no adverse effects on the fresh concrete, with the impression that the internally cured concrete

"looks and feels" like normal concrete and the concrete tended to finish with a little less effort than the control mixture. It has been identified by the research team (Rupnow et al., 2016) that U.S. 80 showed significantly less cracking in nine months, and the trial was deemed successful.

Figure 19. Internally cure concrete project at U.S. 80 near Ada, North Louisiana

2. Western Lafayette Parish on West Congress Street. As illustrated in Figure 20, the placement was a 13"-thick slab with several spans. In this structure, 25-ft center spans were constructed with plain concrete, whereas the 20-ft adjacent spans were constructed with internally cured concrete. In this case, the reduced cracking was also observed at one year after the placement.

Overall, the project showed promising results, and the standard replacement between 225 and 275 pcy of LWFA was suggested by the research group.

Figure 20. Internally cure concrete project at West Congress Street bridge

2.8.5 North Carolina 2017

In 2017, a research team from the University of North Carolina at Charlotte worked with North Carolina DOT and conducted a pilot project for field implementation of internally cured concrete (Cavalline et al. 2019). With regarding stockpile management, NCDOT adopted the

practice from NYDOT to pre-wet the LWFA for a minimum of 48 hours, followed by a draining period of 12-15 hours. The stockpile was also turned and remixed to obtain a homogenous aggregate moisture content prior to batching. As shown in Figure 21, the sprinklers were located on the side of the stockpile and the drainage of the stockpile was directed to the far side of the pole with slab sloped to drain.

Figure 21. Stockpile of prewetted LWFA the day before placement of the internally cured bridge deck

For concrete placement, as shown in Figure 22, the project used a pump line with a minimum 5-inch diameter to decrease the pressure that may prematurely draw the water out of the LWA pores. According to interviews with contractors and concrete suppliers, producing internal curing concrete may be more problematic in rural areas or smaller markets. Specifically, concrete batch plants tend to be smaller, and may not have the capacity (space or weigh bins) or technical expertise to handle prewetted LWFA and successfully batch internal curing concrete mixtures.

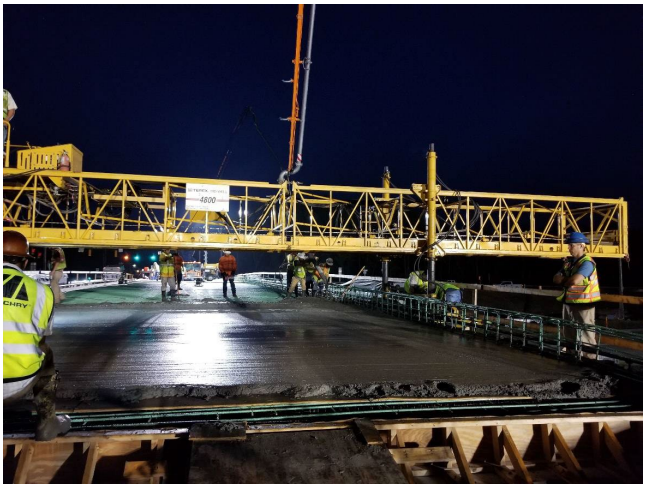

Figure 22. Placement of internally cured concrete mixture

CHAPTER 3. MATERIAL, MIXING METHOD AND TEST PROCEDURES

The experimental work included in this study was divided into three phases based on the needs at different stages. All the phases incorporated the same materials but used different mix designs and test methods. This chapter describes the materials used in the study and cover the experimental program of each phase.

3.1 Materials

The following section of the chapter provides a detailed description of materials used in the project.

3.1.1 Cement and cementitious materials

NDOT Standard Specifications for Highway Construction (2017) requires the use of IP interground/blended cement for pavement application. IP cement was designed to mitigate Alkali-Silica Reaction (ASR), provide sulfate resistance, and reduced chloride permeability. For this study, type IP Portland-pozzolan cement with 25% blended class F fly ash content that meets ASTM C595 "Standard Specification for Blended Hydraulic Cements" (ASTM 2019) was used as the cementitious material. The chemical composition and physical properties of cement used in the study are reported in Table 7.

Table 7. Chemical composition and physical properties of IP cement

Chemical Properties	Pozzolan content, %	25
	MgO, %	2.45
	SO_3, %	3.10
	Loss in Ignition, %	1.00
Physical Properties	Blaine Fineness, cm^2/g	4400
	Specific Gravity	2.95

3.1.2 Natural Aggregates

Plain aggregates, which do not provide any internal curing, will be referred to as natural aggregates hereinafter. As one of the project requirements, local materials were used as normal aggregates in the study. Locally available No. 57 limestone and sand and gravel were utilized as coarse and fine aggregates, respectively. Their physical properties are shown in Table 8.

Table 8. Physical properties of normal aggregates

Aggregate	$G_{sb,\ SSD}$	Absorption (%)	Bulk Density (pcy)
No. 57 Limestone	2.67	0.91	105.65
Sand & Gravel	2.59	0.96	117.24

Figure 23 illustrates the gradation of the normal aggregates.

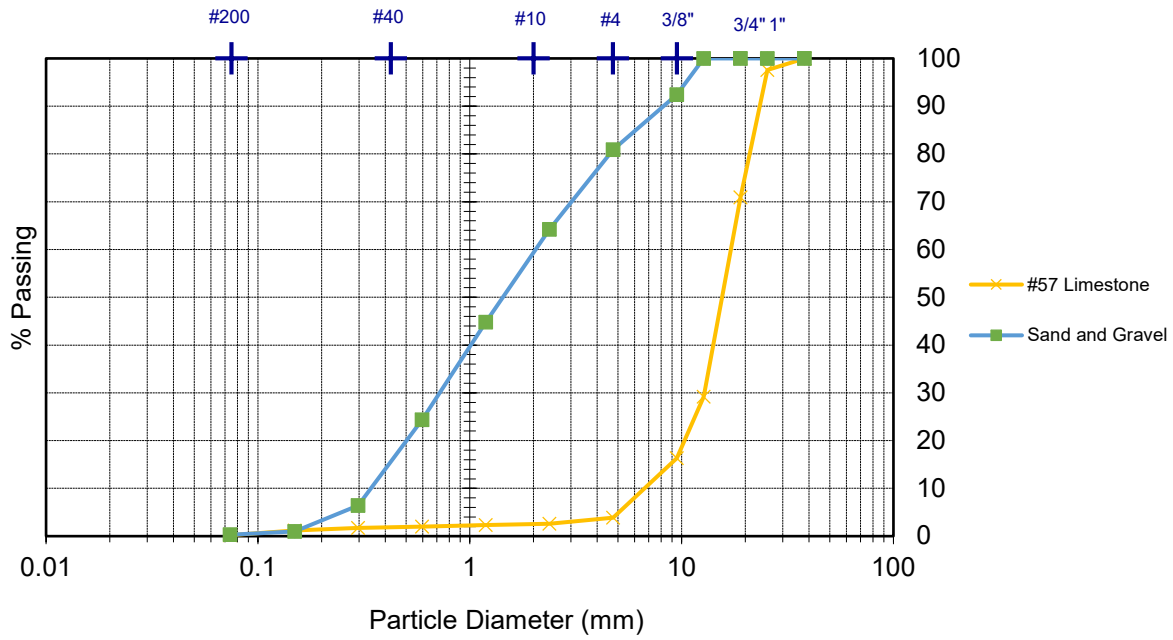

Figure 23. Gradation chart of normal aggregates

3.1.3 Lightweight Fine Aggregate

Based on the project needs, which required to investigate local materials for internal curing, four types of LWFA were identified and ordered. LWFA A is expanded clay supplied from Boulder, Colorado. The LWFA B and C are expanded shale aggregates obtained from the same source located in New Market, Missouri. In general, LWFA B and C are identical aggregates but with different gradations. LWFA D is an expanded slate from Gold Hill, North Carolina. Their general information about the LWFA is presented in Table 9.

Table 9. General information of LWFA used in the study

LWFA ID	LWFA A	LWFA B	LWFA C	LWFA D
Supplier	Trinity/Arcosa	Buildex	Buildex	Stalite
Product name	N/A	3/8" x 0	No. 4 x 0	MS-16
Material type	Expanded clay	Expanded shale	Expanded shale	Expanded slate
Location	Boulder, CO	New Market, MO	New Market, MO	Gold Hill, NC

Table 10 provides the physical properties of LWFA, such as specific gravity, water absorption, and desorption values.

Table 10. Physical properties of LWFAs in the study

LWFA ID:	LWFA A	LWFA B	LWFA C	LWFA D
Specific Gravity, SSD	1.91	1.74	1.80	1.88
Water Absorption (%)	22.4	16.4	12.8	11.5
Water Desorption (%)	85.8	99.1	98.7	N/A

Since the absorption of LWFA D is the smallest among all the four aggregates, it was decided to eliminate that type of aggregate from the study at this stage. The gradation of all types of LWFAs is illustrated on Figure 24, where they are also compared to the gradation of normal aggregates. It can be observed that all lightweight aggregates, especially LWFA A, are finer, in general, compared to sand and gravel.

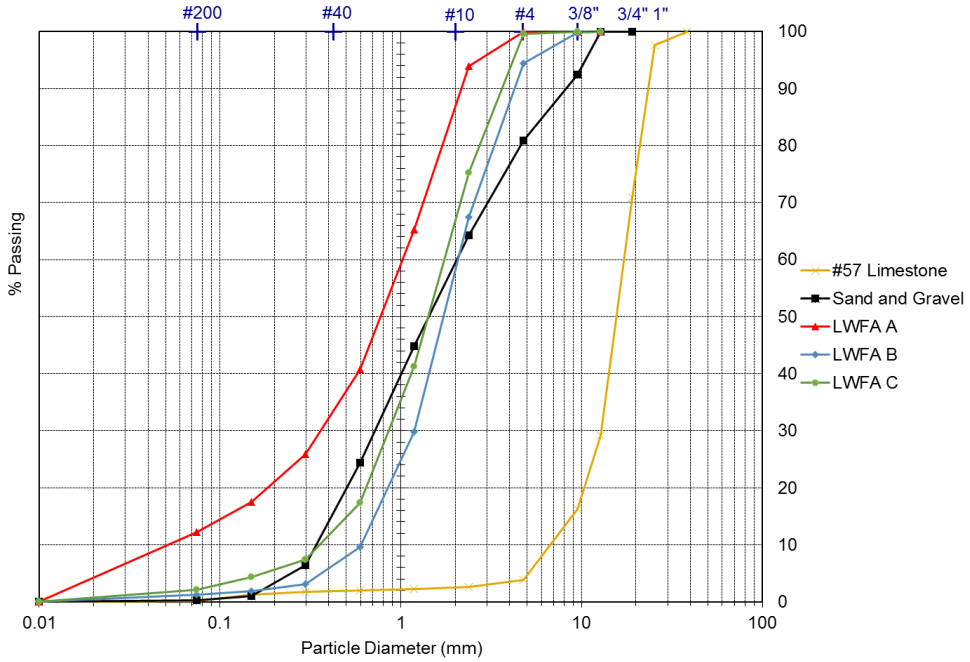

Figure 24. Gradation chart of LWFAs and natural aggregates used in the study

Figure 26 and Figure 20 provide a visual representation of different types of LWFA in their initial state and in the concrete matrix. The porous matrix of each aggregate can be clearly seen and identified in Figure 26.

(a) LWFA A (b) LWFA B (c) LWFA C

Figure 25. Physical appearance of LWFA

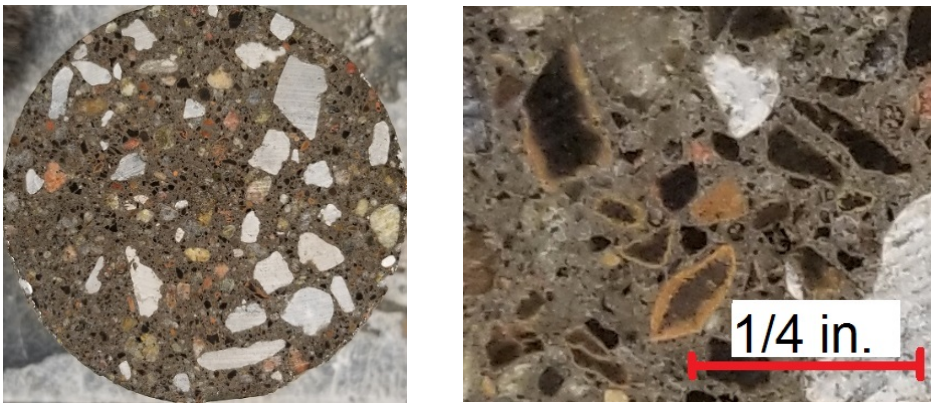

(a) LWFA A

(b) LWFA C

Figure 26. Physical appearance of LWFA in concrete matrix

3.1.4 Chemical Admixtures

Commercially available air-entraining agent (AEA) and mid-range water reducer (MRWR), meeting the standards described in ASTM C494 "Standard Specification for Chemical Admixtures for Concrete" (ASTM 2017), were utilized as chemical admixtures for concrete.

3.2 Control Mixture

A standard bridge deck concrete, identified as 47BD, was used as a basis for the control mixture of this study. Table 11 provides mix design requirements of 47BD (NDOT Pavement Design Manual, 2018).

Table 11. Mix design requirements of 47BD mixture

Mix Type	Cement Type	Total Cement Content (pcy)	Total Aggregate Content (pcy)	Required Air Content (%)	Vol. Proportion of Rock in Aggregate Blend (%)	w/c Max.	Required 28-day Strength (psi)
47BD	IP	658	2500-3000	6.0-8.5	30±3	0.42	4000

Furthermore, NDOT requires bridge deck concrete to be cured with wet burlaps for at least 10 days after placement, followed by 7-day curing using curing compound (Standard Specifications for Highway Construction, 2017). This information will be taken into account in the experimental design of the study.

3.3 Concrete Batching and Mixing

Limestone and sand and gravel were prepared prior to mixing according to guidelines specified in ASTM C192 "Standard Practice for Making and Curing Concrete Test Specimens in the Laboratory" (ASTM 2018). Approximately 72 hours prior to the mixing, sufficient amounts of both coarse and fine aggregates were retrieved from the stockpile. The materials were then oven-dried at 230±18°F for 24 hours. After the drying, aggregates were cooled at room temperature for 2 hours. Then, limestone was soaked in water for the next 24 hours, followed by 1-hour draining. At the same time period, sand and gravel were brought to the wet condition by means of a water sprayer and left in a sealed bucket for 24 hours. Finally, both limestone and sand and gravel were measured for the moisture content according to ASTM C70 "Standard Test Method for Surface Moisture in Fine Aggregate" (ASTM 013). The moisture retained on the surface of the aggregates was then accounted for in the mix design.

LWFAs were prepared according to the following procedure: a representative portion of LWFA from the stockpile was brought to the oven-dry state by keeping it in the oven at a constant temperature of 230±18°F for 24 hours, followed by air-cooling for approximately 2 hours. Then, the required total amount of oven-dry aggregates based on the mix design was weighed in the bucket and left submerged completely in the water for 24 hours. The bucket for saturating aggregates had 10-12 predrilled openings of approximately 1/16" in diameter at random locations of the bucket bottom, as shown in Figure 27, which were sealed with a waterproof tape prior to aggregate soaking. The dimensions of the bottom openings, which should be large enough to drain water and small enough to keep all saturated aggregate particles inside were obtained by trial and error method. 24 hours after soaking, on the day of the mixing, the tape was removed from the bottom to allow the excess non-absorbed water to drain for approximately 1 hour. Since the described procedure leaves some excess water on the aggregate surfaces, the difference between the weight of the obtained aggregates and the theoretical weight of SSD aggregates was accounted for in the mixing water.

Figure 27. Openings at the bottom of the bucket for saturating LWFAs

Concrete mixing was performed following ASTM C192 "Standard Practice for Making and Curing Concrete Test Specimens in the Laboratory" (ASTM 2018) with one additional

modification for the LWFA. Firstly, half of the mixing water was thoroughly premixed with AEA and another half with MRWR. Then, a limestone was discharged into a drum mixer followed by half of the mixing water with AEA. 30 seconds of mixing were given in order to initiate the production of entrained air. Then, the mixer was then stopped, and the following materials were discharged into the mixer in the order of sand and gravel, cement, and remaining half of the water premixed with MRWR. After mixing for another 30 seconds, the mixer was stopped again in order to discharge the last material, prewetted LWFA. The reason LWFA was not added together with sand and gravel is to avoid dry contact of LWFA, which might initiate early desorption. The next step involved mixing for 2.5 minutes, followed by 3-minute rest and final 2-minute mixing. The mixing procedure of the control mix did not include a stop for discharging LWFA as it was not needed.

Upon the completion of mixing, various concrete specimens were prepared according to ASTM C192 (ASTM 2018) and then stored under a wet burlap and plastic sheeting at a room temperature of 73±3.5°F prior to demolding at 24±1 hour. The next section covers the curing periods and testing methods for each of the samples.

3.4 Test Methods

3.4.1 LWFA Absorption and Desorption

Previously, in Chapter 2, three different methods of measuring water absorption of LWFAs, i.e., "brown paper towel" method, "brown paper towel" method, and ASTM C128 method, were described. Out of three, the research team decided to utilize a modified "brown paper towel" method in this study. The wet specimen of LWFAs weighing approximately 750 grams was placed on a No. 200 sieve with a pan underneath for draining water. Then, brown paper towels were used to wipe fine aggregates in a circular motion while continually applying pressure. The wiping process was continued until no further moisture was observed on the paper towels, with which the LWFA was deemed as in SSD condition.

After the LWFAs were brought to SSD condition, a representative sample weighing approximately 500 grams was obtained, weighed to the closest 0.1 gram, and placed in the oven at 212±9°F for 24 hours. After the drying process is over, the moisture loss was recorded, and the absorption capacity was calculated.

The desorption test was conducted in accordance with ASTM C1761 (ASTM 2017). Another representative sample weighing approximately 5 grams from the same batch was obtained, weighed to the closest 0.0001 gram using the scales illustrated in Figure 28, and placed in the controlled environmental mini-chamber, as illustrated in Figure 29.

The mini-chamber, which was kept at a room temperature of 73.0±3.5°F is a sealed plastic container with three cups filled with ~100 grams of super-saturated potassium nitrate solution each. A super-saturated solution of potassium nitrate is supposed to maintain the environment relative humidity at 94.0% ± 0.5%. A plastic mesh was placed on top of the cups in order to accommodate a mini-pan with saturated LWFAs.

Figure 28. High-accuracy scales for desorption test

The weight of the aggregates in the chamber was weighed every 24 hours using the scales illustrated in Figure 28 until the difference between the two subsequent readings is not more than 0.01 gram. After that, a pan with aggregates is placed in the oven at 110ºC ± 5ºC for 24 hours. After the drying process is over, the final moisture loss was recorded, and the desorption capacity of the aggregates was calculated.

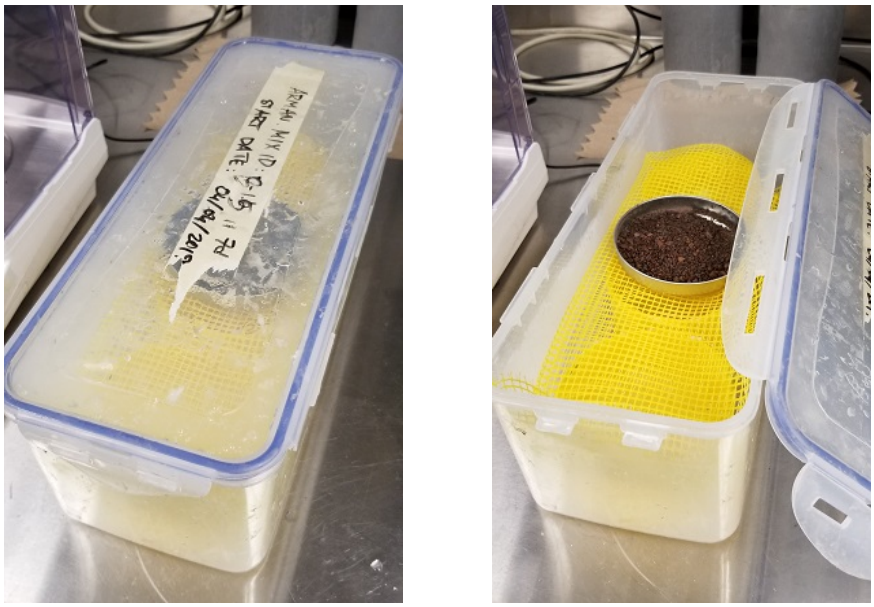

(a) Sealed mini-chamber **(b)** Aggregates being tested for desorption

Figure 29. Environmental mini-chamber for the desorption test

3.4.2 Aggregate Void Content Test

Void contents of each individual coarse and fine aggregates were evaluated based on ASTM C29 "Standard Test Method for Bulk Density ("Unit Weight") and Voids in Aggregate" (ASTM 2017) and ASTM C1252 "Standard Test Methods for Uncompacted Void Content of Fine Aggregate (as Influenced by Particle Shape, Surface Texture, and Grading)" (ASTM 2017) respectively. Prior to the tests, all aggregate were then brought to the oven-dry state by keeping it in the oven at a constant temperature of 230±18°F for 24 hours, followed by air-cooling for approximately 2 hours.

A combined void content test was utilized for the measurement of void content in any given aggregate blend. The test was performed in accordance with ASTM C29. Prior to the testing, sufficient amounts of individual aggregates were obtained from the stockpile, with the total volume of which exceeded the volume of the container for the test by at least 50%. All aggregate were then brought to the oven-dry state by keeping it in the oven at a constant temperature of 230±18°F for 24 hours, followed by air-cooling for approximately 2 hours. At the beginning of the test, all aggregates were mixed in a drum mixer for one minute. Following drum mixer mixing, the aggregate blend was discharged on a pan and further hand-mixed for one minute to ensure uniformity. Then, a steel container with a known volume of 0.250 cu ft ± 0.002 cu ft was filled with the aggregate blend in three layers. Each layer was rodded with 25 strokes of a No. 5 tamping rod. After filling the last layer, the surface of the aggregates was leveled by a straightedge. Finally, the weight of the measure and the container was reported to the nearest 0.01 lb. The test setup is illustrated in Figure 30.

Figure 30. Combined void content test setup

The void content of the aggregate blend was calculated by the following equation:

$$\%Void = \frac{G_{sb,com} \times UW_{water} - Bulk\ Density}{G_{sb,com} \times UW_{water}} \quad \textbf{(Eq. 7)}$$

where

$$Bulk\ Density = \frac{Mass\ of\ aggregate\ blend}{Volume\ of\ the\ container}; \quad \textbf{(Eq. 8)}$$

$$G_{sb,com} = \frac{1}{\frac{P_{LS}}{G_{sb,LS}} + \frac{P_{SG}}{G_{sb,SG}} + \frac{P_{LWFA}}{G_{sb,LWFA}}} \quad \textbf{(Eq. 9)}$$

where G_{sb} and P account for specific gravity and the volumetric fraction of each aggregate in the blend.

3.4.3 Fresh Concrete Properties

The workability of the concrete was evaluated based on the slump test method as specified in ASTM C143 "Standard Test Method for Slump of Hydraulic-Cement Concrete" (ASTM 2015) and is illustrated in Figure 31. Initial mix design for most mixes included the same dosage of MRWR in order to capture the effect of sand and gravel replacement only. After, if the slump of the mix was not within the 4"-6" range, an adjustment of MRWR dosage was made in order to bring the mix to consistency at slump between 4" and 6".

Figure 31. Slump test setup

In the planning stage, both ASTM C231 "Standard Test Method for Air Content of Freshly Mixed Concrete by the Pressure Method" (ASTM 2017) and ASTM C173 "Standard Test Method for Air Content of Freshly Mixed Concrete by the Volumetric Method" (ASTM 2016) were considered for fresh concrete air content measure. However, a thorough literature review of previous DOT studies on internal curing did not identify any issues related to the two different methods for air content measurement. Iowa DOT and Louisiana DOT utilized pressure method. Furthermore, Colorado DOT utilized and compared both methods, and concluded that both methods are valid and do not yield a difference higher than 1.5%, with the pressure method showing slightly higher air content reading. As a result, the research team decided to use the pressure method for air content measurement since it is easier to perform in the field. The type B pressure air meter used in the study is shown in Figure 26.

Figure 32. Type B air pressure meter

The fresh unit weight of the concrete was measured following ASTM C138 “Standard Test Method for Density (Unit Weight), Yield, and Air Content (Gravimetric) of Concrete” (ASTM 2017). A steel container of 0.25 cu ft volume was filled with concrete following the standard specification, and the unit weight of the material was derived from fresh concrete mass in the filled container.

The initial and final setting time of the mortar was evaluated per ASTM C403 “Standard Test Method for Time of Setting of Concrete Mixtures by Penetration Resistance” (ASTM 2016). Each mortar sample was obtained from the corresponding concrete mixtures by sieving with a No. 4 sieve based on the procedure. As soon as a specimen was obtained, it was placed in an open-top container, and the penetration resistance was measured at various times after placement by means of the loading apparatus with penetration needles of various sizes, as shown in Figure 33. As specified in the standard, the initial and final sets occur when the penetration resistance reaches 500psi and 4000 psi, respectively.

Figure 33. The loading apparatus for evaluating set time of concrete

3.4.4 Mechanical Properties

Compressive strength of the concrete was evaluated at the ages of 4, 14, and 28 days in Phases I and II, and at the ages of 3, 7, and 28 days in Phase III, utilizing nine 4"×8" cylinders from each mix. Right after demolding, representative samples were placed inside an environmental chamber satisfying ASTM C511 "Standard Specification for Mixing Rooms, Moist Cabinets, Moist Rooms, and Water Storage Tanks Used in the Testing of Hydraulic Cements and Concretes" (ASTM 2019) with constant relative humidity not lesser than 95% and temperature of 73.5±3.5ºF, where they were continuously cured until testing. The compressive strength test was performed in accordance with ASTM C39 "Standard Test Method for Compressive Strength of Cylindrical Concrete Specimens" (ASTM 2018). Prior to the test, each specimen was end-ground to meet plane requirements for cylinder ends specified by the test method. The loading rate of the test specimens was kept at 440±88 lbs/s throughout the test. Figure 34 illustrates the test setup.

Figure 34. Setup of compressive strength test

Casted flexural beams with the dimensions of 6"×6"×20" (152mm×152 mm×508 mm) were used for modulus of rupture testing in a universal testing machine in accordance with ASTM C78 "Standard Test Method for Flexural Strength of Concrete (Using Simple Beam with Third-Point Loading)" (ASTM 2018). Figure 35 shows the three-point flexural test setup of a concrete beam. As per ASTM C78, the tests were conducted at a loading rate of 125 to 175 psi/min until the rupture occurs. The final modulus of rupture was calculated and reported accordinlgy.

Figure 35. Test setup for flexural strength test

Since concrete deformation is also dependent on the modulus of elasticity, it was decided to include that test in the experimental program. Three 4”x8” cylinders, which were cured for 28 days, were used for modulus of elasticity testing in accordance with ASTM C469 “Standard Test Method for Static Modulus of Elasticity and Poisson’s Ratio of Concrete in Compression” (ASTM 2014). Figure 35 shows the modulus of elasticity test setup. As per ASTM C469, the tests were conducted at the same loading rate as in the compressive strength test at 440±88 lbs/s. The modulus of elasticity was obtained based on the procedure described in ASTM C469 and reported.

Figure 36. Static Modulus of Elasticity test setup

The bond strength of concrete was measured by utilizing ASTM C882 “Standard Test Method for Bond Strength of Epoxy-Resin Systems used with Concrete by Slant Shear” (ASTM 2013) as a basis for the test. In this test, no epoxy-resin systems were used as a binding agent.

Instead, concrete-to-concrete bonding was evaluated. The dummy section for each test was prepared from the control (47BD) mixture. Thus, the bonding strength of the concrete will mean the bonding strength of the corresponding concrete mixture to the control mixture. Figure 37a illustrates prepared dummy sections with the control (47BD) ix. Each dummy section has three equidistant notches with a uniform depth of 0.25-0.50". Before placing fresh concrete, the bonding surface of the dummy section was moistened with water. Each specimen was kept in the mold after placement for 7 days and in an environmental chamber satisfying ASTM C511 with constant relative humidity not lesser than 95% and temperature of 73.5±3.5ºF, for the next 21 days until the test was performed. The loading rate of the specimen was kept at 440±88 lbs/s throughout the test, which is illustrated in Figure 37b. The reported bond strength corresponds to the average peak load divided by the area of the bonding interface.

(a) Dummy sections (b) Test setup

Figure 37. Bond strength test specimen and setup

3.4.5 Volume Stability

Free shrinkage, or length change of concrete, was evaluated at the ages of 1, 3, 7, 14, 28, 56, and 90 days utilizing four 3"×3"×11" prisms. The test method evaluated length change of unrestrained concrete beams at four curing periods (0 days, 5 days, 7 days, and 10 days) and two different environmental conditions (sealed and non-sealed).

In order to study the performance of the developed mixes in different curing durations, four different curing conditions were adopted in this study. 0 days of curing means that the monitoring of the length change began immediately after demolding, with that day being the day one of the tests. Cured specimens were stored inside an environmental chamber satisfying ASTM C511 with constant relative humidity not lesser than 95% and temperature of 73.5±3.5ºF for an additional 5, 7, or 10 days. The monitoring of the length change for that specimen began immediately after the end of the curing period, that day being the day zero of the test.

The sealed environmental condition indicates that the specimen was securely and tightly wrapped with foil and tape to isolate the specimen from the outside environment and prevent moisture loss. The sealed condition was needed to evaluate the autogenous shrinkage of concrete only, meaning that no drying shrinkage took place. The non-sealed environmental condition indicates that the specimen was stored in an environmental chamber at a relative humidity of 50%

and a temperature of 73.5±3.5ºF. The following condition indicates two combined shrinkages: autogenous shrinkage and drying shrinkage. To conclude, the eight different conditions showing below are included in the study, with four of which are illustrated in Figure 38:

- Condition 1: 0 days of curing followed by exposure in a sealed environment (Figure 38, Specimen 1)
- Condition 2: 0 days of curing followed by exposure in a drying environment (Figure 38, Specimen 2)
- Condition 3: 5 days of curing followed by exposure in a sealed environment
- Condition 4: 7 days of curing followed by exposure in a drying environment
- Condition 5: 7 days of curing followed by exposure in a sealed environment (Figure 38, Specimen 3)
- Condition 6: 7 days of curing followed by exposure in drying environment (Figure 38, Specimen 4)
- Condition 7: 10 days of curing followed by exposure in a sealed environment
- Condition 8: 10 days of curing followed by exposure in a drying environment

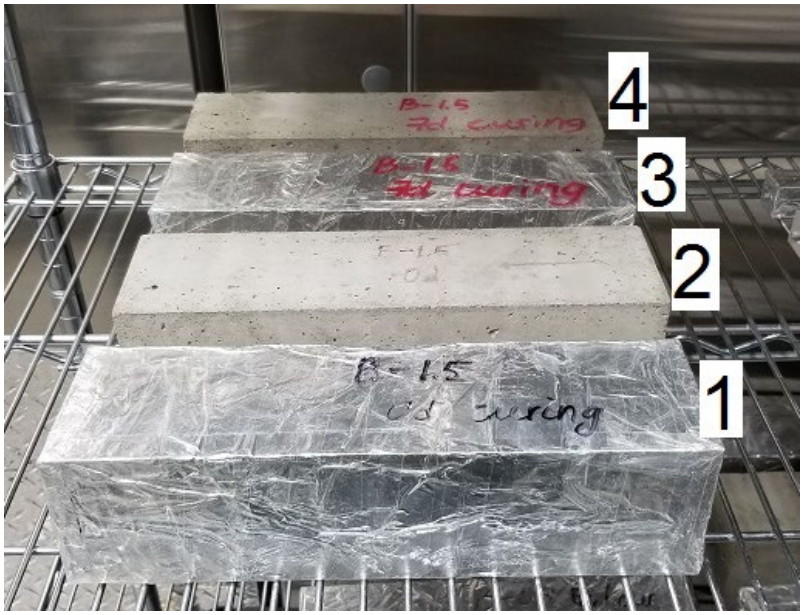

Figure 38. Free shrinkage specimens at four different conditions

The shrinkage test was performed in accordance with ASTM C157 “Standard Test Method for Length Change of Hardened Hydraulic-Cement Mortar and Concrete” (ASTM 2017). The total length of the bar was evaluated at the ages of 1, 3, 7, 14, 28, 56, and 90 days and the difference in length change was reported in microstrains (με). Figure 39 illustrates the test setup.

Figure 39. Setup of a free shrinkage test

The restrained shrinkage test was performed in accordance with ASTM C1581 "Standard Test Method for Determining Age at Cracking and Induced Tensile Stress Characteristics of Mortar and Concrete under Restrained Shrinkage" (ASTM 2018). In general, the idea of the test is to measure the age of cracking of a restrained concrete ring. A fresh concrete ring is poured between a steel ring and a detachable plastic outer ring. Two strain gauges are connected to the steel ring to monitor the stresses induced by shrinking concrete on a ring. The concrete is restrained only from the side, where it is connected to the steel ring. The top part of concrete is waxed to prevent moisture loss from the top. The test is finished at one of the following scenarios:

- If the crack developed in under 28 days. The crack is usually represented by a sudden drop in strain on a strain-time curve with the reduction of strain greater than 30 microstrains. The age at which cracking occurred was reported to the nearest 0.25 day.
- If the test was continuously going for 28 days. In this scenario, the test is stopped and report as no cracking.

At the end of the test, the age of cracking and the strain at cracking is reported together with a strain versus time graph. Figure 40 illustrates the test setup.

(a) Rest setup (b) Example of a crack from the top view

Figure 40. Restrained shrinkage test setup

3.4.6 Durability Performance

Electrical resistivity of the concrete was evaluated at the ages of 3, 7, 14, 21, and 28 days utilizing 4"x8" cylinders in accordance with AASHTO TP 95-11 "Standard Test Method of Test for Surface Resistivity Indication of Concrete's Ability to Resist Chloride Ion Penetration" (AASHTO 2011). The specimens were cured inside an environmental chamber, satisfying ASTM C511 at a constant relative humidity not lesser than 95% and temperature of 73.5±3.5ºF. Surface moisture was removed with a towel prior to testing. The average result of the three cylinders tested was reported. Both surface and bulk electrical resistivity of the concrete were monitored. Figure 41 illustrates the test setup.

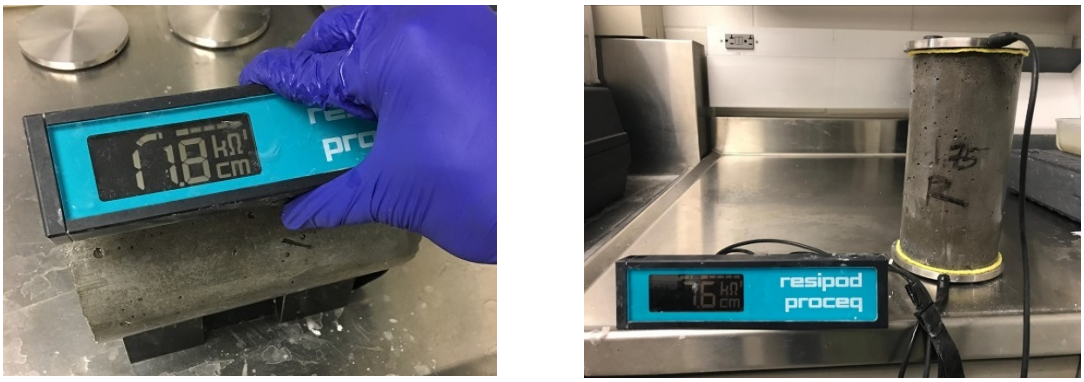

(a) surface resistivity (b) bulk resistivity

Figure 41. Setup of electrical resistivity test

Rapid chloride permeability test was conducted in accordance with ASTM C1202 "Standard Test Method for Electrical Indication of Concrete's Ability to Resist Chloride Ion Penetration" (ASTM 2019). The test was conducted with specimens, which were cured for 56 days. The test setup is shown in Figure 42.

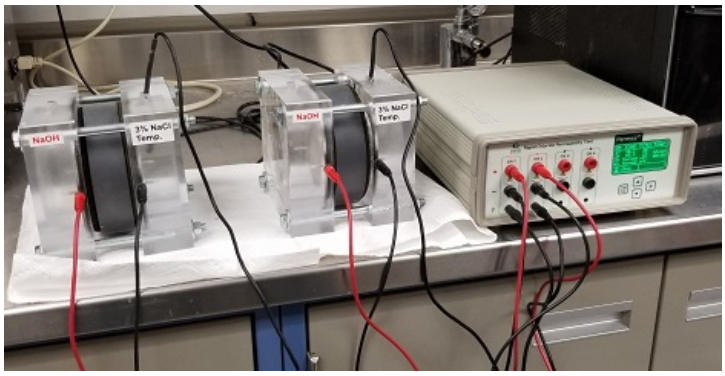

Figure 42. Setup of rapid chloride permeability test

CHAPTER 4. EXPERIMENTAL PROGRAM

Based on the needs and aims of the project, the experimental program was divided into three distinct phases:

- Phase I. Effect of Replacement Rate
- Phase II. Aggregate Blend Optimization
- Phase III. Performance Evaluation

Phase I of the project studied the effect of partial replacement of sand and gravel by LWFA in a 47BD control mix. All mix design parameters were kept unchanged, other than the amount of sand and gravel, amount of LWFA, and the adjustment of MRWR, where needed. Three replacement levels per each type of LWFA were evaluated at this stage. Phase I of the project concluded with the selection of two LWFA types at one replacement level, which demonstrated the best performance in terms of free and restrained shrinkage.

During the scope of Phase I of the study, the research team identified an issue resulted from the incorporation of LWFA, which is that the replacement of sand and gravel by LWFA disturbs the overall gradation of the blend and leads to lower workability. The main aim of Phase II is, therefore to address this workability issue. The following two approaches were used to overcome this issue:

1. General adjustment method. The workability of the mixes was adjusted by the addition of water-reducing admixtures (both Phase I and Phase II).
2. Aggregate blend optimization. This approach will modify the blend proportions of the aggregates based on experimental void content tests, which were also compared to theoretical and empirical particle packing models (Phase II).

The aggregate blends of the two mix designs selected from the previous phase were optimized based on experimental void content. The selection of optimum blend proportions was also supported by the theoretical particle packing model and empirical charts. The properties of the optimized mixes were compared with those of corresponding mixes from Phase I, and one mix design per each type of LWFA was selected to be studied in Phase III.

The final phase of the project evaluated the mechanical behaviors and durability performance of the two best mixes from Phase I, the two corresponding mixes from Phase II, and the two control mixes with non-optimized and optimized aggregate gradations, respectively. Table 12 summarizes the experimental program of the project.

Table 12. Summary of tests included in the different phases of the experimental program

Test		Preparation	Phase I	Phase II	Phase III
Aggregate Testing	Sieve Analysis	X			
	Specific Gravity	X			
	Absorption	X			
	Desorption	X			
	Combined Aggregate Void Content			X	
Fresh Concrete Properties	Slump		X	X	X
	Air Content		X	X	X
	Unit Weight		X	X	X
	Setting Time				X
Mechanical Properties	Compressive Strength		X	X	X
	Modulus of Rupture				X
	Modulus of Elasticity				X
	Bond Strength				X
Volume Stability	Free Shrinkage		X	X	X
	Restrained Shrinkage		X	X	X
Durability Properties	Electrical Resistivity		X	X	X
	Free and Thaw Resistance				X
	Rapid Chloride Permeability				X

4.1 Phase I – Effect of Replacement Rate

The main aim of Phase I was to evaluate the impact of sand and gravel replaced by different dosages of LWFA on the fresh, mechanical, and physical properties of the concrete. Three replacement levels for each aggregate based on Equation 2 were investigated. All other parameters, other than contents of sand & gravel, LWFA, and chemical admixtures, remained constant from mix to mix. At the end of Phase I, the two most promising aggregates and the respective dosage rate were identified and utilized further in Phase II and Phase III study.

In order to meet the project objectives, three types of LWFA were identified based on local availability, and their effects on the following properties of concrete were studied:

- Fresh concrete properties: slump, air content, and unit weight;
- Hardened concrete properties: compressive strength, and electrical resistivity;
- Volume stability: free shrinkage at sealed and drying environmental conditions with no curing, and restrained shrinkage;

The control mix, or 47BD mix, which is a common bridge deck concrete utilized in the state of Nebraska, and eleven additional mixes incorporating three different types of LWFA at three replacement levels for LWFA A and B, and five replacement levels for LWFA C were studied. Additional dosage rates for LWFA C are explained by the fact that the research team identified that a higher amount of LWFA C is more suitable during the project. As a result, it was decided to incorporate two additional dosage rates for LWFA C. Equation 2 was used to calculate the theoretical amount of LWFA needed to compensate chemical shrinkage of the concrete. Based on that amount, three levels of LWFA dosage were estimated for each mix design. Each of the replacement levels incorporated 50% (0.5), 100% (1.0), and 150% (1.5) of the theoretical amount. Additional replacement levels of 125% (1.25) and 175% (1.75) were studied for the case of LWFA

C. The reason behind the different levels of dosage is to study the effect of under- and over-dosage of LWFA as well.

4.1.1 Phase I Mix Designs

The explanation of mixture IDs is shown in Figure 43. Mix designs for each concrete mixture are shown in Table 13. As it was stated earlier, after the physical properties of the LWFAs were obtained, individual mix designs were adjusted based on Equation 2.

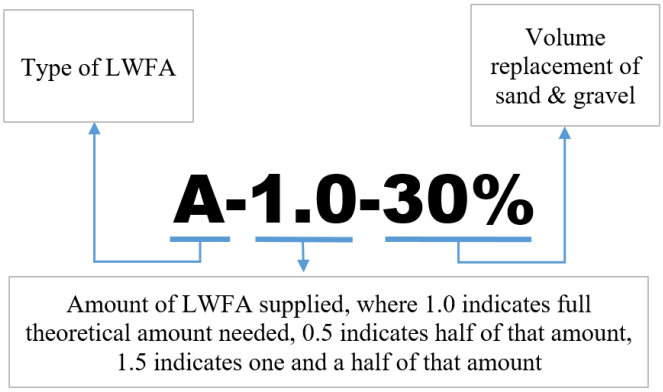

Figure 43. Explanation of mix ID

It should be noted that the same initial dosage of MRWR was utilized for all mixes, except B-1.5-54%, for the purpose of observing the effect of aggregate replacement only. If the required workability was not met, the additional MRWR was added to the mix, which is shown in the "Final' column of Table 13.

Table 13. Mix designs of Phase I

Mix ID	Cement (pcy)	Water (pcy)	Limestone (pcy)	Sand and Gravel (pcy)	LWFA (pcy)	AEA (fl oz/cwt)	MRWR (fl oz/cwt)	
							Initial	Final
Control	658	250	854	1992	0	1.5	5.0	5.0
A-0.5-14%	658	250	854	1713	212	1.5	5.0	12.5
A-1.0-29%	658	250	854	1400	450	1.5	5.0	14.0
A-1.5-43%	658	250	854	1129	636	2.5	5.0	12.0
B-0.5-18%	658	250	854	1637	239	1.5	5.0	8.0
B-1.0-36%	658	250	854	1281	477	1.5	5.0	5.0
B-1.5-54%	658	250	854	926	716	1.5	0.0	0.0
C-0.5-21%	658	250	854	1563	298	1.5	5.0	10.0
C-1.0-43%	658	250	854	1135	596	1.5	5.0	9.0
C-1.25-54%	658	250	854	921	745	1.5	5.0	13.0
C-1.5-64%	658	250	854	854	706	1.5	5.0	19.0
C-1.75-75%	658	250	854	492	1042	1.5	5.0	12.0

4.1.2 Phase I Results and Discussion

4.1.2.1 Fresh Properties

Results showed that the replacement of sand and gravel by LWFA has a significant impact on the workability of the mix. It was noticed the replacement of sand and gravel with finer LWFAs, i.e., LWFA A and C, leads to lower workability, as illustrated in Figure 44. Lower fineness modulus and/or void content of combined aggregate blend are believed to play a significant role in the workability of the mix. This significant effect will be further studied and assessed in Phase II of the project. The introduction of LWFA B, which is closer to sand and gravel in terms of gradation, resulted in a required little-to-no adjustment.

It was also observed that the slump of internal curing mixes could be closely correlated with air content. Likely due to the relatively small particle size, the introduction of LWFA tends to interference with the air entrainment in the system. As illustrated in Figure 44, some mixtures in Phase I do not necessarily have the air content within the air content limits. As the focus of Phase I study was mostly to identify the most effective types and dosages of LWFAs based on shrinkage results, the amount of air-entrainment was not adjusted in this Phase. In the Phase III study, all mixes will be adjusted to ensure to mee the air content requirement, and the corresponding slump values will be reported.

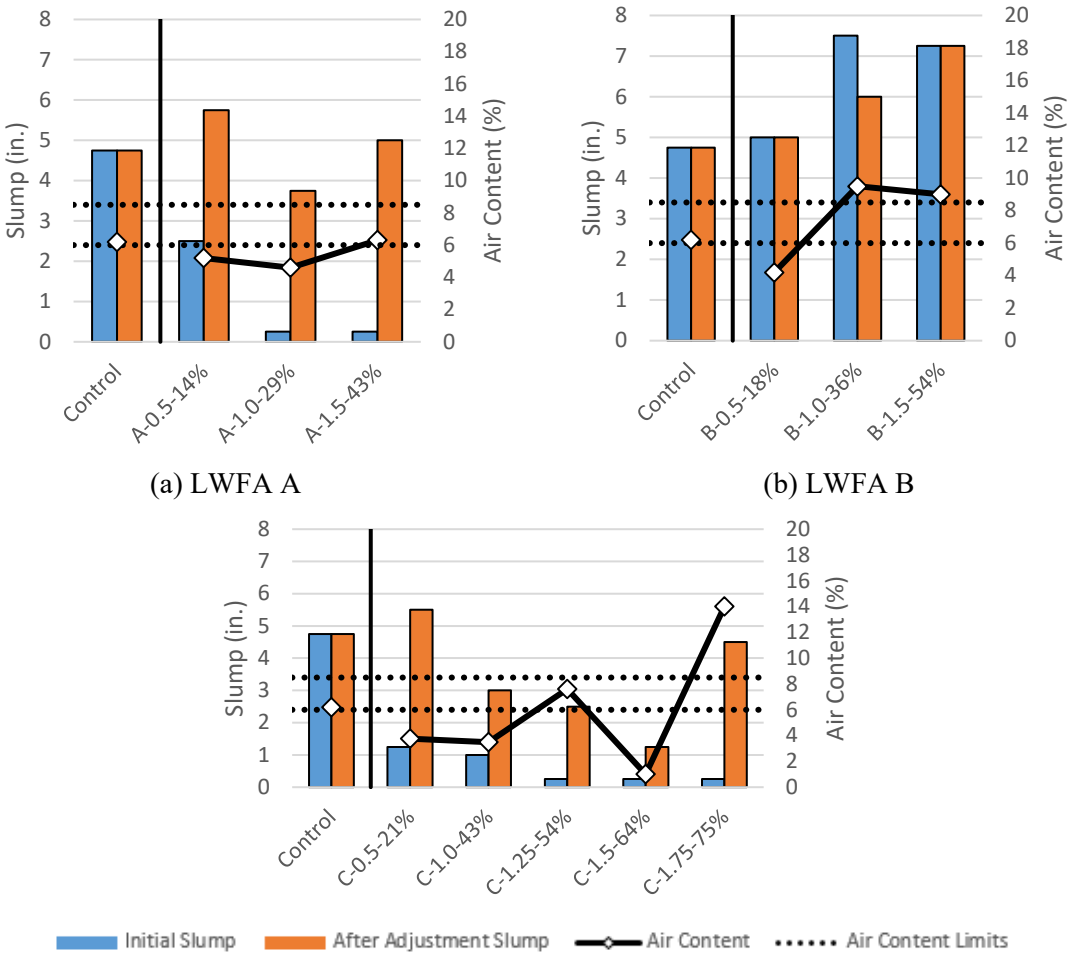

(a) LWFA A

(b) LWFA B

(c) LWFA C

Figure 44. Workability of Phase I mixes

As expected, the replacement of sand and gravel with LWFA will result in a decrease in the unit weight of the concrete mixes. A design unit weight of the control mix is 139.0 pcf, whereas the unit weights of the developed internal curing mixes varied from 125.5 to 136.5 pcf, as shown in Figure 45. The actual unit weights did not vary significantly from the design values, except for the LWFA C, which was mainly linked to the air content.

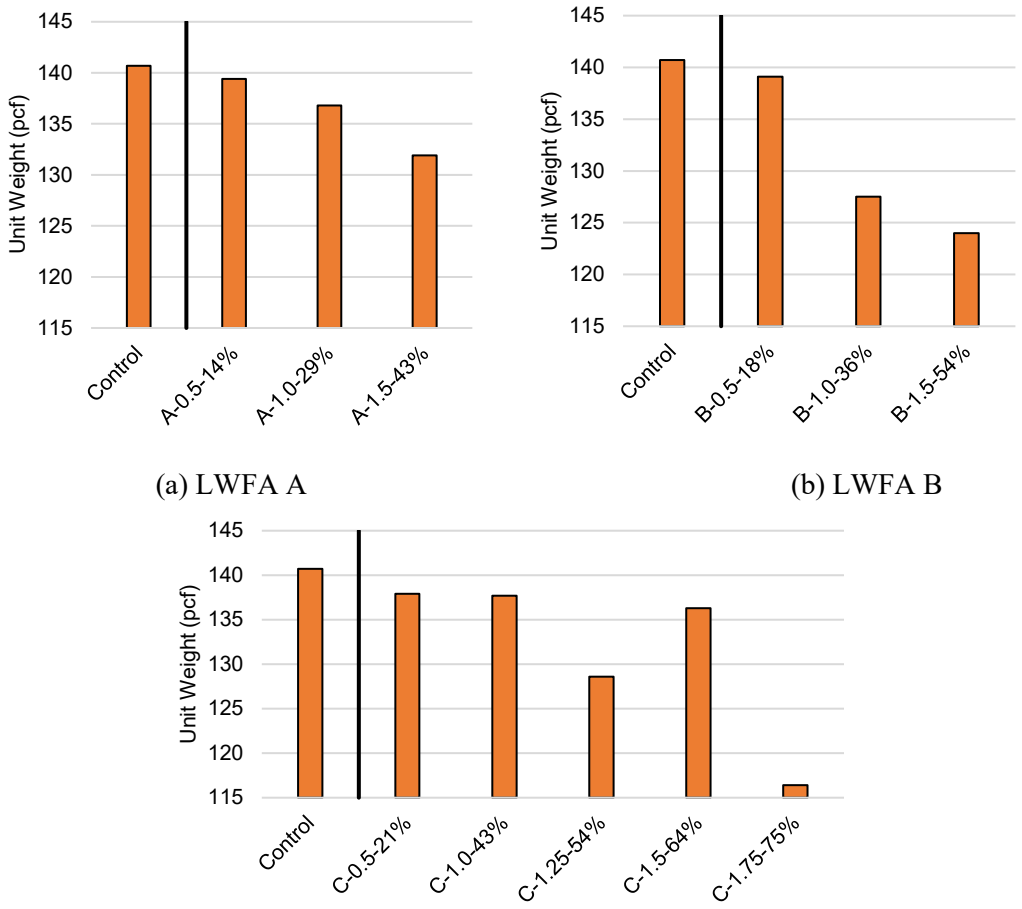

(a) LWFA A

(b) LWFA B

(c) LWFA C

Figure 45. Unit weight of Phase I mixes

4.1.2.2 Mechanical Properties

As shown in Figure 46, in general, it seems that most of the mixes are capable of reaching the NDOT 28-day requirement of 4000 psi. Similar to slump, the compressive strength of mixes can also be closely correlated to the air content. Since the air content seems to be the major influencing factor on compressive strength, a clear effect of LWFA in the compressive strength of the mixes cannot be determined at this stage.

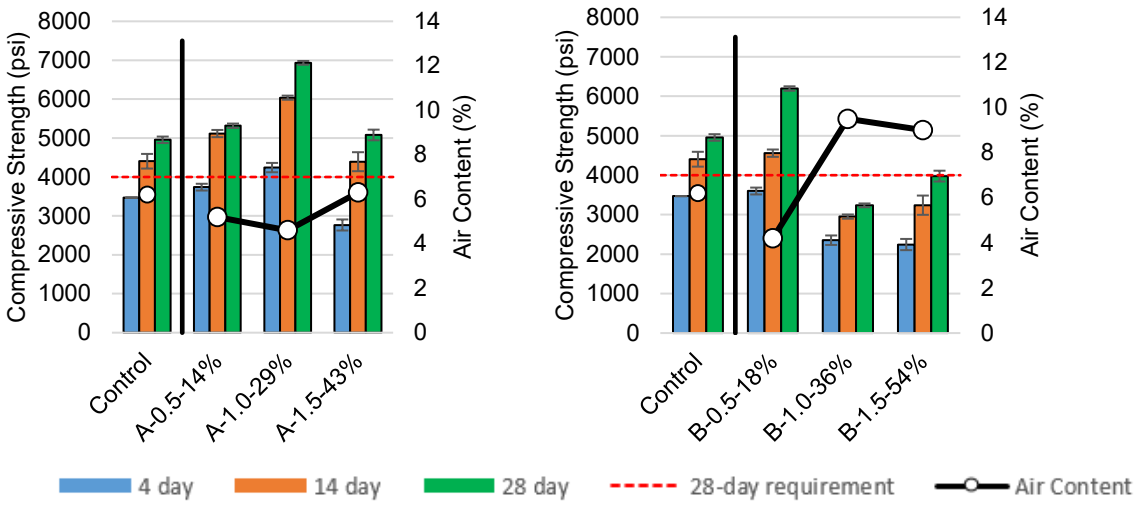

(a) LWFA A

(b) LWFA B

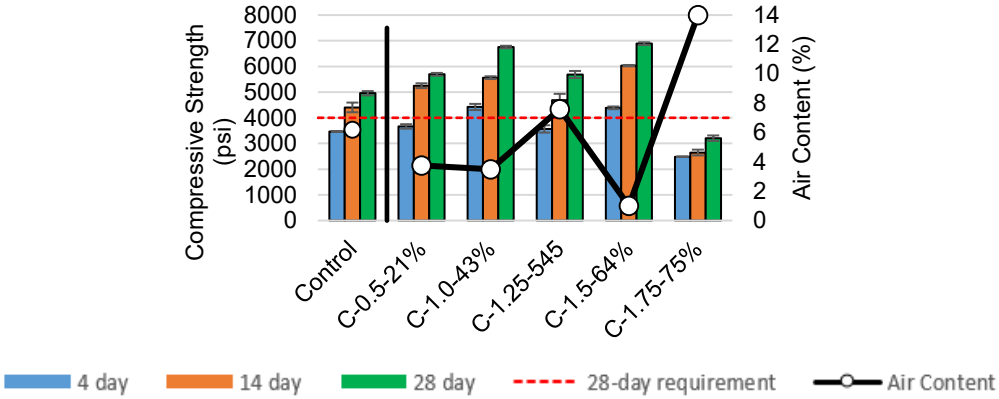

(c) LWFA C

Figure 46. Compressive strength of Phase I mixes

The important issue is the control of air content, since it has a direct influence on compressive strength, as demonstrated in Figure 47. The air content issue will be addressed in Phase II of the project, where the air-entrainment agent contents in all mixes will be adjusted to meet the air content requirement.

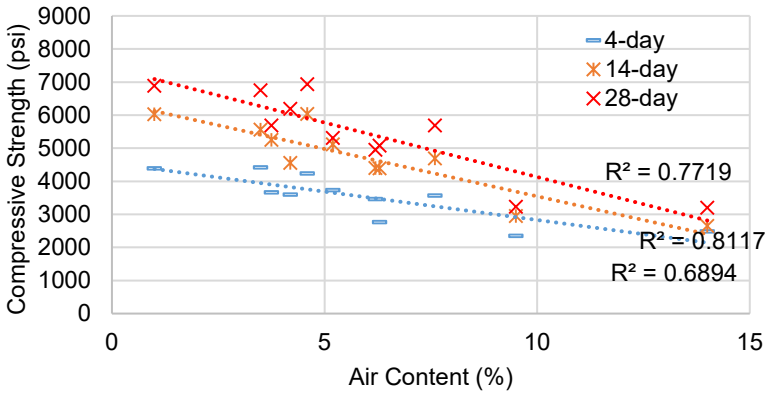

Figure 47. Correlation between compressive strength and air content for Phase I mixes

As mentioned in Chapter 2 of the report, most DOT projects on internal curing reported either no effect or a slight improvement of compressive strength, which is comparable to the findings of our project.

4.1.2.3 Durability Properties and Volume Stability

When comparing internal curing mixes with the control mix, almost all mixes, except for A-1.0-29%, yielded lower surface and bulk resistivity, as shown in Figure 48 and Figure 49, respectively. The possible reason for this feature might be the fact that both the control mix and A-1.0-29% were cured in the curing room, whereas specimens from the remaining mixes were cured in the water tank. Phase II and III will provide consistent curing conditions for all specimens.

When comparing internal curing mixes at different dosage rates of LWFA, it can be noticed that in most cases, higher replacement values lead to lower resistivity, which is attributed to the conductive characteristic of saturated porous aggregate. As showed in previous studies, it is believed that at the later stages of concrete, curing the water inside the LWFA will transport to the concrete matrix and contribute to improved hydration, which in turn will improve the electrical resistivity (Di Bella et al., 2012; Vosoughi et al., 2017).

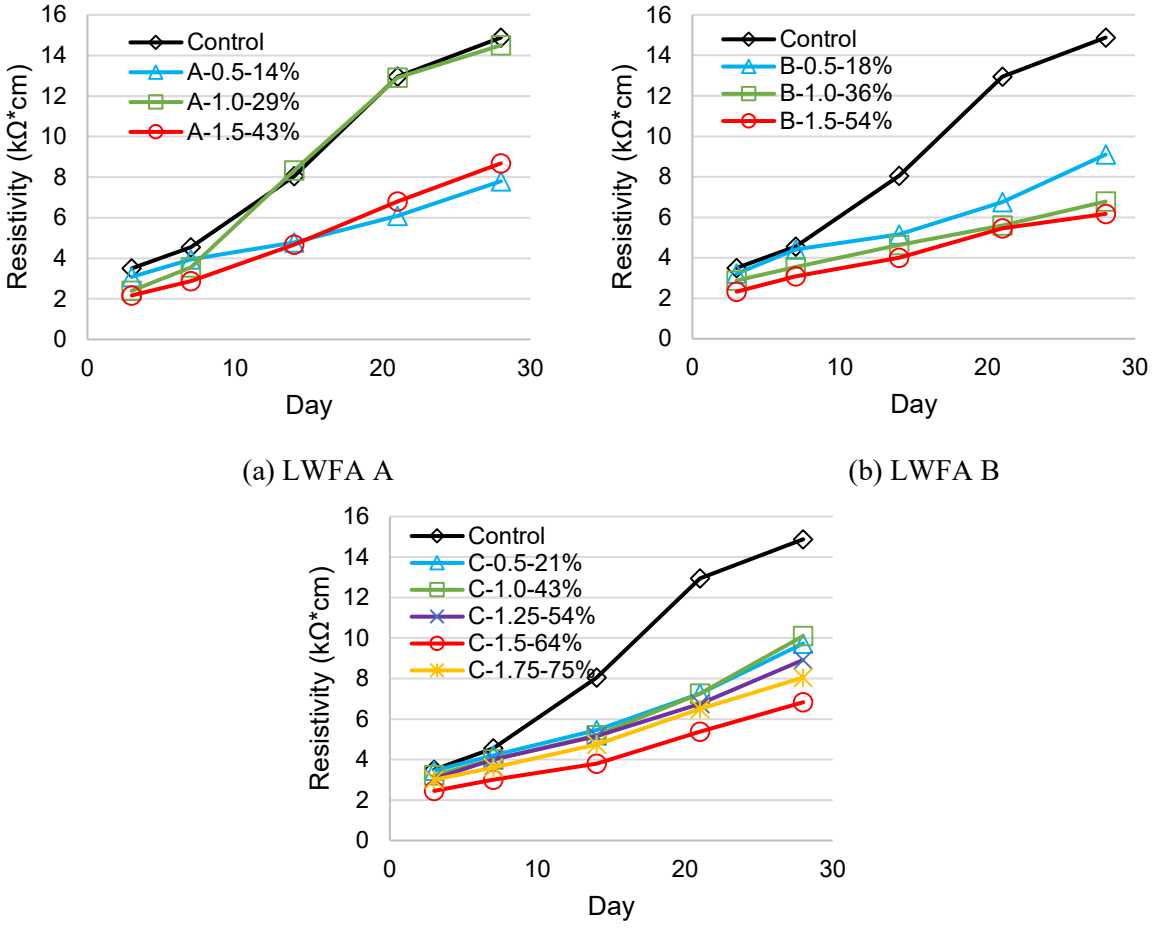

(a) LWFA A

(b) LWFA B

(c) LWFA C

Figure 48. Surface resistivity results of Phase I mixes

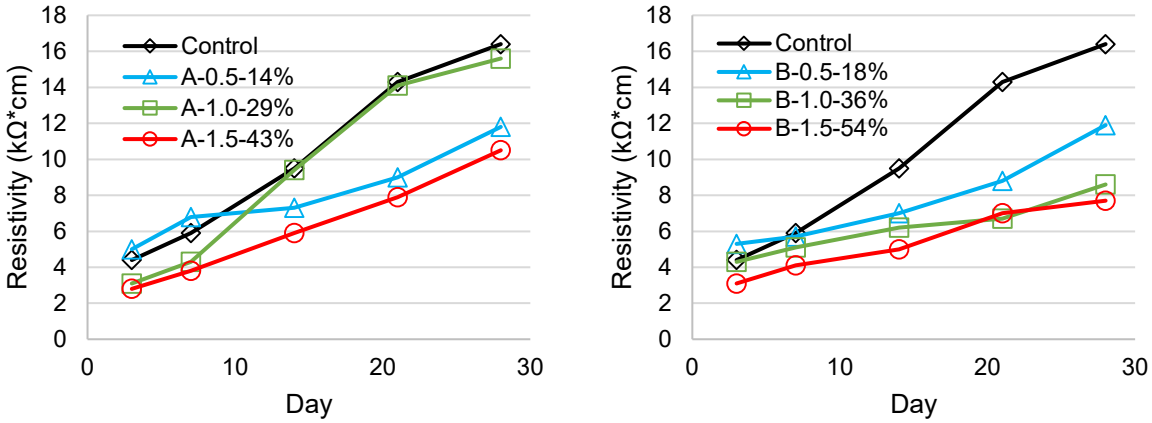

(a) LWFA A (b) LWFA B

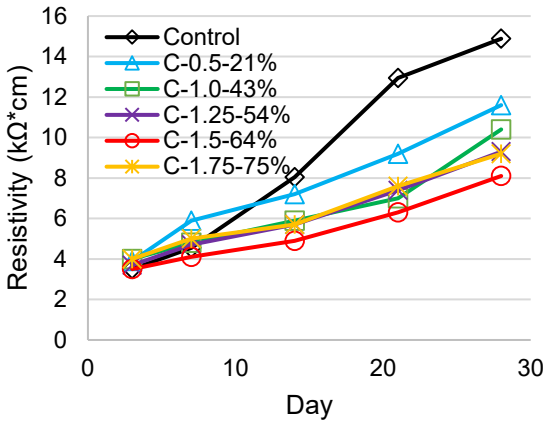

(c) LWFA C

Figure 49. Bulk resistivity results of Phase I mixes

Figure 50 provides the results on free shrinkage of sealed prisms for all mixes. It is clearly noticed that the autogenous portion of the chemical shrinkage, which is controlled by the sealed environmental condition, is significantly lower at all dosage rates of every type of LWFA compared to the control specimen.

Introducing LWFA A and LWFA B at a replacement rate of 0.5 (50% of the theoretical amount) generally results in a delayed shrinkage, meaning that the specimens were observed to shrink correspondingly with the control specimen at later age. 150% of LWFA A results in initial expansion due to the immediate abundance of curing water, which is likely attributed to a larger surface area of finer aggregates. With regards to individual LWFAs, the best performance, or in other words, the lowest autogenous shrinkage was observed at the replacement rates of 1.0 for LWFA A, at a replacement rate of 1.5 for LWFA B, and at replacement rates of 1.25, 1.5, and 1.75 for LWFA C.

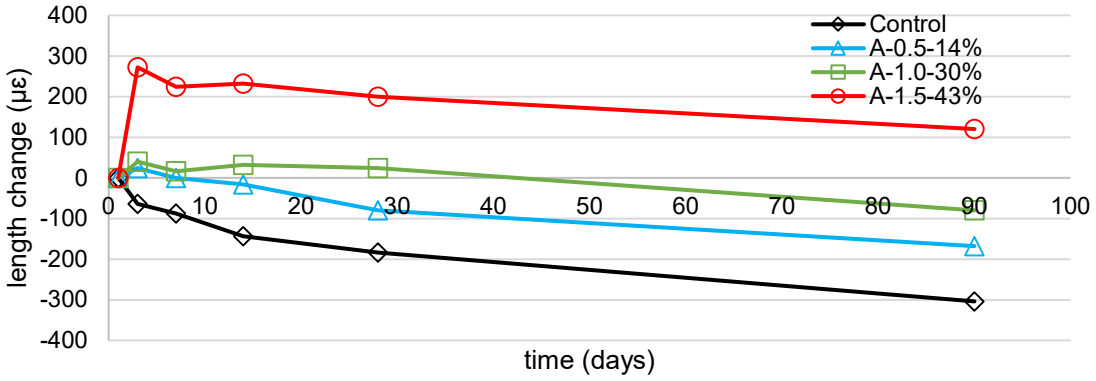

(a) Sealed condition, no curing, LWFA A

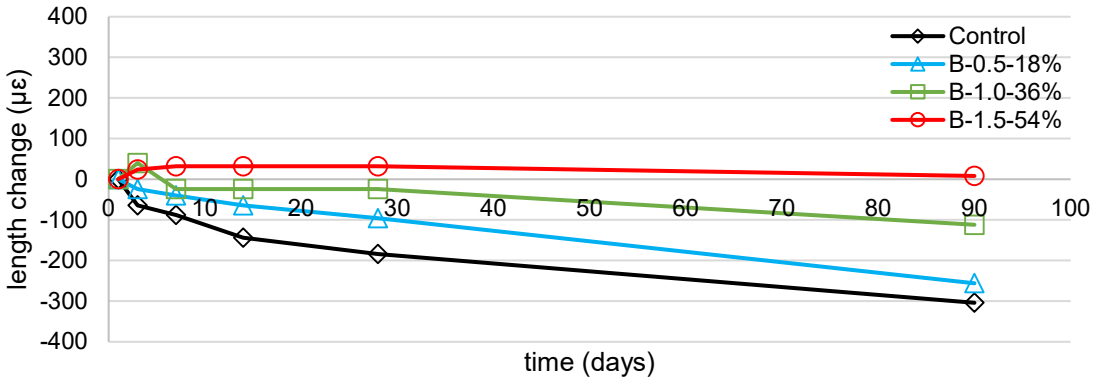

(b) Sealed condition, no curing, LWFA B

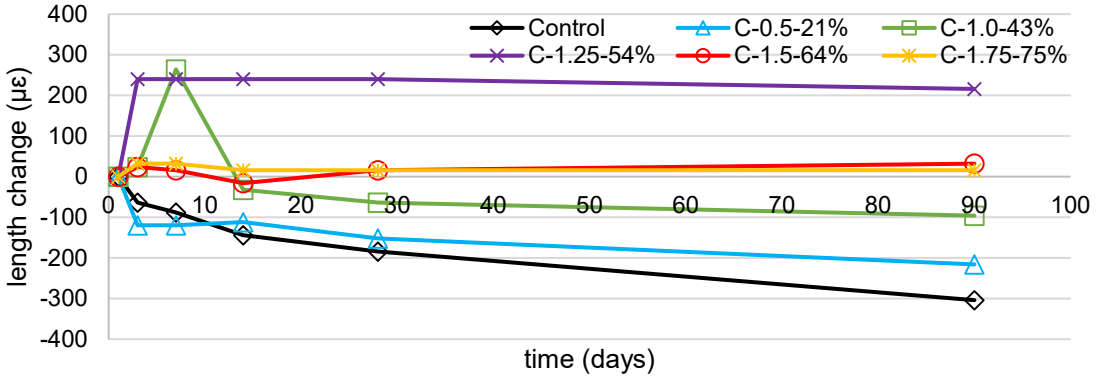

(c) Sealed condition, no curing, LWFA C

Figure 50. Free shrinkage of uncured specimens at sealed condition of Phase I mixes

As shown in Figure 51, with regards to free shrinkage at the drying environmental conditions, a similar trend was observed for LWFA A and B, matching to the control line. In addition, a higher dosage of LWFA results in higher shrinkage, which is believed to be a direct impact from two factors:

- Varying modulus of elasticity, which will be evaluated in Phase III of the project;
- Water loss, which is larger with a higher dosage of LWFA, as shown in Figure 52;

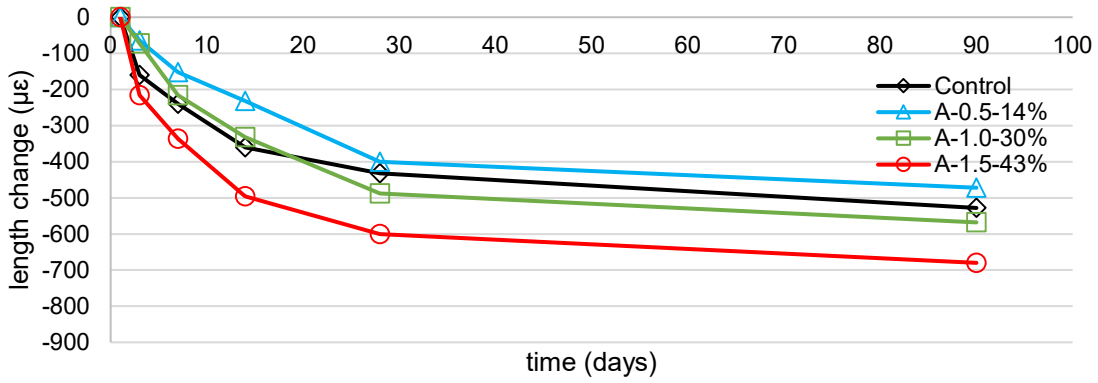

(a) Drying condition, no curing, LWFA A

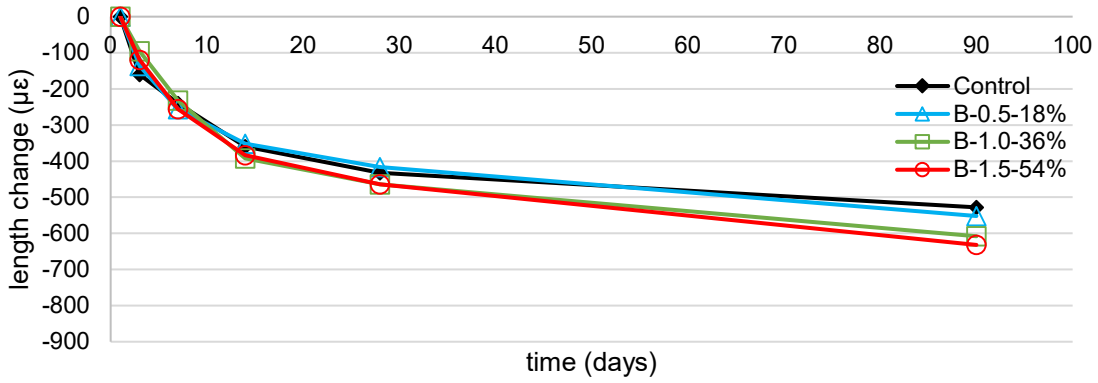

(b) Drying condition, no curing, LWFA B

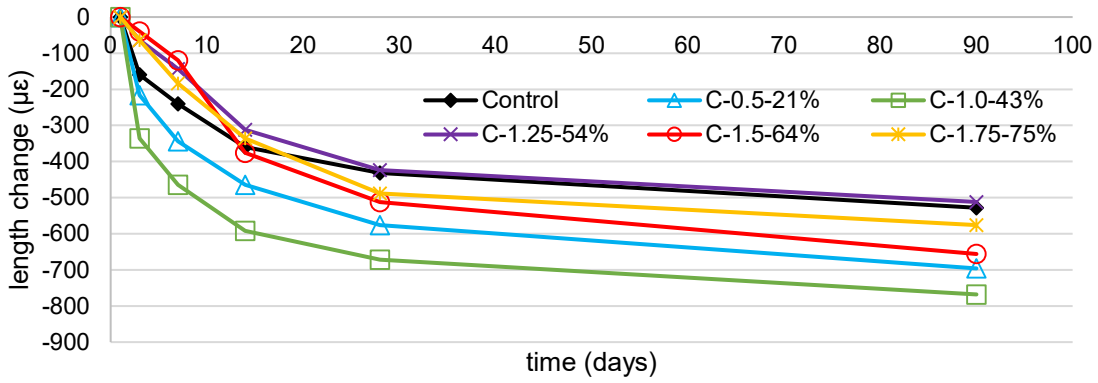

(c) Drying condition, no curing, LWFA C

Figure 51. Free shrinkage of uncured specimens at drying condition, Phase I

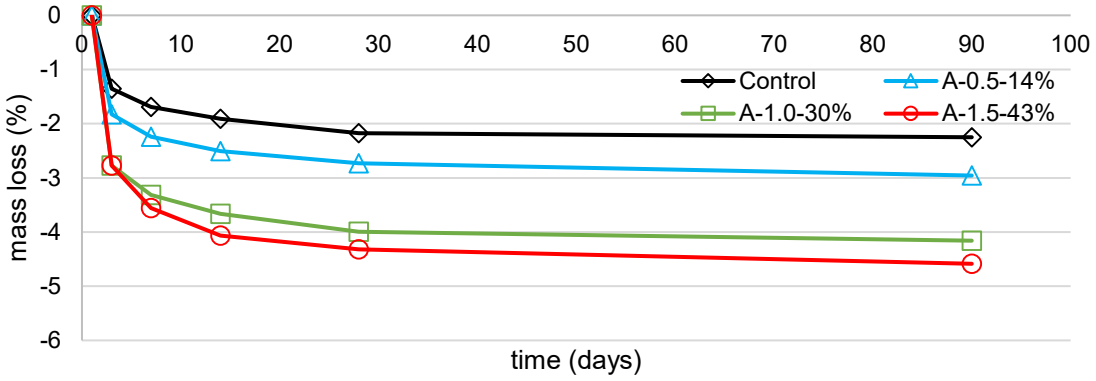

(a) Mass loss, LWFA A

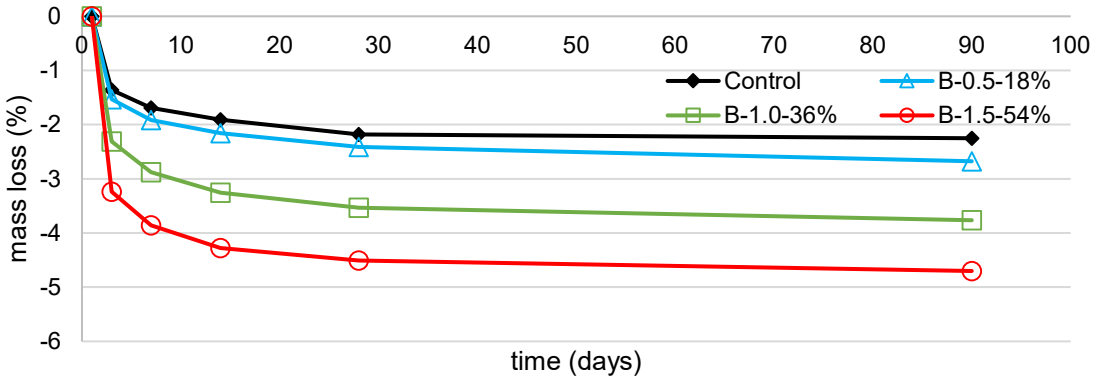

(b) Mass loss, LWFA B

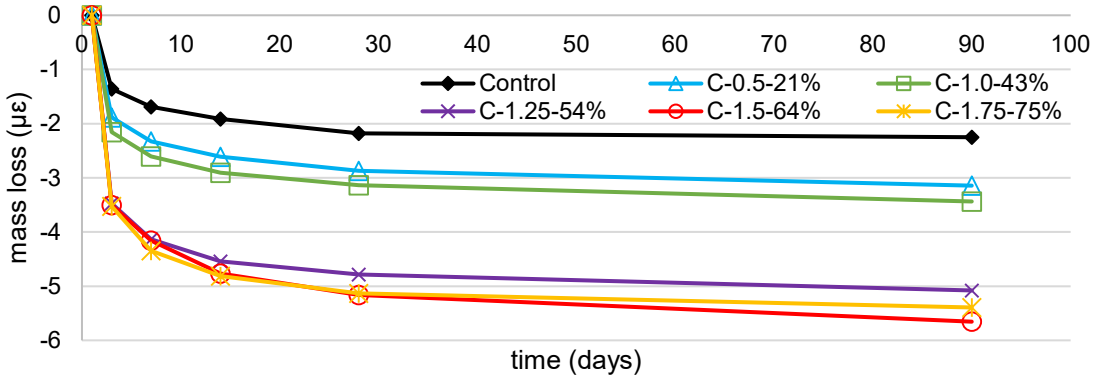

(c) Mass loss, LWFA C

Figure 52. Moisture loss of samples at drying condition from Figure 51

Figure 53 provides the results for the restrained shrinkage test for all mixes of Phase I. Results showed that, in general, the introduction of LWFA improves restrained shrinkage test

results at all ages. Both delayed cracking age and lower strain at the crack are observed in most of the cases.

Results also showed that overdosage of LWFA, as it can be noticed for the case of LWFA A, does not necessarily improve restrained shrinkage behavior. On the other hand, under dosage of LWFA resulted in poor restrained shrinkage behavior compared to those of dosage 1.0 in all cases.

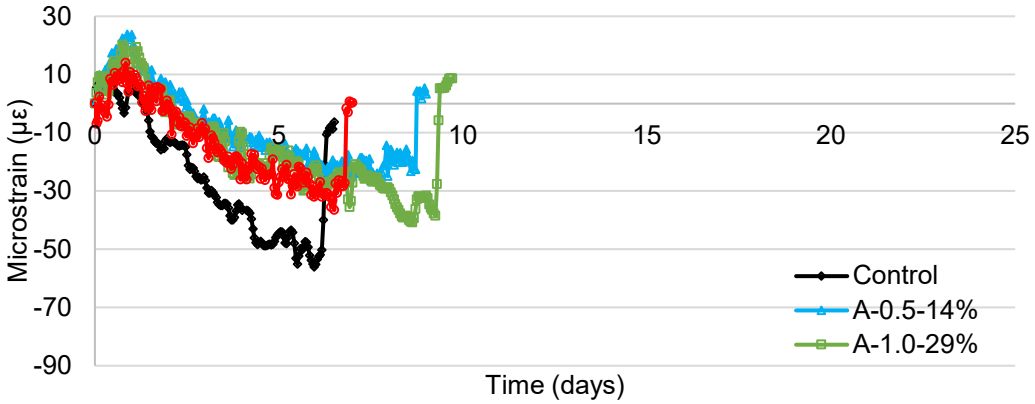

(a) Restrained shrinkage, LWFA A

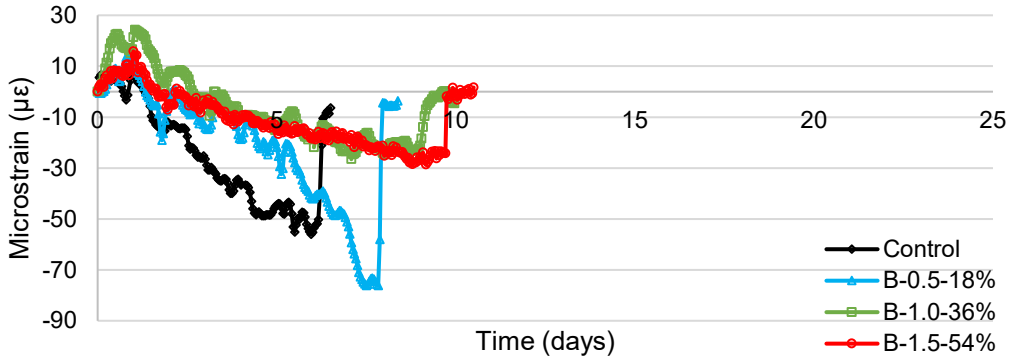

(b) Restrained shrinkage, LWFA B

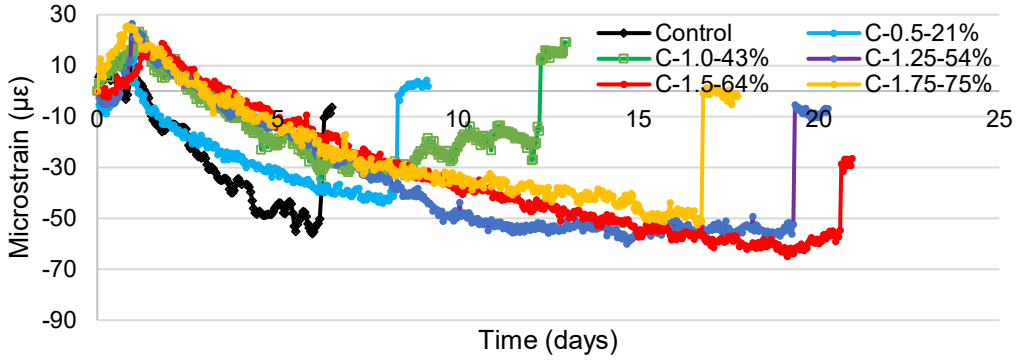

(c) Restrained shrinkage, LWFA C

Figure 53. Restrained shrinkage test results

Table 14 summarizes the cracking age of the restrained shrinkage rings from different mixes. As it can be observed from both Figure 53 and Table 14, the introduction of LWFAs successfully delays the cracking age of concrete rings. Even though almost all mixes experienced slightly higher free shrinkage at drying conditions, which was previously illustrated in Figure 51, the same concrete cracked at a much later age. This observation can be explained by the fact that modulus of elasticity of internally cured concrete decreases, which means that the same level of free shrinkage in internally cured concrete and conventional concrete is caused actually by the lesser amount of internally built pressure in the former. This reasoning will be further observed and discussed in Phase III of the project.

It is worth noting that since the free shrinkage test setup has the test specimens experiencing a very aggressive drying condition and not necessarily reflect the real field situation, results from the test were not considered in determining the most promising types and dosages of LWFA for internal curing. Since restrained shrinkage test setup simulates testing environment and conditions, which are the most similar to the real-case situation, the results of the test were utilized as a basis for the selection of potential mixes. Mixes A-1.0-29%, and C-1.25-54% were chosen to be studied further.

Table 14. Summary of restrained shrinkage cracking age in Phase I mixes

Dosage	LWFA A	LWFA B	LWFA C	Control
0.5	8.75 days	7.75 days	8.25 days	6.25 days
1.0	**9.25 days**	9.00 days	12.25 days	
1.25	-	-	**19.25 days**	
1.5	6.75 days	9.75 days	20.50 days	
1.75	-	-	16.75 days	

4.2 Phase II - Aggregate Blend Optimization

Results from Phase I study revealed a strong need to address the workability issue of internally cured concrete. The replacement of sand and gravel with finer LWFA adversely impacted the workability of the mix. As it was covered in Chapter 2, the aggregate blend gradation plays a vital role in the workability of the mix. The main aims of Phase II are to analyze the effect of plain aggregate replacement on aggregate blend gradation, to optimize the mix in order to have better compaction and workability, and compare to the mix complying to NDOT specifications (70SG:30LS).

Based on results of Phase I study, it was decided to continue the study with LWFA A and C at the dosage rate of 1.0 and 1.25 respectively, which correspond to 423.7 pcy (20.4% by volume of the aggregate blend) and 744.5 pcy (38.0% by volume of the aggregate blend) of LWFA respectively. The volume of LWFA in the aggregate blend will remain constant, and only the volumetric portions of limestone and sand and gravel are varied. The detailed process of mix adjustment will be explained further.

Following properties of concrete were studied in Phase II:

- Aggregate testing: combined void content test;
- Fresh concrete properties: slump, air content, and unit weight;
- Hardened concrete properties: compressive strength, and electrical resistivity;

- Volume stability: free shrinkage at sealed and drying environmental conditions with no curing, and restrained shrinkage

4.2.1 Phase II Mix Designs

Mix designs for concrete mixtures included in the Phase II study are shown in Table 15. The justification of each aggregate amount is explained in the next section. It should be noted that the same initial dosage of MRWR as in Phase I was utilized for both mixes to observe the effect of aggregate replacement on workability. If the required workability was not met, additional MRWR was added to the mix. The sum of initial and additional MRWR is shown in the column identified as "Total" in Table 15.

Table 15. Mix designs of Phase II study

Mix ID	Cement (pcy)	Water (pcy)	Limestone (pcy)	Sand and Gravel (pcy)	LWFA (pcy)	AEA (fl oz/cwt)	MRWR (fl oz/cwt)	
							Initial	Total
A-1.0-OPT	658	264	1438	851	424	1.5	5.0	5.0
C-1.25-OPT	658	264	1291	497	745	1.5	5.0	10.0

4.2.2 Phase II Results and Discussion

4.2.2.1 Particle Packing of LWFA A

It was discussed previously that the volumetric proportion of each LWFA in the aggregate blend would remain constant in the mix. That value corresponds to 0.204 for LWFA A and 0.380 for LWFA C. In order to adjust the mix, void contents of each individual aggregate were evaluated first, which are shown in Table 16.

Table 16. Void contents of individual aggregate

Aggregate	Limestone	Sand and Gravel	LWFA A	LWFA C
Void content (%)	38.5	27.3	25.7	34.4

Experimental combined void content test for various proportions of limestone and sand and gravel was conducted for both LWFA A and LWFA C. As shown in Figure 54, the dotted black line represents the void content of the aggregate blend of control mix. Again, the volume of each LWFA was kept constant, and only the relative amount of limestone and sand and gravel has been varied. The x-axis represents the volumetric fraction of limestone in the aggregate blend only and not the entire mix. As shown in Equation 10, the volumetric fraction of the sand and gravel can be estimated by subtracting the volumetric fraction of limestone and the corresponding LWFA from 1.0.

$$Vol.Pr.of\ S\&G = 1.0 - Vol.Pr.of\ LS - Vol.Pr.of\ LWFA \qquad \textbf{(Eq. 10)}$$

For example, a volumetric fraction of 0.494 for the case of LWFA A means that sand & gravel occupies 0.302 of the aggregate blend by volume.

$$Vol.Pr.of\ S\&G = 1.0 - 0.494 - 0.204 = 0.302$$

The experimental void content test results were also compared to theoretical values computed from Modified Toufar model, which was described in Chapter 2. The model is proven to be the most suitable for the pavement concrete of Nebraska in a recently completed NDOT study (Mamirov et al., 2020).

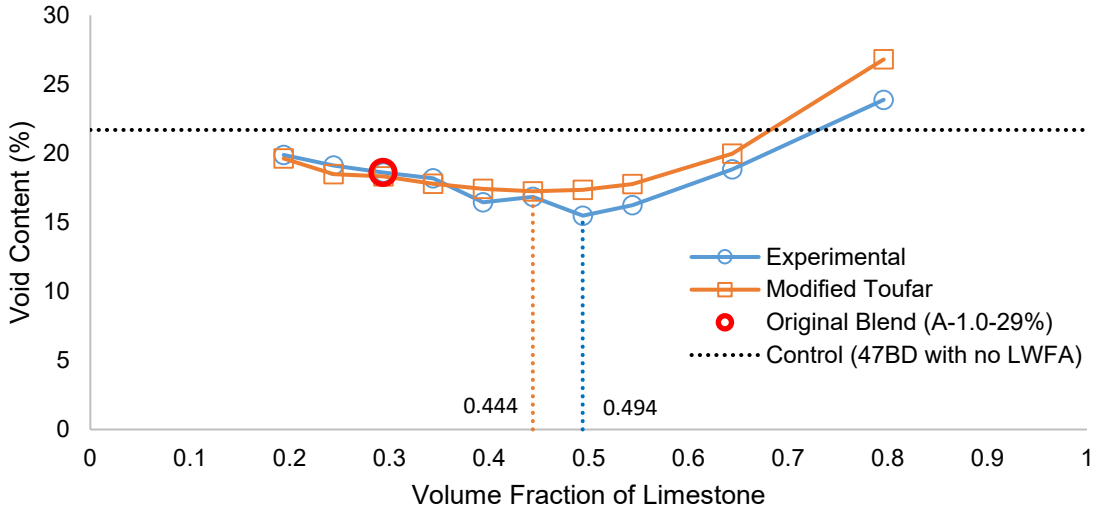

(a) LS-SG-LWFA A aggregate blend, vol. fraction of LWFA A = 0.204

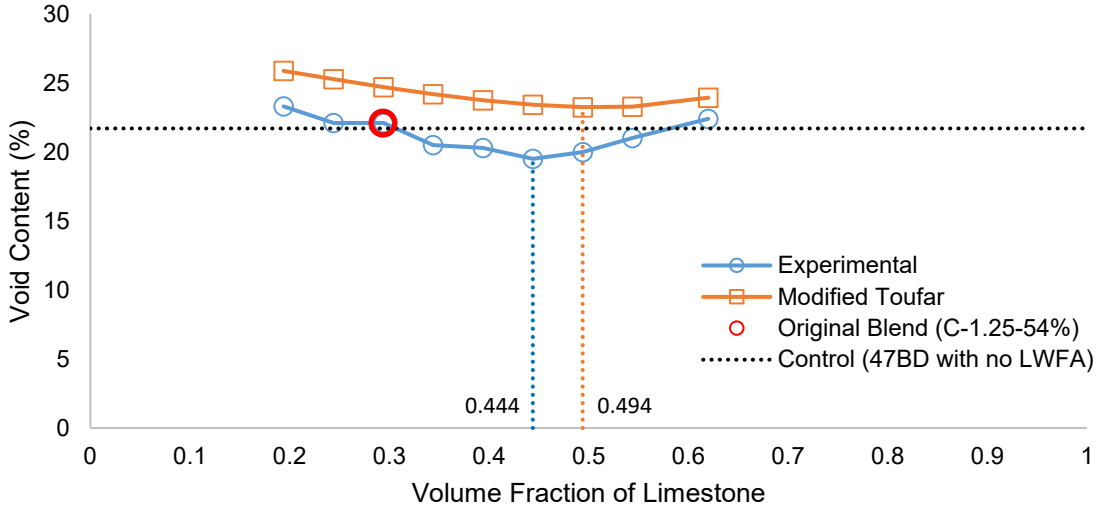

(b) LS-SG-LWFA C aggregate blend, vol. fraction of LWFA C = 0.380

Figure 54. Combined void content test results compared with theoretical values

Results from Figure 54 illustrate that aggregate blends of mixes from Phase I, which are denoted by thick red circles, do not provide the best compaction degree. Based on the experimental test results, the best compaction is achieved at the following aggregate proportions:

- LWFA A: 0.494-0.302-0.204 (LS-SG-LWFA A, respectively). The combined void content of the blend is 15.5%, compared to 21.7% of the control mix with no LWFA (47BD) and 18.6% of the original blend (A-1.0-29%).
- LWFA C: 0.444-0.176-0.380 (LS-SG-LWFA C, respectively). The combined void content of the blend is 19.5%, compared to 21.7% of the control mix with no LWFA (47BD) and 22.1% of the original blend (C-1.25-54%).

The experimental results are also supported by the theoretical values from the Modified Toufar model. Although the results did not match identically, a close correlation with the

theoretical model can be observed. Finally, a decision on the blend selection was made based on the experimental test results and following are the final aggregate blend proportions and their corresponding mix IDs, which will be further evaluated in Phase II study:

- A-1.0-OPT: 0.494-0.302-0.204 (LS-SG-LWFA A respectively);
- C-1.25-OPT: 0.444-0.176-0.380 (LS-SG-LWFA C respectively);

The need for blend adjustment of selected aggregate blends was further justified and compared to Phase I mixes in terms of various empirical models and theoretical concepts related to workability.

Figure 55 illustrates that the introduction of and further increase in the dosage of both LWFA reduces the fineness modulus of the aggregate blend. The consequent increase in the total aggregate surface area with the paste volume remaining constant may harm the workability of the mix, which was observed in Phase I results. Optimized mixes, on the other hand, resulted in the increase in the total fineness modulus of both blends.

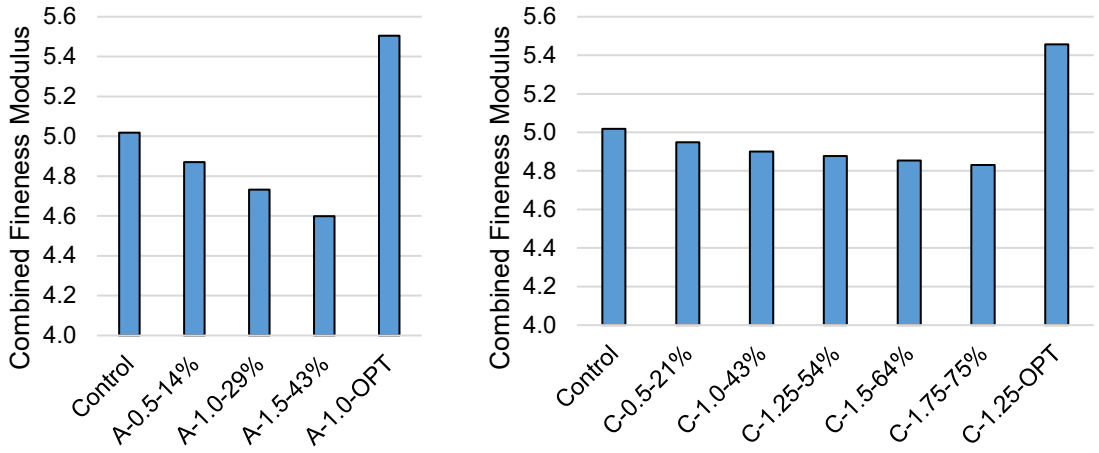

(a) LWFA A **(b)** LWFA C

Figure 55. Combined fineness moduli of Phase I and Phase II aggregate blends

Figure 56 illustrates the aggregate gradation of Phase I and II mixes in a 0.45 power gradation chart. As mentioned earlier in Chapter 2, the ideal compaction case is represented by the black dotted line. The closer the blend gradation curve to the dotted line, the better compaction is. As can be noticed, the introduction of and further increase in the dosage of both LWFA shifts the curve to the left, which means that the gradation becomes more disturbed, and the workability of the mix can be negatively influenced by that shift. The optimized aggregate blends, on the other hand, are better graded and closer to the best-fit line.

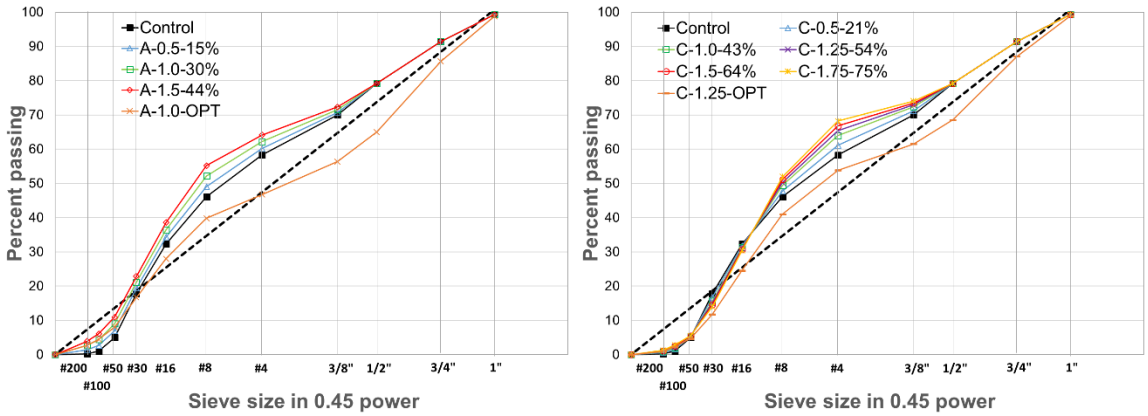

(a) LWFA A (b) LWFA C

Figure 56. 0.45 power gradation chart with Phase I and II aggregate blends

Figure 57 shows the Shilstone chart with the mixes from Phase I and II. Results showed that every mix, including the control mix, are located in Zone I, which refers to the zone with excess fines. Moreover, the higher dosage of LWFA aggravated the situation and moved the blend further from the optimum zone (Zone II). The optimized aggregate blends for both LWFAs are located exactly at the transition line between Zones I and II. Results showed that the Shilstone chart also supports the selection of optimized blends.

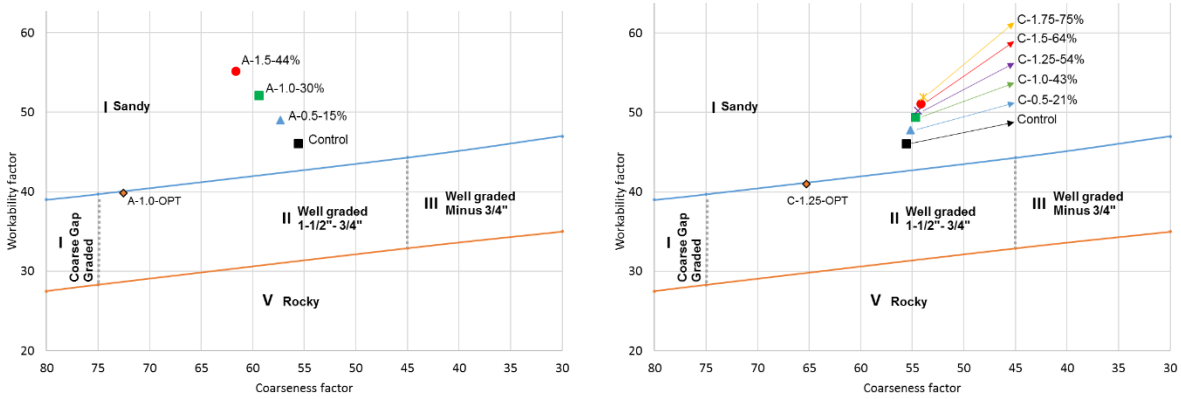

(a) LWFA A (b) LWFA C

Figure 57. Shilstone chart with Phase I and II aggregate blends

To summarize, the aggregate blends of A-1.0-29% and C-1.25-54% were optimized to achieve the highest degree of compaction based on the experimental combined void content test. The selection of optimized blends for LWFAs A and C was further justified by theoretical particle packing model, various empirical models, and theoretical concepts.

4.2.2.2 Fresh Properties

The effect of the optimized aggregate gradation on fresh concrete properties is discussed in this section. Figure 58 compares the slump of optimized mixes with the corresponding mixes from Phase I, as well as with the control mix. It can be noticed that with the optimized aggregate blend, the initial dosage of MRWR (5.0 fl oz/cwt) resulted in better workability for both LWFAs.

Mix A-1.0-OPT has met the workability requirements with a slump of 5.25," and no additional MRWR was necessary, whereas an additional 9.0 fl oz/cwt of MRWR was necessary for A-1.0-29% to increase the slump from 0.25" to 3.75" before aggregate blend optimization.

Even though the additional MRWR was necessary for C-1.25-OPT, the needed additional amount of chemical admixture was lesser compared to those of C-1.25-54%, at 5.0, and 8.0 fl oz/cwt respectively.

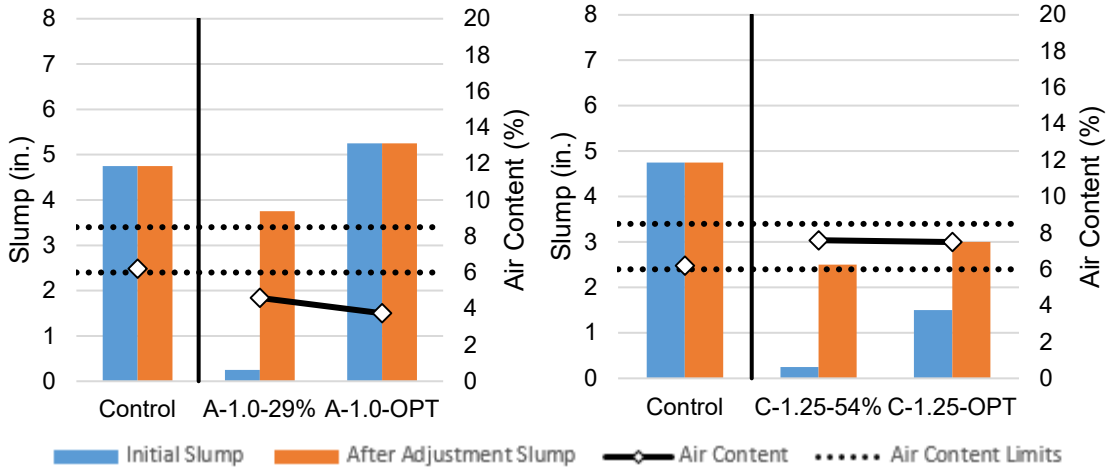

(a) LWFA A **(b)** LWFA C

Figure 58. Workability of Phase II mixes compared to Phase I mixes

As expected, the unit weight of internally cured concrete was lower for almost all cases, as illustrated in Figure 59. The fact that as-cast unit weights are slightly higher than the design unit weights is attributed to the low air content of the mixes. As it was mentioned before, the air content requirements will be adjusted in Phase III study.

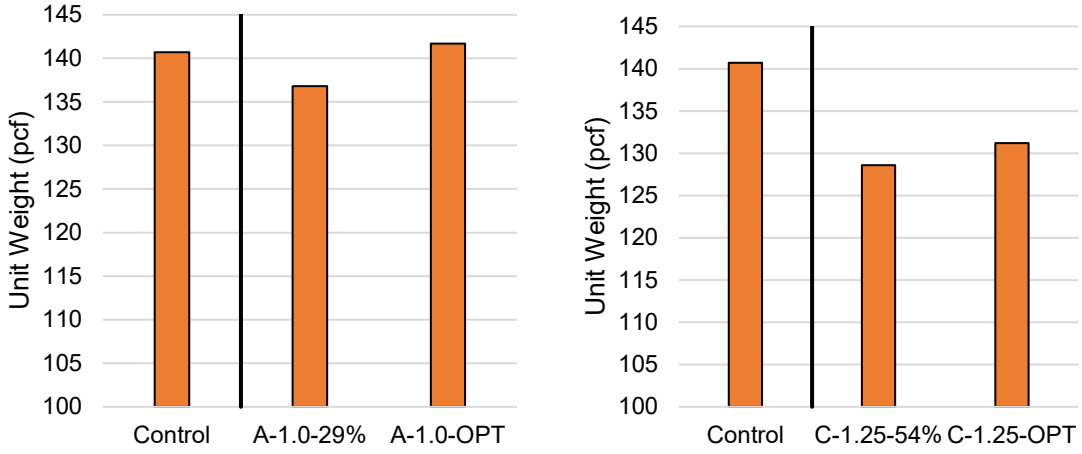

(a) LWFA A **(b)** LWFA C

Figure 59. Unit weight results of Phase II mixes

In general, optimized aggregate blends of Phase II mixes were mostly able to address the workability issues Phase I mixes. The overall aim of Phase II study was successfully met. Results of the mechanical, durability, and volume stability of the optimized mixes, are to be presented and discussed next.

4.2.2.3 Mechanical Properties

Results from the compressive strength test of mixes with optimized aggregate blends are presented in Figure 60, where they are also compared to those of the control mix and corresponding internally cured mixes from Phase I study. It should be noted that no clear effect of aggregate blend optimization on compressive strength was observed. Although the compressive strength of A-1.0-OPT is slightly lower compared to standard A-1.0-29% mix, it is higher than those of the control mix, and it still meets the 28-day compressive requirement.

In the case of LWFA C, no significant effect of aggregate blend optimization is observed. The results are comparable for both C-1.25-54% and C-1.25-OPT.

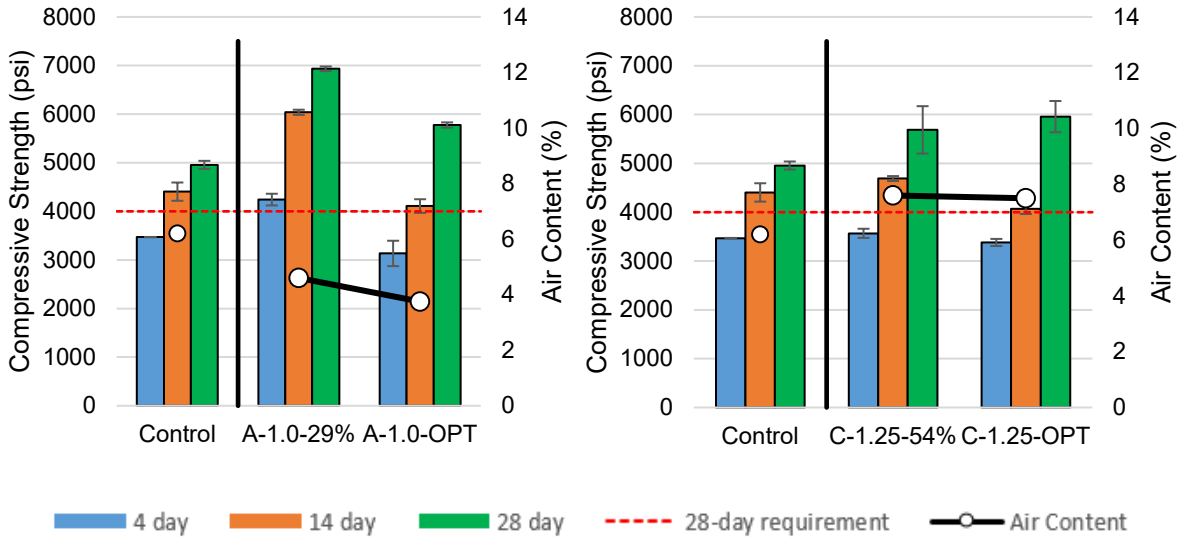

(a) LWFA A (b) LWFA C

Figure 60. Compressive strength results of Phase II mixes

Based on the results of the mechanical properties of Phase II mixes, it can be concluded that while both optimized mixes met 28-day requirements, compressive strength is not affected greatly by the aggregate blend optimization.

4.2.2.4 Durability Properties and Volume Stability

As shown in Figure 61 and Figure 62, the same overall trend of the surface and electrical resistivity as in Phase I can be observed. As was previously explained, the saturated LWFA act as the conductive medium, which results in lower resistivity at an early age, when the aggregates are still saturated.

The optimized aggregate blend resulted in a higher surface and bulk resistivity for the case of C-1.25-OPT compared to those of C-1.25-54%. Although it is still lower compared to the control mix, it can be noticed that at later ages, i.e., 28 days, the rate of resistivity increase becomes higher and almost reaches the bulk resistivity of the control mix. As was mentioned in earlier, for

internally cured concrete, it is not uncommon to have lower resistivity at an early age. However, at later ages, the rate of resistivity increase will become higher and will eventually exceed conventional concrete.

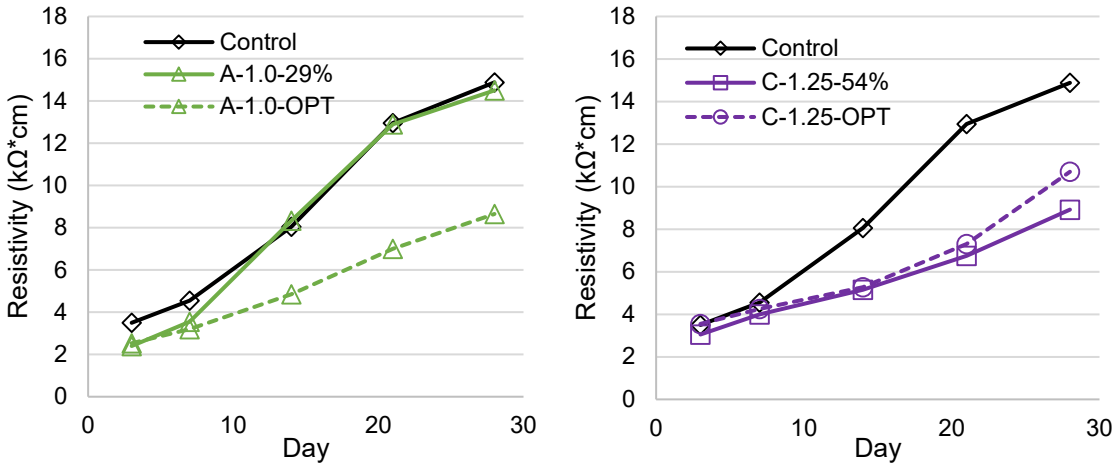

(a) LWFA A (b) LWFA C

Figure 61. Surface resistivity results, Phase II

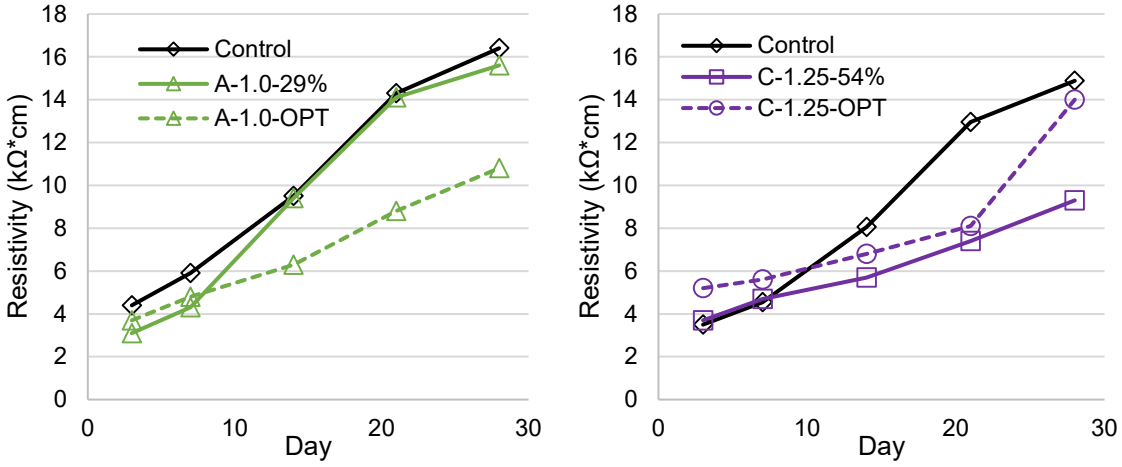

(a) LWFA A (b) LWFA C

Figure 62. Bulk resistivity results, Phase II

Figure 63 illustrates the free shrinkage results of specimens in a sealed condition for both LWFAs. The results are also compared to those of the control mix and corresponding internally cured mixes from Phase I. In general, it can be stated the overall trend of autogenous shrinkage is the same for both A-1.0-OPT and C-1.25-OPT in comparison with their corresponding mixes from Phase I. The only major difference is that no early expansion was observed in C-1.25-OPT. Other than that, both optimized mixes were observed to have horizontal lines, which means almost no autogenous shrinkage.

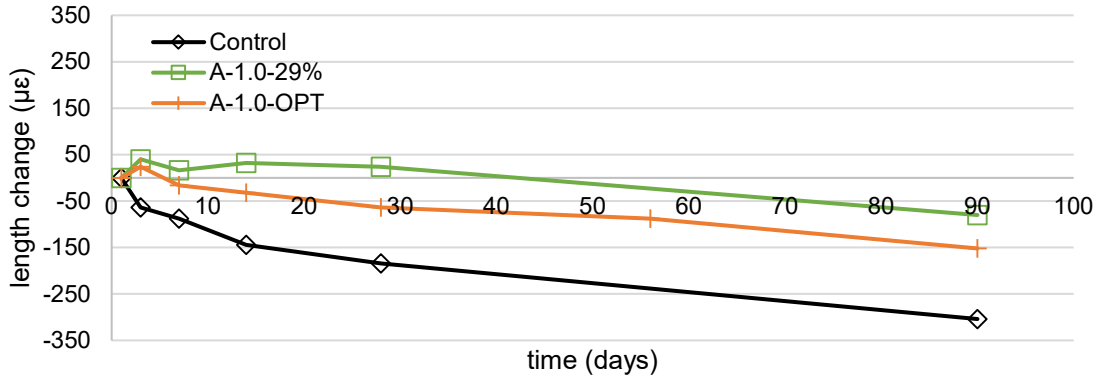

(a) Sealed condition, no curing, LWFA A

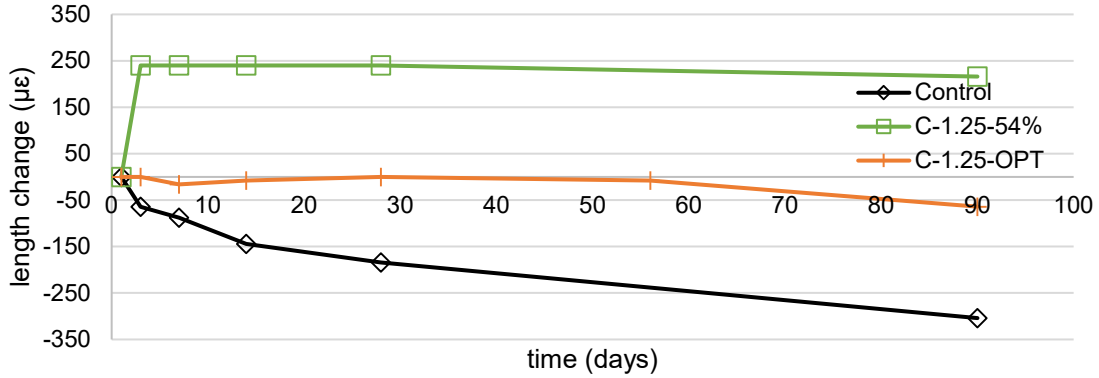

(b) Sealed condition, no curing, LWFA C

Figure 63. **Free shrinkage of uncured specimens at sealed conditions of Phase II mixes**

Free shrinkage of the specimens at drying conditions for the same mixes is shown in Figure 64. The same trend relative to their corresponding Phase I mixes is observed here as well. The free shrinkage at drying condition of A-1.0-OPT and C-1.25-OPT is comparable and close to A-1.0-29% and C-1.25-54%, respectively.

Moisture loss of samples at drying conditions is provided in Figure 65. The moisture loss is observed to be consistent and comparable between mixes with identical aggregates.

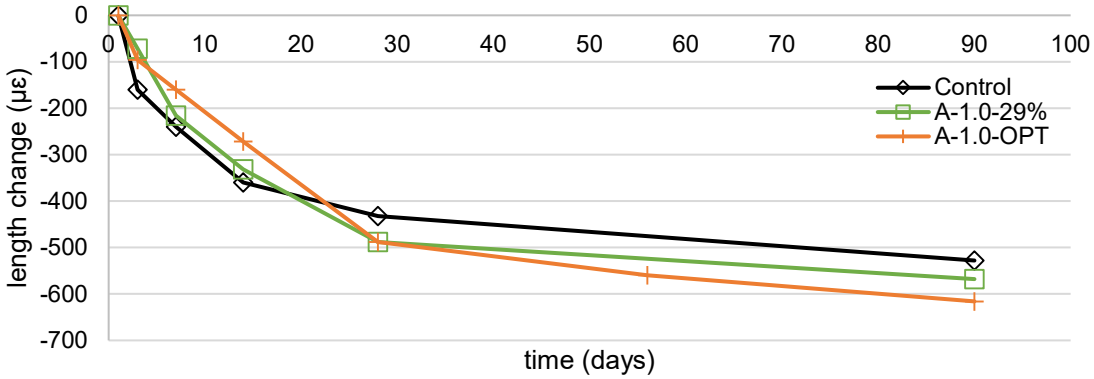

(a) Drying condition, no curing, LWFA A

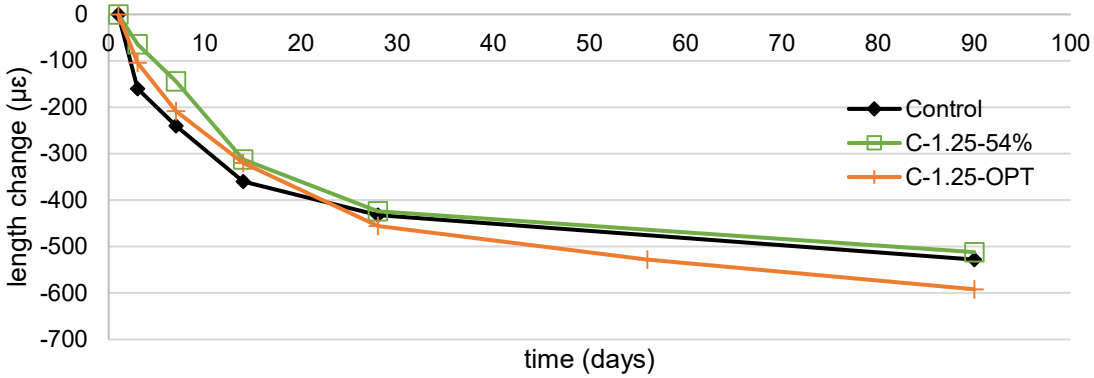

(b) Drying condition, no curing, LWFA C

Figure 64. Free shrinkage of uncured specimens at drying conditions of Phase II mixes

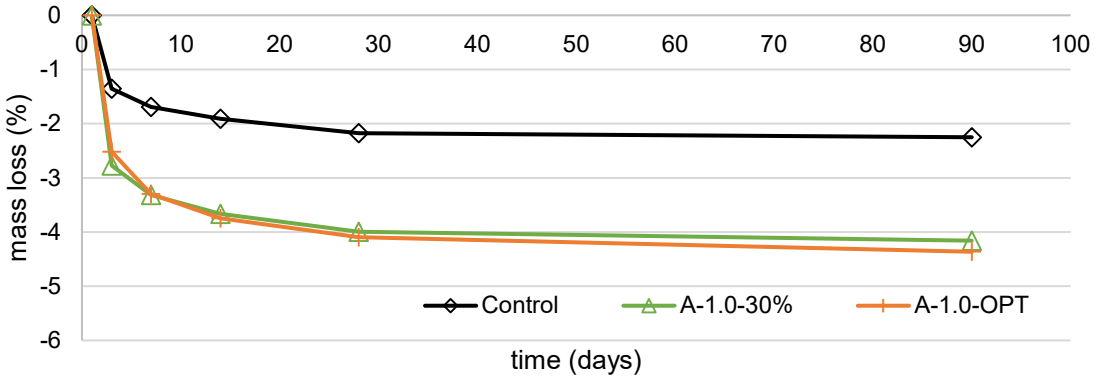

(a) Mass loss, LWFA A

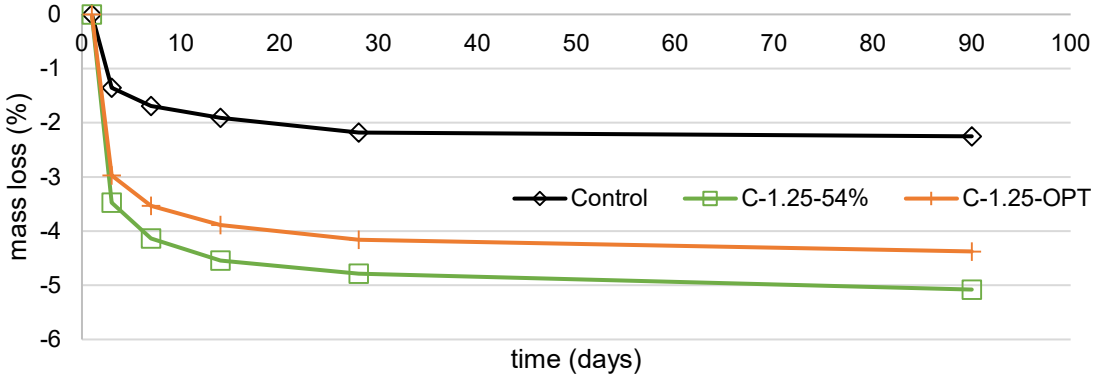

(b) Mass loss, LWFA C

Figure 65. Moisture loss of specimens from Phase II mixes

The restrained shrinkage curves and cracking age data are shown in Figure 66 and Table 17, respectively. The aggregate blend optimization did not have a significant impact on the mix with LWFA A, with their cracking age difference being only 0.50 days. However, with regards to LWFA C, the optimized blend C-1.25-OPT cracked 4.50 days earlier than C-1.25-54%.

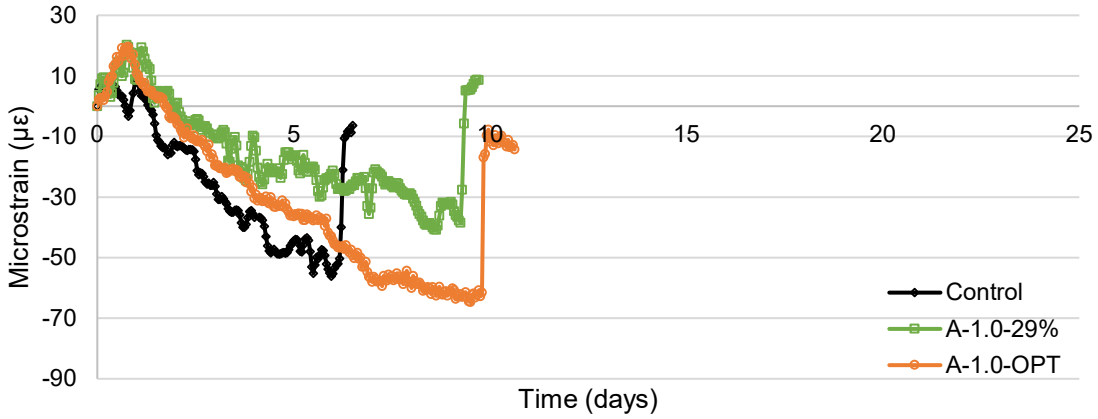

(a) Restrained shrinkage, LWFA A

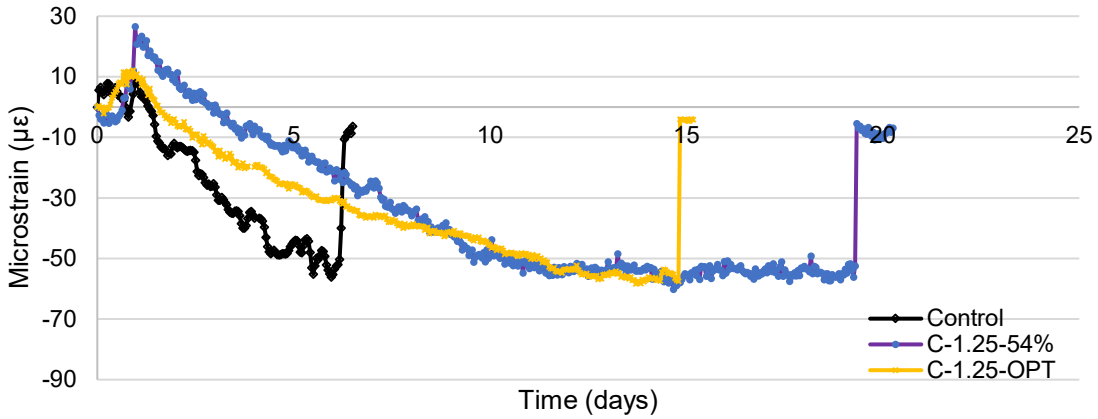

(b) Restrained shrinkage, LWFA C

Figure 66. Restrained shrinkage test results of Phase II mixes

Table 17. Summary of restrained shrinkage cracking age, Phase II

Mix ID	Cracking age (days)
Control	6.25
A-1.0-29%	9.25
A-1.0-OPT	9.75
C-1.25-54%	19.25
C-1.25-OPT	14.75

4.3 Phase III – Performance Evaluation

The final phase of the project was to evaluate the performance of the four internally cured mixes from the previous mixes, as well as two control mixes. In particular, two internally cured mixes from Phase I (A-1.0-29% and C-1.25-54%), two internally cured mixes from Phase II (A-1.0-OPT and C-1.25-OPT), the control mix from Phase I (Control) and optimized control mix with

45:55 gradation (limestone: sand and gravel by volume) were included in Phase III study. Following properties of concrete were studied in Phase III:

- Fresh concrete properties: slump, air content, unit weight, and setting time;
- Hardened concrete properties: compressive strength, modulus of elasticity, modulus of rupture, bond strength;
- Volume stability: free shrinkage at sealed and drying environmental conditions at 5, 7, and 10 days of curing, and restrained shrinkage at 5 and 10 days of curing;
- Durability performance: electrical resistivity, rapid chloride permeability test, freeze/thaw resistance;

The following subsection of the chapter will provide the test results of the Phase III study and discussion of findings.

4.3.1 Phase III Mix Designs

Mix designs for each concrete mixture in the Phase III study are shown in Table 18. The initial amount of chemical admixtures was adjusted based on the fresh properties results obtained from Phase II. If the required workability was not met, an additional MRWR was added to the mix. The sum of initial and additional MRWR is shown in the column identified as "Total" in Table 18. It should also be noted that as the required workability for mixes with LWFA C was not achieved at the initial w/c of 0.38, it was increased to 0.41 to meet the slump requirements.

Table 18. Mix designs of Phase III mixes

Mix ID	Cement (pcy)	Water (pcy)	Limestone (pcy)	Sand and Gravel (pcy)	LWFA (pcy)	AEA (fl oz/cwt)	MRWR (fl oz/cwt]	
							Initial	Total
Control	658	250	854	1992	0	2.5	5.0	8.0
A-1.0-29%	658	250	854	1417	424	3.0	8.0	8.0
C-1.25-54%	658	270	828	893	745	3.5	7.0	14.0
Control-OPT	658	250	1287	1573	0	2.5	5.0	7.5
A-1.0-OPT	658	250	1438	851	424	3.0	6.0	6.0
C-1.25-OPT	658	270	1271	479	733	3.5	7.0	11.0

4.3.2 Phase III Results and Discussion

4.3.2.1 Fresh Properties

Workability and air content of Phase III mixes are illustrated in Figure 67. In Phase III of the study, the dosage of AEA was adjusted to assure that all mixes met the NDOT air content requirements of 6.5-8.0% by volume. The acceptable range of air content is between black dotted lines in Figure 67.

Results, as shown in Table 18 and Figure 67, demonstrated that optimized gradation helped to improve workability in all three optimized mixes. Not only the higher slump was achieved for all the cases, but also a lesser amount of chemical admixtures was needed.

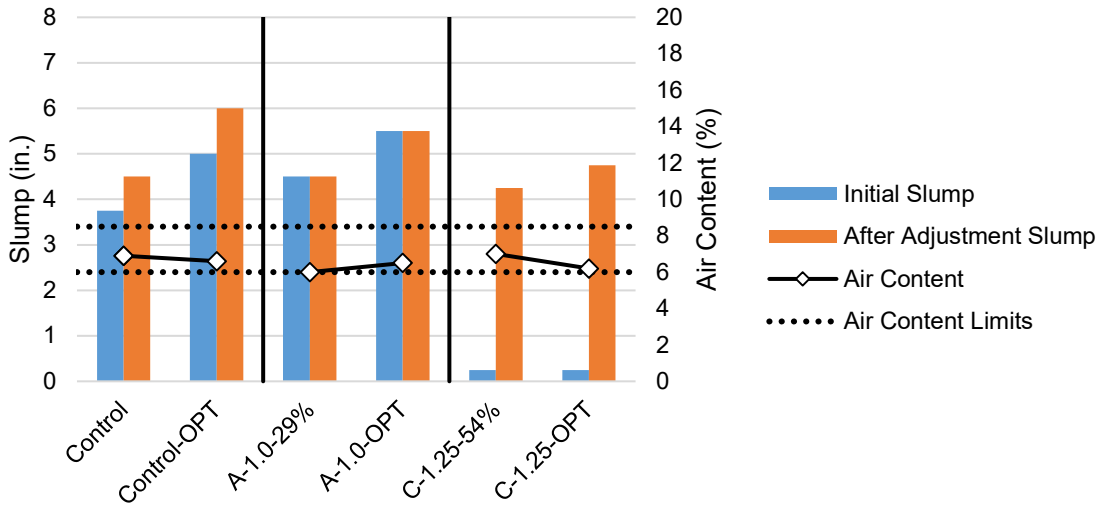

Figure 67. Workability and air content of Phase III mixes

Unit weight of all Phase III mixes are illustrated in Figure 68. The actual unit weights did not vary significantly compared to the design values.

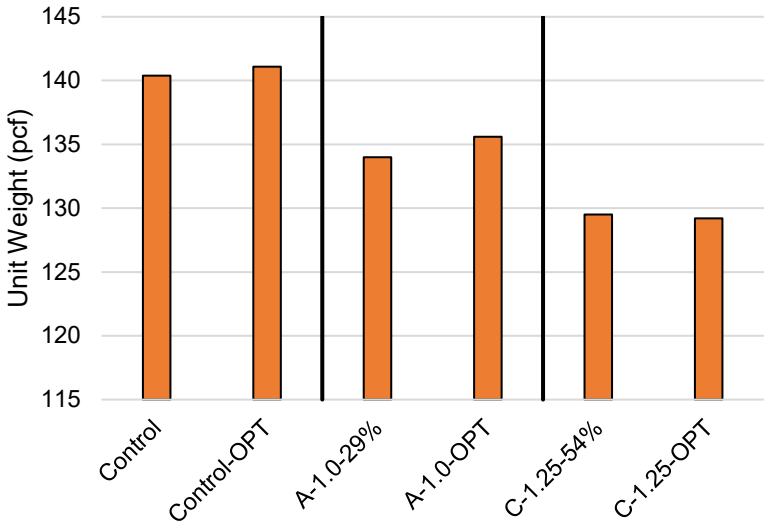

Figure 68. Unit weight of Phase III mixes

The initial and final setting times for each concrete mixture are illustrated in Figure 69. Firstly, it should be pointed out that the difference between standard mixes and their optimized counterparts is insignificant for all cases. Secondly, the control mixtures and internal curing mixtures with LWFA A have comparable initial and final setting time, yet the internal curing mixes with LWFA C tend to set at much later ages.

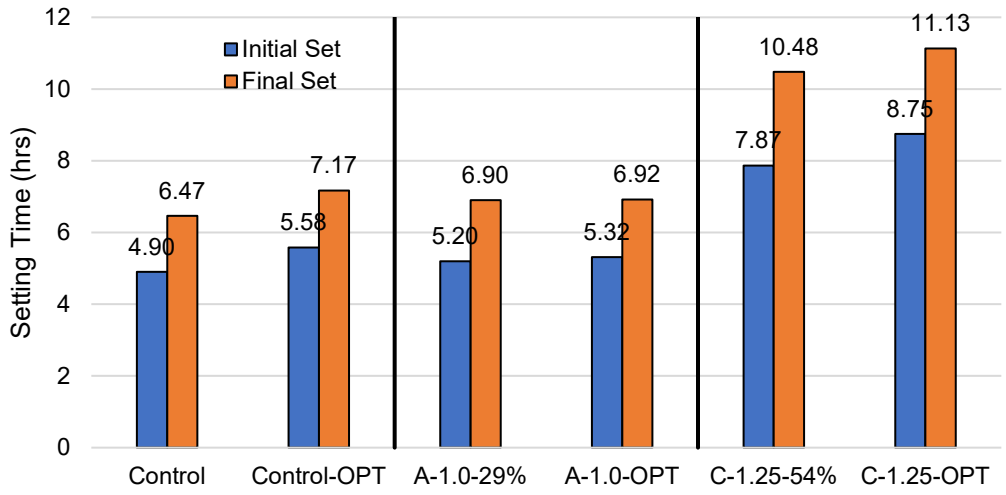

Figure 69. Setting times Phase III mixes

4.3.2.2 Mechanical Properties

Figure 70 shows compressive strength results for Phase III mixes. Previously, there was a significant variation in compressive strength among the mixes, which was linked to the air content. Results showed that with the controlled air content, the 28-day compressive strength requirement of 4000 psi could be easily met with all the mixes. Furthermore, all internally cured mixes show higher 28-day strength, which can be explained by a higher degree of cement hydration resulted from internal curing. Finally, the effect of aggregate optimization on compressive strength is minimal.

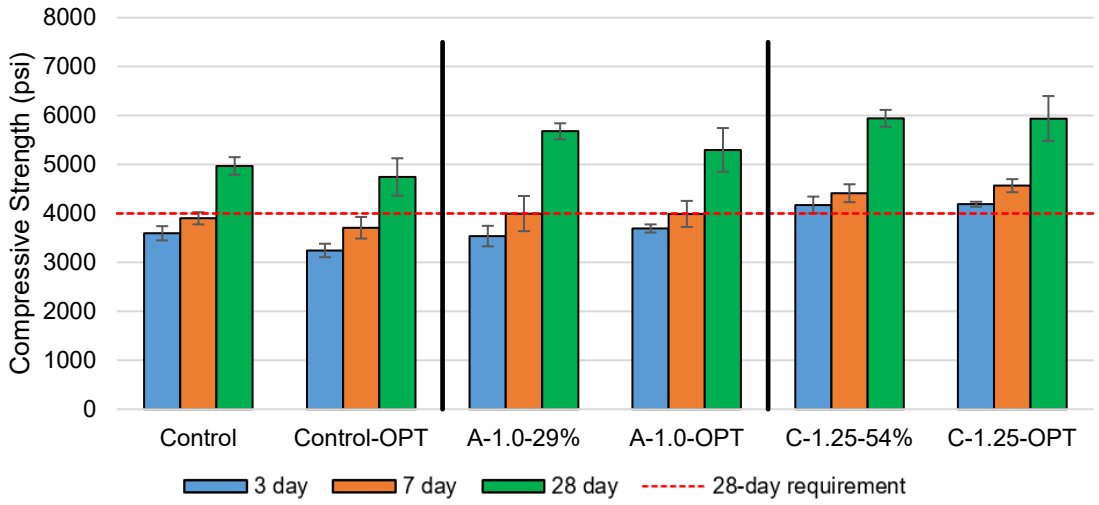

Figure 70. Compressive strength results of Phase III mixes

Figure 71 presented the results of the modulus of elasticity of all Phase III mixes. As it was reported by other researchers, LWFAs lead to a slight decrease the modulus of elasticity of concrete. Modulus of elasticity was measured as 5345ksi and 5095ksi for the Control and Control-OPT mix, respectively, which is comparable to the modulus of elasticity of normal-weight

concrete. In comparison, A-1.0-29%, A-1.0-OPT, C-1.25-54%, and C-1.25-OPT were measured to have 4453 ksi, 4759 ksi, 4155 ksi, and 4485 ksi, respectively. Overall, the modulus of elasticity of internally cured concrete decreased by 7% to 23% compared to control mixes. As explained previously, the effect is expected and contributed by soft and porous nature of LWFA.

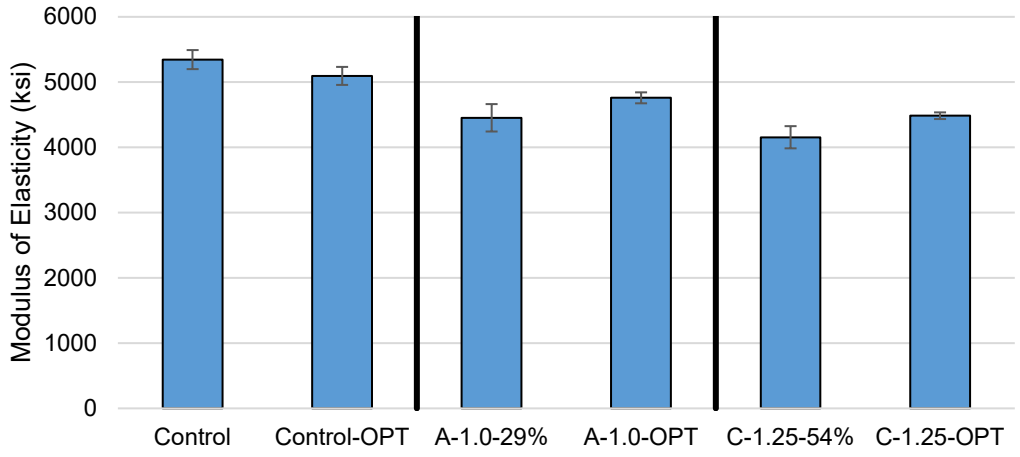

Figure 71. Modulus of elasticity results of Phase III mixes

The results of the modulus of rupture are shown in Figure 72. It can be observed, internally cured mixes have a lower modulus of rupture, in general. The control mixture has a modulus of rupture of 958.7 psi, whereas the modulus of rupture of internally cured mixtures are 19.9% (767.8 psi) and 34.7% (626.4 psi) lower for A-1.0-29% and C-1.25-54% respectively. One potential reason behind that is the porous nature of lightweight aggregates, which may act as a weak cracking interface for tensile failure. Based on the trend, it may also be suggested that the decrease in modulus of rupture may be somewhat linearly proportional to the volumetric content of lightweight aggregates in the concrete.

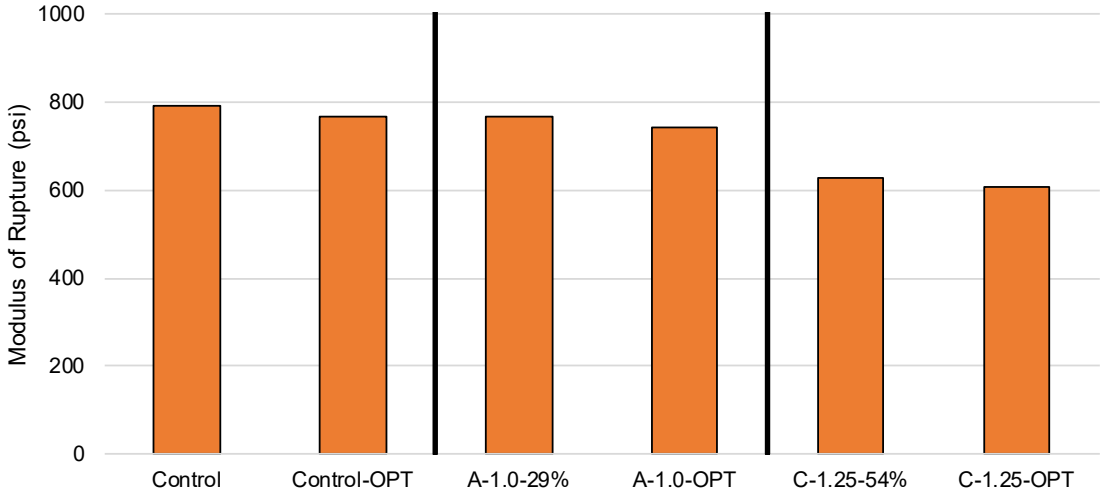

Figure 72. Modulus of rupture results of Phase III mixes

The same trend as modulus of rupture can be observed with the bond strength. Figure 73 illustrates the data on the bond strength of concrete mixtures. Bond strength of the control mixture

is 4078 psi, whereas A-1.0-29% and C-1.25-54% mixes have a bonding strength 10.2% (3662 psi) and 23.2% (3130 psi) lower respectively.

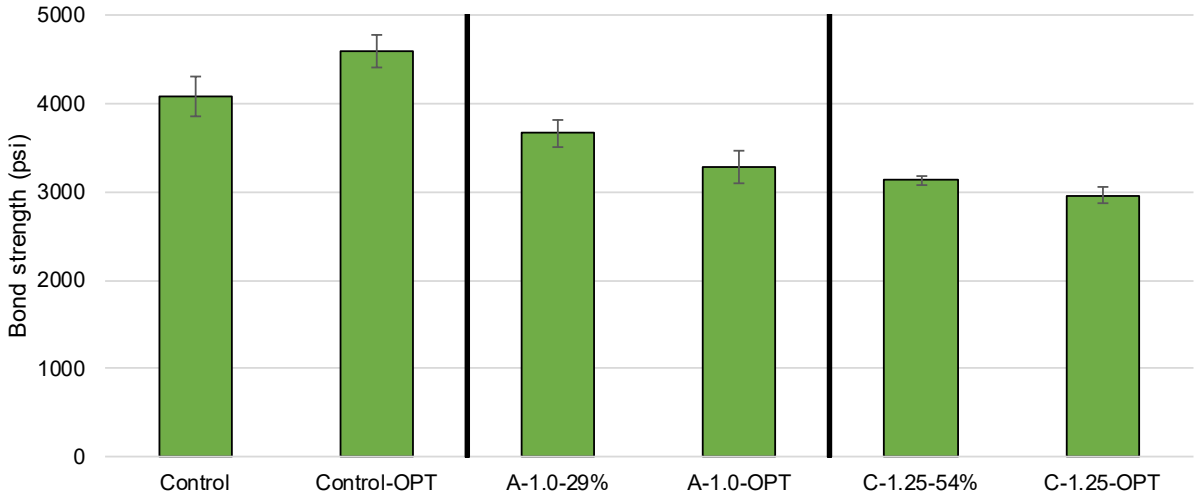

Figure 73. Bond strength results of Phase III mixes

The measured mechanical properties and their comparison to the prediction from LRFD equations (AASHTO 2017) are presented in Table 18. Results showed that LRFD euqations tend to underpredict the modulus of elasticity and modulus of rupture. The high variance of the measured and predicted mechanical properties indicated that likely due to the softer nature of introduced LWFA, modulus of elasticity and modulus of rupture equations from AASHTO LRFD is not adequate for predicting key parameters these of internally cured concrete. Further study and data collection are needed to develop revised LRFD equations for internally cured concrete in bridge design should the direct measurement of parameters such as modulus of elasticity, modulus of elasticity not available.

Table 19. Measured and predicted mechanical properties of Phase III mixes

	$f'_{c,28}$ (ksi)	$E'_{c,28}$ (ksi)		$MOR_{,28}$ (ksi)		$f_{b,28}$ (ksi)	$f'_{sp,28}$ (ksi)
	Measured	Measured	LRFD	Measured	LRFD	Measured	LRFD
Control	4.971	5345	3871	0.959	0.535	4.078	0.513
A-1.0-29%	5.679	4453	3858	0.768	0.572	3.662	0.548
C-1.25-54%	5.944	4155	3749	0.626	0.585	3.130	0.561
Control-OPT	4.746	5095	3810	0.766	0.523	3.284	0.501
A-1.0-OPT	5.299	4759	3793	0.744	0.552	4.591	0.529
C-1.25-OPT	5.940	4485	3735	0.606	0.585	2.185	0.561

4.3.2.3 Durability Properties and Volume Stability

Figure 74 and Figure 75 illustrate surface and bulk electrical resistivity of Phase III mixes, respectively. A similar trend is noticed in the previous research phases. In most cases, internally cured concrete has lower resistivity at an early age, mainly because of saturated porous LWFAs.

However, it is expected that the resistivity of internally cured concrete will reach the values of control mixes and even overpass them at later ages.

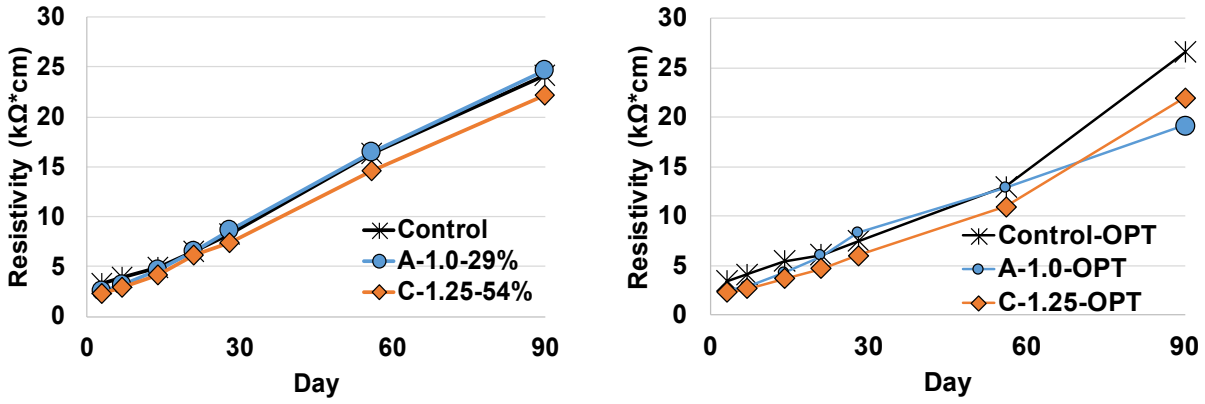

(a) Regular mixes **(b)** Optimized mixes

Figure 74. Surface resistivity of Phase III mixes

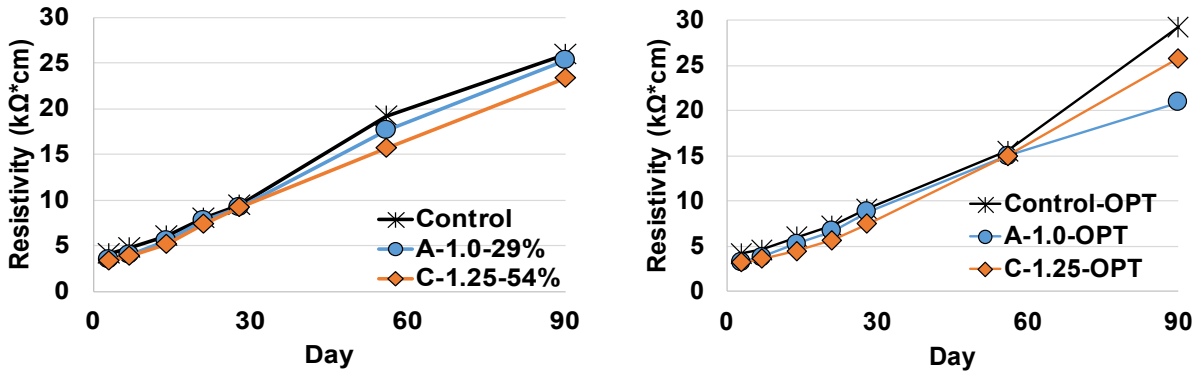

(a) Regular mixes **(b)** Optimized mixes

Figure 75. Bulk resistivity of Phase III mixes

Results from the rapid chloride permeability test, as presented in Table 20, showed that the developed internally curing mixes have comparable chloride penetrability compared to the control mix and were also categorized as either very low or low chloride ion penetrability based on ASTM C1202 guidance.

Table 20. Rapid chloride permeability test results of Phase III mixes

Mix ID	Total Charge Passed (C)	Chloride Ion Penetrability
Control	1081	Low
Control-OPT	1365	Low
A-1.0-29%	975	Very Low
A-1.0-OPT	1107	Low
C-1.25-54%	1012	Low
C-1.25-OPT	1388	Low

Results of free shrinkage of Phase III mixes at sealed and drying conditions are illustrated in Figure 76 and Figure 77, respectively. Each Figure is subdivided into six separate charts based on the age of curing (5, 7, or 10 days) and aggregate blend optimization (non-optimized and optimized blends). Various curing durations were proposed to study the effect of reduction of curing duration with internally cured mixes.

The first observation is that internal curing allows minimizing or eliminating autogenous shrinkage, regardless of curing age and aggregate blend. It can be observed in Figure 76 that most charts of internally cured mixes keep close to the neutral x-axis, which means that the specimens do not experience any length change. Control mixes, on the other hand, tend to experience autogenous shrinkage, which starts at a later age.

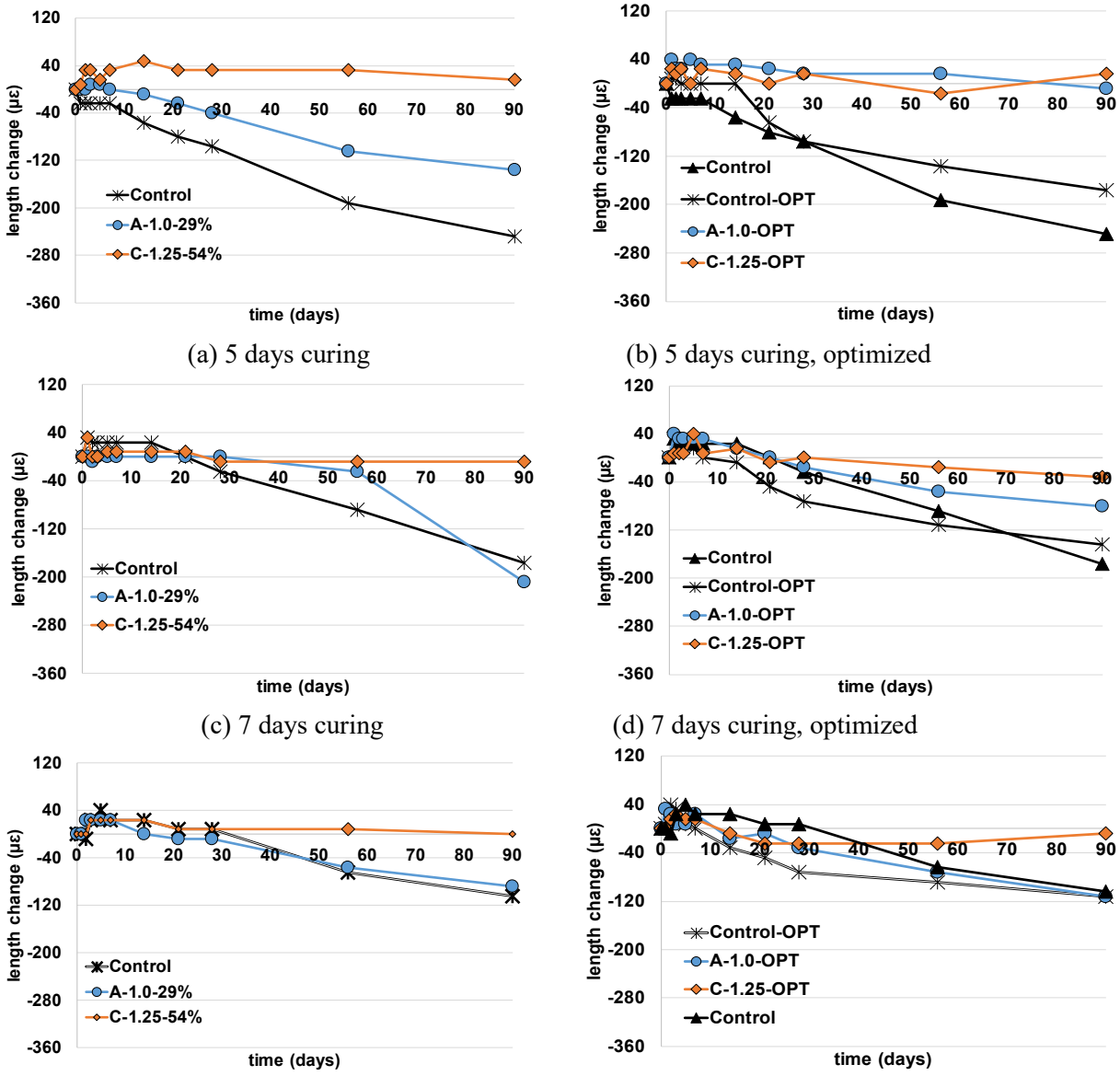

(a) 5 days curing

(b) 5 days curing, optimized

(c) 7 days curing

(d) 7 days curing, optimized

(e) 10 days curing

(f) 10 days curing, optimized

Figure 76. Free shrinkage at sealed condition at different curing ages of Phase III mixes

Secondly, it can be clearly observed that the longer duration of curing reduces the amount of autogenous shrinkage for both optimized and non-optimized control mixes. At 10 days of curing, the autogenous shrinkage behavior of control mixes and internally cured mixes is comparable. As the curing age decreases, the autogenous shrinkage of control mixes increases, whereas internally cured mixes are unaffected because saturated LWFAs provide curing water from within the concrete matrix. This finding may mean that internal curing could potentially decrease the required amount of curing period in the field.

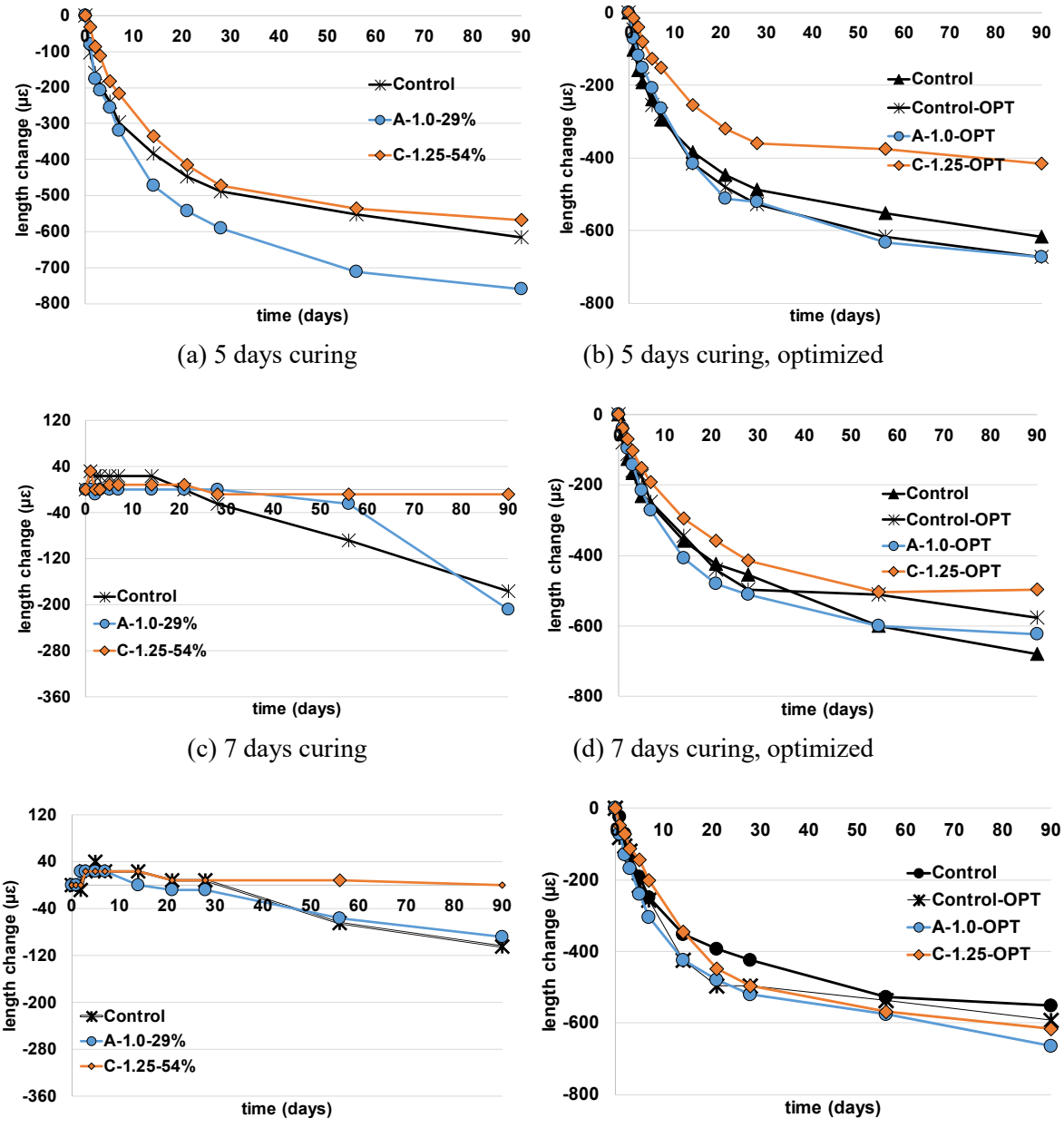

(a) 5 days curing

(b) 5 days curing, optimized

(c) 7 days curing

(d) 7 days curing, optimized

(e) 10 days curing

(f) 10 days curing, optimized

Figure 77. Free shrinkage at drying condition at different curing ages of Phase III mixes

Thirdly, free shrinkage at drying conditions, or drying shrinkage of internally cured concrete mixes is similar in general to those of control mixes. However, it should be noted that the

following two factors play a vital role:

- Moisture loss. Shrinkage specimens have a high ratio of surface area to the total volume of the concrete. This high ratio is the main reason behind moisture loss, which is lost from the specimen before it could be used for continuous cement hydration. Actual field structures are expected to have a much lower surface area to total volume ratios and are believed to provide a more appropriate sealed environment for the internally cured concrete.
- Modulus of elasticity. The previous section of the chapter provided the values of modulus of elasticity for all mixes. Internally cured mixes had a lower modulus of elasticity, which means that even though the amount of drying shrinkage is the same or a bit higher compared to those of control mixes, the actual internal pressure causing the shrinkage is lower for specimens with lightweight aggregates.

Restrained shrinkage findings are provided in Figure 78 and Table 21. As explained earlier, in order to simulate different field curing periods, it was decided to provide external curing to restrained shrinkage rings by means of wet burlaps. As was observed in previous phases, LWFAs help to significantly delay the crack formation. It was observed that rings cured by LWFA C tend to crack at later ages compared to LWFA A. As expected, prolonged (10 days over 5 days) curing resulted in delayed cracking age. Table 20 includes the cracking age for the mixes. Unfortunately, the test was not performed on optimized mixes because of the equipment issues.

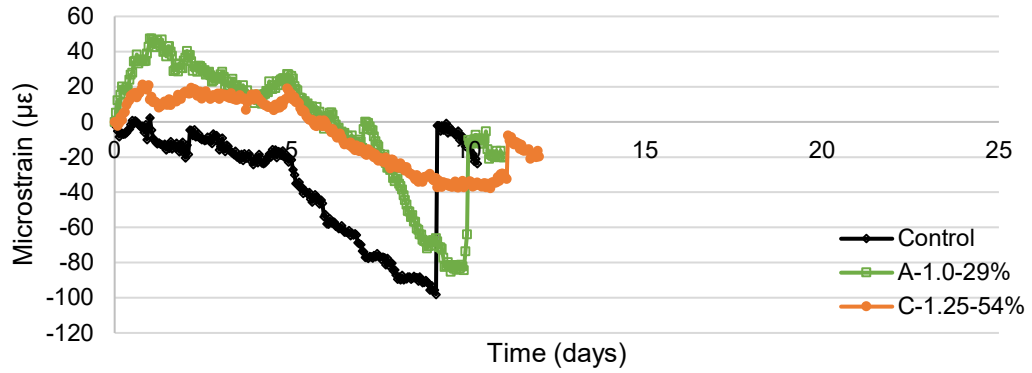

(a) 5 days curing

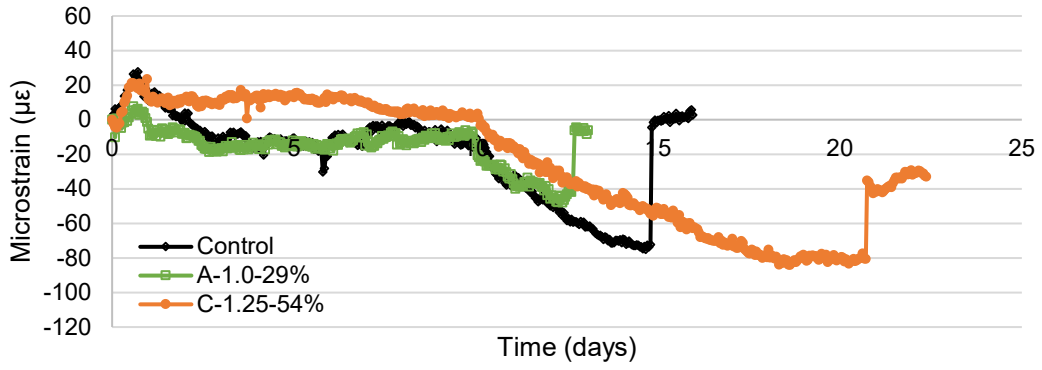

(b) 10 days curing

Figure 78. Restrained shrinkage of Phase III mixes

Table 21. Summary of restrained shrinkage cracking age of Phase III mixes

Mix ID	Cracking age (days)	
	5 days curing	10 days curing
Control	9.00	14.75
A-1.0-29%	10.00	12.75
C-1.25-54%	11.00	20.75

4.4 Results Summary

Table 22 provides a summary of all test results from Phase III study. As expected, aggregate blend optimization successfully enhanced the workability of internally cured mixes. Better workability was achieved with a lesser amount of chemical admixtures for both internal curing mixes and control mix.

Furthermore, internal curing had a direct impact on the mechanical properties of concrete. Compressive strength increased by 7% to 20%, whereas modulus of elasticity, modulus of rupture, and bond strength experienced a slight decreases were observed. Both trends were attributed to enhanced cement hydration and "soft" LWFA, respectively.

Table 22. Summary of results of Phase III mixes

Properties		Control	A-1.0	C-1.25	Control-OPT	A-1.0-OPT	C-1.25-OPT
Slump (in.)		4.50	4.50	4.25	6.00	5.50	4.75
Air Content[1] (%)		6.9	6.0	7.0	6.0	6.5	6.2
Unit Weight (pcf)		140.4	134.0	129.5	141.1	135.6	129.2
Setting Time	Initial Set(hrs)	4.90	5.20	7.87	5.58	5.32	8.75
	Final Set (hrs)	6.47	6.90	10.48	7.17	6.92	11.13
Compressive Strength[1], 28d (psi)		4971	5679	5944	4746	5679	5940
Modulus of Elasticity, 28d (ksi)		5345	4453	4155	5095	4759	4485
Modulus of Rupture, 28d (psi)		792	768	626	766	744	606
Slant Shear Bond Strength, 28d (psi)		4078	3662	3130	4591	3284	2963
Electrical Resistivity, 90d (kΩ*cm)	Surface	24.15	24.63	22.20	26.58	19.15	21.95
	Bulk	25.90	25.30	23.33	29.20	20.90	25.80
Chloride Ion Penetration, 90d (Coulombs)		1081	975	1012	729	1107	697
90d Autogenous Shrinkage, (με)	5d curing	-248	-136	16	-176	-8	16
	7d curing	-176	-208	-8	-144	-80	-32
	10d curing	-104	-88	0	-112	-112	-8
90d Free Drying Shrinkage, (με)	5d curing	-616	-760	-568	-672	-672	-416
	7d curing	-680	-672	-680	-576	-624	-496
	10d curing	-552	-672	-608	-592	-664	-616
Restrained Shrinkage Cracking Age, (d)	0d curing	6.25	9.25	19.25	N/A	N/A	N/A
	5d curing	9.00	10.00	11.00	N/A	N/A	N/A
	10d curing	14.75	12.75	20.75	N/A	N/A	N/A

[1] NDOT requirement: 6.0%-8.5% [2] NDOT requirement: minimum 4000psi

Internal curing successfully minimizes and, in some cases, even eliminates autogenous shrinkage. In addition, it was found that the same trends of autogenous shrinkage were observed for internally cured mixes at early curing ages (5 to 7 days) as for control mixes at later ages (10 days). This fact provides a basis to suggest that the curing age for internally cured mixes may be potentially reduced. Finally, a restrained shrinkage cracking age was delayed by means of internal curing in all cases.

The findings on electrical resistivity are consistent with studies from other researchers; that is, resistivity is slightly lower compared to the reference mix at an early age. Long-term continuous monitoring of electrical resistivity is suggested, when most of the internal curing water is desorbed. Chloride ion penetrability of internal curing mixtures was found to be comparable to the reference mix, all in very low or low range.

CHAPTER 5. ANALYSIS OF FEASIBILITY AND COST EFFECTIVENESS

5.1 Cost Effectiveness Analysis

With the identified materials sources and developed mixture designs, a cost analysis was performed to estimate the mixtures production cost based on raw material costs, as shown in Table 23. The results are to be used to justify if the developed concrete mixtures are cost-effective to be implemented in the state of Nebraska.

Table 23. Costs of raw materials

Material	Unit Cost	Unit
IP Cement	$135	Ton
Limestone	$25	Ton
Sand & Gravel	$18	Ton
LWFA A	$50	Ton
LWFA C	$50	Ton
Water	$2.5	Ton
Water Reducer	$9	Gallon
Air Entraining Agent	$7	Gallon

The production cost of each mixture based on the cost of raw materials and mix designs is provided in Table 24. It should be noted that the exact cost depends on the location and availability of materials. Also, the unit costs of raw materials are subject to change.

Table 24. Production cost of each mixture

Mixture	Base Cost ($/cu yd)
Control	77.93
A-1.0-29%	83.54
C-1.25-54%	89.50
Control-OPT	79.34
A-1.0-OPT	84.82
C-1.25-OPT	89.62

5.2 Feasibility Analysis

Many aspects make internally cured mixtures feasible in the state of Nebraska. First of all, sources of LWFA identified through the study are located relatively close, in the neighboring state of Missouri and Colorado. In terms of concrete production, while attention is needed for pre-wetting LWFA, no significant change is needed for mixing and handling of internally cured concrete. Final mixes are workable and have no issues with finishability. As demonstrated by the experimental study, with appropriate mix design, it was possible to achieve promising mixes utilizing local materials with sufficient fresh concrete, mechanical, and durability performance that meet NDOT requirements.

It is worth noting that there are still some issues that should be taken into account before the successful use of internally curing mixtures in the field. Mixtures need to be carefully designed

to ensure appropriate air content and workability. Special attention is need for soaking and control the mixture content of LWFA prior to batching. Also, it should be kept in mind that internal curing comes with changes in mechanical properties, such as decreased modulus of elasticity, modulus of rupture, and bond strength, which needed to be accounted for in the structural design.

5.3 Recommendations for Construction Practice of Internally Cured Concrete

5.3.1 Field Handling of Lightweight Fine Aggregates

According to NY State DOT (Streeter et al. 2015) and Indiana DOT (Barrett et al. 2015) studies, and CP Tech Center Guide Specification (Weiss and Montanari, 2017), the same concept of prewetting coarse aggregates should be adopted to LWFA. Stockpiles for LWFA should be used, where a sprinkler system continuously provide water for at least 48 hours, or until the absorbed moisture content of LWFA reached the required value. Besides, stockpiles should be turned several times during the prewetting period for uniform soaking of aggregates. After the prewetting process is completed, stockpiles should be drained of excess water for 12 to 15 hours. At the end of the draining, LWFAs should be immediately used in batching. Variability in moisture states within a stockpile of prewetted lightweight aggregate should be controlled or monitored and accounted for throughout concrete production.

5.3.2 Concrete Production and Mixing Procedure

According to New York State DOT (Streeter et al., 2015), Indiana DOT (Barrett et al. 2015), and North Carolina DOT (Cavalline et al. 2019) studies, in smaller batch plants in rural areas or smaller markets, producing internal curing concrete may be more problematic as they might not have the capacity (space of aggregate bins) to accommodate LWFA. In that case, hoppers might be used to load LWFA. Another practice that was reportedly used was to pre-combine aggregates and freed up an aggregate bin for LWFA. In general, no differences in batching and mixing are needed to accommodate internally cured concrete.

5.3.3 Placing

According to New York State DOT (Streeter et al., 2015) and North Carolina DOT (Cavalline et al. 2019) studies, the internally cured concrete can be pumped onto the deck, where no difference in pumpability is expected between internally cured and conventional concrete. Studies from North Carolina DOT (Cavalline et al. 2019) recommended a minimum 5-inch diameter pump line is to be used to decrease the pressure that may prematurely draw the water out of the LWFA pores.

5.3.4 Finishing

According to New York State DOT (Streeter et al., 2015) and Louisiana DOT studies (Rupnow et al. 2016), finishability of internally cured concrete is expected to be either no difference or slightly better compared to conventional concrete.

5.3.5 Curing

According to New York State DOT (Streeter et al., 2015) and Louisiana DOT studies (Rupnow et al. 2016), it is recommended to maintain the conventional curing practice and duration. It should be noted that while the current lab study demonstrated that there is potential to reduce the required curing time, as the drying condition and geometries from the lab shrinkage tests are

different compared to field conditions, field demonstration projects are needed to justify if a reduced curing time can be adopted without causing higher cracking potential.

5.3.5 Quality control

According to New York State DOT (Streeter et al., 2015) study, quality control tests (slump, air content, and strength) should be conducted in the same manner as for regular bridge deck mixes, and no adjustment for the criteria is needed.

Chapter 6. Conclusions and Recommendations

6.1 Conclusions

The main goal of the project was to develop and evaluate an internally cured concrete based on local bridge deck concrete mix design by means of partial replacement of sand and gravel with saturated LWFA. The research study demonstrated that it is possible to develop a local internally cured concrete mix that is both technical and economically feasible.

- Due to the relatively small particle size, the introduction of LWFA tends to interference with the overall aggregate gradation and air entrainment in the system. Adjustment of water reducer and air entrainment agent dosages might be needed to ensure appropriate fresh concrete behavior.
- Aggregate blend optimization is an effective measure of addressing the workability issue, which might arise from aggregate replacement in internal curing concrete.
- Even though the replacement of fine aggregates by LWFAs results in an increase of 28-day compressive strength, and slight decreases of modulus of elasticity, and modulus of rupture, the overall mechanical properties still meet bridge deck criteria.
- Likely due to the softer nature of introduced LWFA, modulus of elasticity and modulus of rupture equations from AASHTO LRFD is not adequate for predicting key parameters these of internally cured concrete.
- Internally cured concrete was found to successfully reduce autogenous shrinkage of concrete and effectively delay the cracking age of in restrained shrinkage test.
- As the curing age decreases, internally cured mixes were found to be less affected because of the curing water from within the concrete matrix provided by the saturated LWFAs, which demonstrated that internal curing could potentially decrease the required amount of curing period in the field.
- At the very early ages (up to 3-4 weeks) the resistivity of internally cured mixes is slightly lower compared to the control mixes. However, at the later ages, due to the contribution of LWFAs to hydration of surrounding paste matrix, the resistivity of internally cured mixes could catch up with those of control mixes.
- The developed internally curing mixes have comparable chloride penetrability compared to the control mix and were categorized as either very low or low chloride ion penetrability.

6.2 Recommendations for Future Studies

Based on the results and findings, as well as the personal experience throughout the course of the project, it is believed that studies related to the concrete crack formation with internal curing will further benefit the state of Nebraska. As it was previously mentioned, none of the available tests represent the real conditions of field-scale concrete. Therefore, one of the potential recommendations is the field-scale demonstration project to study the impact of internal curing on full-scale concrete bridge decks with embedded strain gauges and temperature/moisture sensors, which can serve several purposes:

- While the experience from other states, particularly New York and Indiana are extremely beneficial, it is important for NDOT engineers and contractors to have the experience of

production and construction of internally cured concrete based on Nebraska bridge deck mix design, materials, and construction practice.

- Monitoring crack formation at different locations and different curing durations. In the present study, the free drying shrinkage test was found to post specimens in an extreme and aggressive testing environment, which resulted in massive moisture loss. Furthermore, autogenous shrinkage test results indicate the potential of reduction of curing age. As the drying condition and geometries of both free shrinkage and autogenous shrinkage tests are different compared to the real field condition, the potential of reducing required curing duration should be further studied in field-scale projects.
- Monitoring relative humidity inside concrete at different locations in order to evaluate the degree of moisture loss in the real field applications and to determine if a further adjustment of the level of internal curing is needed.
- Monitoring deterioration resistance of internal curing concrete from various mechanism, including freezing/thawing and de-icing agents.

The direct measurements of parameters such as modulus of elasticity, modulus of elasticity are always desirable for bridge deck design. However, as the modulus of elasticity, and modulus of rupture equations from AASHTO LRFD is not adequate for predicting these key parameters of internally cured concrete, further study and data collection are needed to develop revised LRFD equations to better predict mechanical properties of internally cured concrete should the direct measurement of above-mentioned parameters not feasible. Also, bridge design parameters are to be adjusted to account for the different mechanical properties of internally cured concrete.

Lastly, the internal curing mechanism could potentially be applied to ultra-high-performance concrete (UHPC). Since the w/c is usually lower than 0.20 in UHPC, there is a considerable portion of unhydrated cement left in the concrete matrix. Internal curing may facilitate further hydration of those cement particles and lead to better mechanical and durability performance of the material.

REFERENCES

AASHTO LRFD Bridge Design Specifications, American Association of State Highway and Transportation Officials. *American Association of State Highway and Transportation Officials*, 2017.

AASHTO TP 95-11. Standard Test Method of Test for Surface Resistivity Indication of Concrete's Ability to Resist Chloride Ion Penetration. *American Association of State and Highway Transportation Officials*, 2011.

ACI Committee 211. *Standard Practice for Selecting Proportions for Structural Lightweight Concrete.* American Concrete Institute, 1990.

ACI Committee 209. *Prediction of Creep, Shrinkage, and Temperature Effects in Concrete Structures.* American Concrete Institute, 1992.

ACI Committee 209. *Report on Factors Affecting Shrinkage and Creep of Hardened Concrete*. American Concrete Institute, 2005.

ACI Committee 308. *Report on Internally Cured Concrete Using Prewetted Absorptive Lightweight Aggregate.* American Concrete Institute, 2013.

Arcosa Lightweight. *Internal Curing*. https://arcosalightweight.com/applications/internal-curing. Accessed Jan. 14, 2019.

ASTM C29. Standard Test Method for Bulk Density ("Unit Weight") and Voids in Aggregate. *ASTM International*, 2017.

ASTM C39. Standard Test Method for Compressive Strength of Cylindrical Concrete Specimens. *ASTM International*, 2018.

ASTM C70. Standard Test Method for Surface Moisture in Fine Aggregate. *ASTM International*, 2013.

ASTM C78. Standard Test Method for Flexural Strength of Concrete (Using Simple Beam with Third-Point Loading). *ASTM International,* 2018.

ASTM C128. Standard Test Method for Relative Density (Specific Gravity) and Absorption of Fine Aggregate. *ASTM International*, 2015.

ASTM C138. Standard Test Method for Density (Unit Weight), Yield, and Air Content (Gravimetric) of Concrete. *ASTM International*, 2017.

ASTM C143. Standard Test Method for Slump of Hydraulic-Cement Concrete. *ASTM International*, 2015.

ASTM C150. Standard Specification for Portland Cement. *ASTM International*, 2019.

ASTM C157. Standard Test Method for Length Change of Hardened Hydraulic-Cement Mortar and Concrete. *ASTM International*, 2017.

ASTM C173. Standard Test Method for Air Content of Freshly Mixed Concrete by the Volumetric Method. *ASTM International*, 2016.

ASTM C192. Standard Practice for Making and Curing Concrete Test Specimens in the Laboratory. *ASTM International*, 2018.

ASTM C231. Standard Test Method for Air Content of Freshly Mixed Concrete by the Pressure Method. *ASTM International*, 2017.

ASTM C403. Standard Test Method for Time of Setting of Concrete Mixtures by Penetration Resistance. *ASTM International*, 2016.

ASTM C469. Standard Test Method for Static Modulus of Elasticity and Poisson's Ratio of Concrete in Compression. *ASTM International*, 2014.

ASTM C494. Standard Specification for Chemical Admixtures for Concrete. *ASTM International*, 2017.

ASTM C511. Standard Specification for Mixing Rooms, Moist Cabinets, Moist Rooms, and Water Storage Tanks Used in the Testing of Hydraulic Cements and Concretes. *ASTM International*, 2019.

ASTM C595. Standard Specification for Blended Hydraulic Cements. *ASTM International,* 2019.

ASTM C882. Standard Test Method for Bond Strength of Epoxy-Resin Systems Used With Concrete by Slant Shear. *ASTM International,* 2013.

ASTM C1202. Standard Test Method for Electrical Indication of Concrete's Ability to Resist Chloride Ion Penetration. *ASTM International,* 2019.

ASTM C1252. Standard Test Methods for Uncompacted Void Content of Fine Aggregate (as Influenced by Particle Shape, Surface Texture, and Grading) . *ASTM International,* 2017.

ASTM C1581. Standard Test Method for Determining Age at Cracking and Induced Tensile Stress Characteristics of Mortar and Concrete under Restrained Shrinkage. *ASTM International*, 2018.

ASTM C1698. Standard Test Method for Autogenous Strain of Cement Paste and Mortar. *ASTM International*, 2009.

ASTM C1761. Standard Specification for Lightweight Aggregate for Internal Curing of Concrete. *ASTM International,* 2017.

Barrett, T. J., Miller, A. E., and Weiss, W. J. *Documentation of the INDOT experience and construction of the bridge decks containing internal curing in 2013.* Technical Report. Indiana Department of Transportation, 2015.

Bentz, D. P., Lura. P, and Roberts J. W. *Mixture Proportioning for Internal Curing*. Concrete International*,* 2005, 27: 35-40.

Bentz, D. P., and Snyder K. A. *Protected paste volume in concrete. Extension to internal curing using saturated lightweight fine aggregate*. Cement and Concrete Research, 1999, 29: 1863-1867.

Castro, J. *Moisture Transport in Cement Based Materials: Application to Transport Tests and Internal Curing.* PhD Dissertation. Purdue University, 2011.

Cavalline, T. L., Tempest, B. Q., Leach, J. W., Newsome, R. A., Loflin, G. D., and Fitzner, M. J., *Internal Curing of Concrete Using Lightweight Aggregate*, Technical Report, North Carolina Department of Transportation, 2019.

Delatte, N., Mack, E., and Cleary, J. *Evaluation of High Absorptive Materials to Improve Internal Curing of Low Permeability Concrete*. Technical Report. Ohio Department of Transportation, 2007.

Dewar, J.D. *Computer Modelling of Concrete Mixtures.* E & FN Spon, 1999.

Di Bella, C., Schlitter, J., Carboneau, N., and Weiss, J. *Documenting the Construction of a Plain Concrete Bridge Deck and an Internally Cured Bridge Deck.* Technical Report. Indiana Local Technical Assistance Program Technical Reports, 2012.

Expanded Shale, Clay and Slate Institute. *What is Internal Curing (IC)?* https://www.escsi.org/internal-curing/. Accessed Jan. 14, 2019.

Goad D. R., Jones, C. M., and Hale W. M. *Internal Curing*, Technical Report. Arkansas Highway and Transportation Department, 2014.

Goltermann, P., Johansen, V., and Palbol, L. *Packing of Aggregates: An Alternative Tool to Determine the Optimal Aggregate Mix*. ACI Materials Journal 94-M51, 1997: 435-442.

Guthrie, W. S., and Stevens D., *Internal Curing of Concrete Bridge Decks in Utah: Preliminary Evaluation*. Utah Department of Transportation Research Newsletter, Spring 2013.

Ideker, J. H., Deboodt, T., and Fu T. *Internal Curing of High-Performance Concrete for Bridge Decks*, Technical Report. Oregon Department of Transportation, 2013.

Jensen, O. M., and Lura P. *Techniques and materials for internal water curing of concrete*. Materials and Structures, 2006, 39: 817-825.

Jones, M. R., Zheng, L., and Newlands, M. D. *Comparison of particle packing models for proportioning concrete constituents for minimum voids ratio*. Materials and Structures, 2002, 35: 301-309.

Jones, W. A., House, M. W., and Weiss, W. J. *Internal Curing of High Performance Concrete Using Lightweight Aggregates and Other Techniques.* Technical Report. Colorado Department of Transportation, 2014.

Henkensiefken, R., Bentz, D., Nantung, T., and Weiss, J. *Volume change and cracking in internally cured mixtures made with saturated lightweight aggregate under sealed and unsealed conditions*. Cement & Concrete Composites, 2009, 31: 427-437.

Kosmatka, S. H., and Wilson, M. L. *Design and Control of Concrete Mixtures. The guide to applications, methods, and materials*. Portland Cement Association, 2011.

Ley, T., Cook, D., and Fick, G. *Concrete Pavement Mixture Design and Analysis (MDA): Effect of Aggregate Systems on Concrete Properties*. National Concrete Pavement Technology Center, Ames, IA, 2012.

Li, Z. *Advanced Concrete Technology*. John Wiley & Sons, Inc., 2011.

Lindquist, W. D., Darwin, D., Browning, J., and Miller, G. G. *Effect of Cracking on Chloride Content in Concrete Bridge Decks*. ACI Materials Journal, 2006, 103: 467-473.

Liu, J., Shi, C., Ma, X., Khayat, K. H., Zhang, J., and Wang, D. *An overview on the effect of internal curing on shrinkage of high performance cement-based materials*. Construction and Building Materials, 2017, 146: 702-712.

Ma, X., Liu, J., and Shi, C. *A review on the use of LWA as an internal curing agent of high performance cement-based materials*. Construction and Building Materials, 2019, 218: 385-393.

M. Mamirov, Hu, J., and Kim, Y. R. *Evaluation Reducing Cement Content in NDOR Class R Combined Aggregate Gradations*, Nebraska Department of Transportation, SPR-P1(18) M 069, 2020.

Miller, A. E. *Using a Centrifuge for Quality Control of Pre-Wetted Lightweight Aggregate in Internally Cured Concrete.* Master's Thesis. Purdue University, 2014.

MNDOT, *Bridge Deck Cracking*. Transportation Research Synthesis. Minnesota Department of Transportation, 2011.

NDOT, *Bridge Inspection Database*. Nebraska Department of Transportation.

Neville, A. M. *Properties of Concrete*. Pearson Education Limited, 2011.

NDOT, *NDOT Pavement Design Manual*. Nebraska Department of Transportation, 2018.

NY 703-19 E, Moisture Content of Lightweight Fine Aggregate. New York State Department of Transportation, 2008.

Pavement Interactive. *Gradation and Size.* https://www.pavementinteractive.org/reference-desk/materials/aggregate/gradation-and-size/. Accessed Jan. 10, 2019.

Raoufi, K., Schlitter, J., Bentz, D., and Weiss, J. *Parametric Assessment of Stress Development and Cracking in Internally Cured Restrained Mortars Experiencing Autogenous Deformations and Thermal Loading*. Advances in Civil Engineering, 2011.

Rettner, D. L., Fiegen, M. S., Snyder, M. B., and MacDonald, K. A. *Analysis of Bridge Deck Cracking Data*. Technical Report. Minnesota Department of Transportation, 2014.

Reynolds, D., Browning, J., and Darwin, D. *Lightweight Aggregates as an Internal Curing Agent for Low-Cracking High-Performance Concrete.* Technical Report. Transportation Pooled Fund, 2009.

Roberts, F. L., Kandhal, P. S., Brown, E. R., Lee, D. Y., and Kennedy, T. W. *Hot Mix Asphalt Materials, Mixture Design, and Construction.* National Asphalt Paving Association, 1996.

Rupnow, T., Collier, Z., Raghavendra, A., and Icenogle, P. *Evaluation of Portland Cement Concrete with Internal Curing Capabilities.* Technical Report. Louisiana Department of Transportation and Development, 2016.

Schlitter, J., Henkensiefken, R., Castro, J., Raoufi, K., and Weiss, J. *Development of Internally Cured Concrete for Increased Service Life.* Technical Report. Indiana Department of Transportation, 2010.

Standard Specifications for Highway Construction. Nebraska Department of Transportation, 2017.

Streeter, D. A., Wolfe, W. H., and Vaughn, R. E. *Field Performance of Internally Cured Concrete Bridge Decks in New York State.* New York State Department of Transportation, 2015.

Tia, M., Subgranon, T., Kim, K., Rodriguez, A. M., and Algazlan, A. *Internally Cured Concrete for Pavement and Bridge Deck Applications*. Technical Report. Florida Department of Transporation, 2015.

Vosoughi, P., Taylor, P., and Ceylan, H. *Impacts of Internal Curing on the Performance of Concrete Materials in the Laboratory and the Field.* Technical Report. Iowa Department of Transportation, 2017.

Wang, K., Schlorholtz, S. M., Sritharan, S., Seneviratne, H., and Wang, X. *Investigation into Shrinkage of High-Performance Concrete Used for Iowa Bridge Decks and Overlays.* Technical Report. InTrans Project Reports, 2013, 22.

Weiss, W. J., and Montanari, L. *Guide Specification for Internally Cured Concrete.* Technical Report. InTrans Project Reports, 2017, 13.